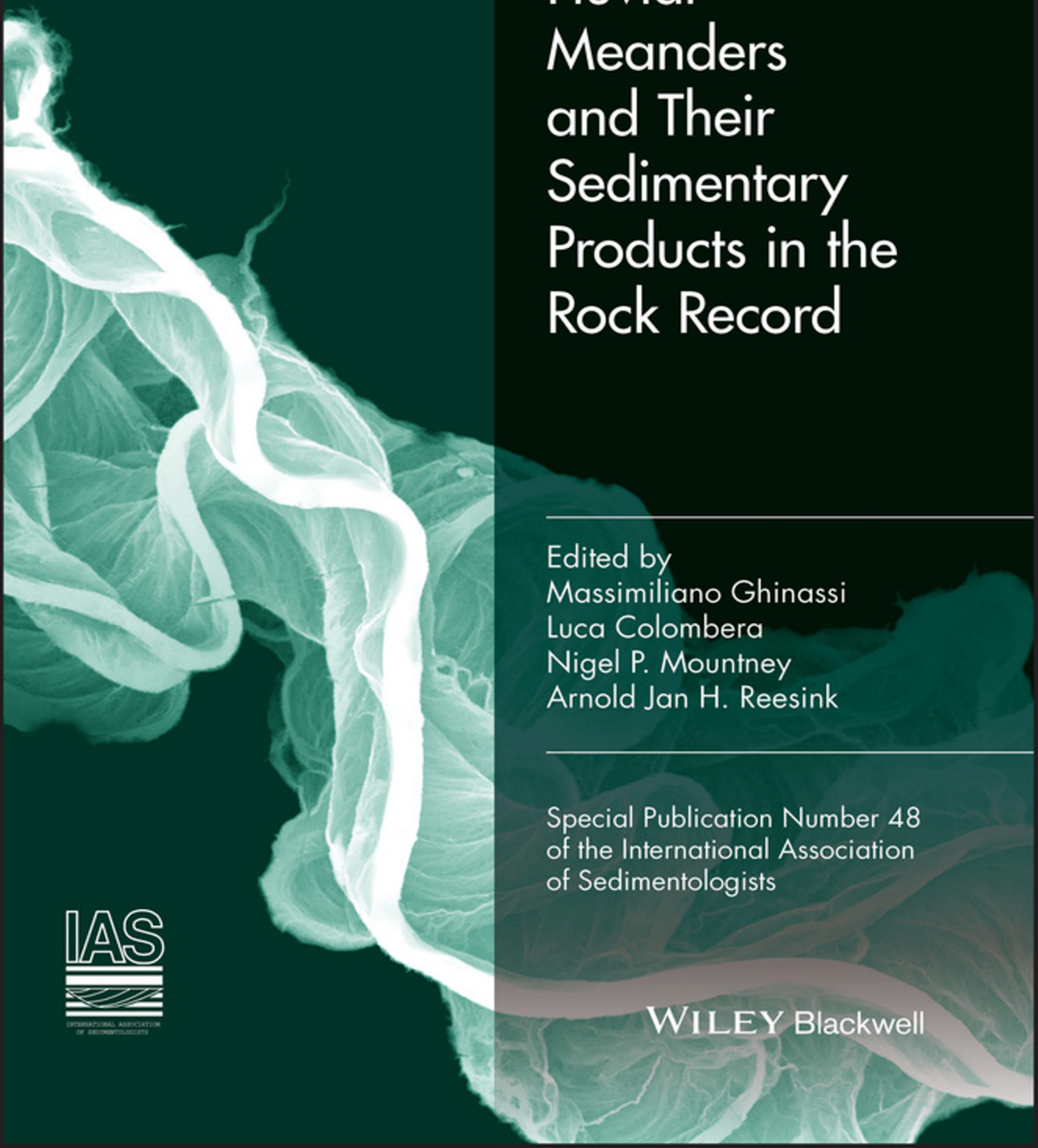

Fluvial Meanders and Their Sedimentary Products in the Rock Record

Edited by
Massimiliano Ghinassi
Luca Colombera
Nigel P. Mountney
Arnold Jan H. Reesink

Special Publication Number 48
of the International Association
of Sedimentologists

IAS
INTERNATIONAL ASSOCIATION
OF SEDIMENTOLOGISTS

WILEY Blackwell

FLUVIAL MEANDERS AND THEIR SEDIMENTARY PRODUCTS IN THE ROCK RECORD

Other publications of the International Association of Sedimentologists

SPECIAL PUBLICATIONS

47 Contributions to Modern and Ancient Tidal Sedimentology
Proceedings of the Tidalites 2012 Conference
Edited by Bernadette Tessier and Jean-Yves Reynaud
2016, 349 pages, 195 illustrations

46 From Depositional Systems to Sedimentary Successions on the Norwegian Continental Margin
Edited by A.W. Martinius, R. Ravnås, J.A. Howell, R.J. Steel and J.P. Wondham 2014, 698 pages, 337 illustrations

45 Linking Diagenesis to Sequence Stratigraphy
Edited by Sadoon Morad, J. Marcelo Ketzer and Luiz F. De Ros
2012, 522 pages, 246 illustrations

44 Sediments, Morphology and Sedimentary Processes on Continental Shelves
Advances in Technologies, Research and Applications
Edited by Michael Z. Li, Christopher R. Sherwood and Philip R. Hill
2012, 440 pages, 231 illustrations

43 Quaternary Carbonate and Evaporite Sedimentary Facies and Their Ancient Analogues
A Tribute to Douglas James Shearman
Edited by Christopher G. St. C. Kendall and Abdulrahman S. Alsharhan
2010, 494 pages, 263 illustrations

42 Carbonate Systems During the Olicocene-Miocene Climatic Transition
Edited by Maria Mutti, Werner E. Piller and Christian Betzler
2010, 304 pages, 154 illustrations

41 Perspectives in Carbonate Geology
A Tribute to the Career of Robert Nathan Ginsburg
Edited by Peter K. Swart, Gregor P. Eberli and Judith A. McKenzie
2009, 387 pages, 230 illustrations

40 Analogue and Numerical Modelling of Sedimentary Systems
From Understanding to Prediction
Edited by P. de Boer, G. Postma, K. van der Zwan, P. Burgess and P. Kukla 2008, 336 pages, 172 illustrations

39 Glacial Sedimentary Processes and Products
Edited by M.J. Hambrey, P. Christoffersen, N.F. Glasser and B. Hubbard
2007, 416 pages, 181 illustrations

38 Sedimentary Processes, Environments and Basins
A Tribute to Peter Friend
Edited by G. Nichols, E. Williams and C. Paola
2007, 648 pages, 329 illustrations

37 Continental Margin Sedimentation
From Sediment Transport to Sequence Stratigraphy
Edited by C.A. Nittrouer, J.A. Austin, M.E. Field, J.H. Kravitz, J.P.M. Syvitski and P.L. Wiberg
2007, 549 pages, 178 illustrations

36 Braided Rivers
Process, Deposits, Ecology and Management
Edited by G.H. Sambrook Smith, J.L. Best, C.S. Bristow and G.E. Petts
2006, 390 pages, 197 illustrations

35 Fluvial Sedimentology VII
Edited by M.D. Blum, S.B. Marriott and S.F. Leclair
2005, 589 pages, 319 illustrations

34 Clay Mineral Cements in Sandstones
Edited by R.H. Worden and S. Morad
2003, 512 pages, 246 illustrations

33 Precambrian Sedimentary Environments
A Modern Approach to Ancient Depositional Systems
Edited by W. Altermann and P.L. Corcoran
2002, 464 pages, 194 illustrations

32 Flood and Megaflood Processes and Deposits
Recent and Ancient Examples
Edited by I.P. Martini, V.R. Baker and G. Garzón
2002, 320 pages, 281 illustrations

31 Particulate Gravity Currents
Edited by W.D. McCaffrey, B.C. Kneller and J. Peakall
2001, 320 pages, 222 illustrations

30 Volcaniclastic Sedimentation in Lacustrine Settings
Edited by J.D.L. White and N.R. Riggs
2001, 312 pages, 155 illustrations

29 Quartz Cementation in Sandstones
Edited by R.H. Worden and S. Morad
2000, 352 pages, 231 illustrations

28 Fluvial Sedimentology VI
Edited by N.D. Smith and J. Rogers
1999, 328 pages, 280 illustrations

27 Palaeoweathering, Palaeosurfaces and Related Continental Deposits
Edited by M. Thiry and R. Simon Coinçon
1999, 408 pages, 238 illustrations

26 Carbonate Cementation in Sandstones
Edited by S. Morad
1998, 576 pages, 297 illustrations

25 Reefs and Carbonate Platforms in the Pacific and Indian Oceans
Edited by G.F. Camoin and P.J. Davies
1998, 336 pages, 170 illustrations

24 Tidal Signatures in Modern and Ancient Sediments
Edited by B.W. Flemming and A. Bartholomä
1995, 368 pages, 259 illustrations

REPRINT SERIES

4 Sandstone Diagenesis: Recent and Ancient
Edited by S.D. Burley and R.H. Worden
2003, 648 pages, 223 illustrations

3 Deep-water Turbidite Systems
Edited by D.A.V. Stow
1992, 479 pages, 278 illustrations

2 Calcretes
Edited by V.P. Wright and M.E. Tucker
1991, 360 pages, 190 illustrations

Fluvial meanders and their sedimentary products in the rock record

Edited by

Massimiliano Ghinassi
Università degli Studi di Padova

Luca Colombera
School of Earth and Environment,
University of Leeds, UK

Nigel P. Mountney
School of Earth and Environment,
University of Leeds, UK

Arnold Jan H. Reesink
Lancing College, UK

SERIES EDITOR

Mark Bateman
Professor in Palaeoenvironments,
Deputy Head of Department,
Department of Geography,
Winter St., University of Sheffield,
Sheffield, UK

IAS

WILEY Blackwell

This edition first published 2019

Registered Office(s)
John Wiley & Sons, Inc., 111 River Street, Hoboken, NJ 07030, USA
John Wiley & Sons Ltd, The Atrium, Southern Gate, Chichester, West Sussex, PO19 8SQ, UK

Editorial Office
9600 Garsington Road, Oxford, OX4 2DQ, UK
For details of our global editorial offices, customer services, and more information about Wiley products visit us at www.wiley.com.

Wiley also publishes its books in a variety of electronic formats and by print-on-demand. Some content that appears in standard print versions of this book may not be available in other formats.

Library of Congress Cataloging-in-Publication Data

Names: Ghinassi, Massimiliano, editor. | Colombera, Luca, editor. | Mountney, Nigel P., editor. | Reesink, Arnold Jan H., editor. | International Association of Sedimentologists.
Title: Fluvial meanders and their sedimentary products in the rock record / edited by Massimiliano Ghinassi (Università degli Studi di Padova), Luca Colombera (School of Earth and Environment, University of Leeds, UK), Nigel P. Mountney (School of Earth and Environment, University of Leeds, UK), Arnold Jan H. Reesink (Lancing College, UK).
Description: Hoboken, NJ : John Wiley & Sons, Inc., [2019] | Series: Special publication ; 48 | Copyrighted by International Association of Sedimentologists. | Includes bibliographical references and index. |
Identifiers: LCCN 2018043693 (print) | LCCN 2018045025 (ebook) | ISBN 9781119424451 (Adobe PDF) | ISBN 9781119424321 (ePub) | ISBN 9781119424468 (hardcover)
Subjects: LCSH: Sedimentary rocks. | Meandering rivers.
Classification: LCC QE471 (ebook) | LCC QE471.F5785 2018 (print) | DDC 551.3/55–dc23
LC record available at https://lccn.loc.gov/2018043693

Cover Image: LiDAR topography of the Quinault River (Washington, USA), courtesy of Daniel Coe and the Washington Geological Survey.
Cover Design: Wiley

Set in 10/12pt Melior by SPi Global, Pondicherry, India

10 9 8 7 6 5 4 3 2 1

Contents

List of contributors

Rolf Aalto
College of Life and Environmental Sciences,
University of Exeter, Exeter, UK

Koen Blanckaert
Technische Universität Wien Fakultät für
Bauingenieurwesen, Institute of Hydraulic
Engineering and Water Resources Management,
Wien, Austria

Dan S. Chaney
Department of Paleobiology,
National Museum of Natural History,
Smithsonian Institution,
Washington, DC, USA

Luca Colombera
Fluvial & Eolian Research Group,
School of Earth and Environment,
University of Leeds, Leeds,
UK

Neil S. Davies
Department of Earth Sciences,
University of Cambridge, Cambridge,
UK

William A. DiMichele
Department of Paleobiology,
National Museum of Natural History,
Smithsonian Institution, Washington,
DC, USA

Robert M. Dorrell
Institute of Energy and Environment,
University of Hull, Hull, UK

Paul R. Durkin
Department of Geological Sciences,
University of Manitoba, Winnipeg,
Manitoba, Canada

Milovan Fustic
Department of Geoscience, University of Calgary,
Calgary, Alberta, Canada

Fernando Garcia-Garcia
Sedimentary Reservoirs Workgroup,
Department of Stratigraphy and Palaeontology,
University of Granada, Spain

Massimiliano Ghinassi
Department of Geoscience, University of Padova,
Padova, Italy

Martin R. Gibling
Department of Earth Sciences,
Dalhousie University, Halifax,
Nova Scotia, Canada

Adrian J. Hartley
Department of Geology & Petroleum Geology,
University of Aberdeen, Aberdeen,
UK

Saturnina Henares
Sedimentary Reservoirs Workgroup,
Department of Stratigraphy and Palaeontology,
University of Granada, Spain

David M. Hodgson
Fluvial & Eolian Research Group,
School of Earth and Environment,
University of Leeds, Leeds, UK

John Holbrook
Texas Christian University, Fort Worth,
Texas, USA

Stephen M. Hubbard
Department of Geoscience, University of Calgary,
Calgary, Alberta, Canada

John Howell
Department of Geology and Petroleum Geology, University of Aberdeen, Aberdeen, UK

Alessandro Ielpi
Harquail School of Earth Sciences, Laurentian University, Sudbury, Canada

Shelby Johnston
Texas Christian University, Fort Worth, Texas, USA

Rebecca Koll
Florida Museum of Natural History, University of Florida, Gainesville, USA

Kory Konsoer
Department of Geography and Anthropology, Louisiana State University College of Humanities and Social Sciences, Baton Rouge, Louisiana, USA

Stefano Lanzoni
Department of Civil, Environmental and Architectural Engineering, University of Padova, Padova, Italy

Dale A. Leckie
Department of Geoscience, University of Calgary, Calgary, Alberta, Canada

Sergio Lopez Dubon
Department of Civil, Environmental and Architectural Engineering, University of Padova, Padova, Italy

William J. Mcmahon
Faculty of Geosciences, Utrecht University, Utrecht, The Netherlands

Nigel P. Mountney
Fluvial & Eolian Research Group, School of Earth and Environment, University of Leeds, Leeds, UK

Andrew Nicholas
College of Life and Environmental Sciences, University of Exeter, Exeter, UK

Amanda Owen
School of Geographical and Earth Sciences, University of Glasgow, Glasgow, UK

Daniel Parsons
School of Environmental Sciences, University of Hull, Hull, UK

Robert H. Rainbird
Department of Natural Resources, Geological Survey of Canada, Ottawa, Canada

Arnold Jan H. Reesink
Lancing College, Lancing, West Sussex, UK

Derek Richards
Department of Geography and Anthropology, Louisiana State University College of Humanities and Social Sciences, Baton Rouge, Louisiana, USA

Catherine E. Russell
School of Geography, Geology and the Environment, University of Leicester, Leicester, UK

Arved Schwendel
School of Environmental Sciences, University of Hull, Hull, UK;
College of Life and Environmental Sciences, University of Exeter, Exeter, UK;
School of Humanities, Religion and Philosophy, York St John University, York, UK

Louis Scuderi
University of New Mexico, Department of Earth and Planetary Sciences, Albuquerque, New Mexico, USA

Richard P. Sech
Chevron Energy Technology Company, Houston, TX, USA

Michelle N. Shiers
CASP, West Bldg, Madingley Rise, Madingley Road, Cambridge, UK

Sharane S.T. Simon
Department of Earth Sciences, Dalhousie University, Halifax, Nova Scotia, Canada

Derald G. Smith†
Department of Geography, University of Calgary, Calgary, Alberta, Canada

Rudy Strobl
EnerFox Enterprise, Calgary, Alberta, Canada

Alistair Swan
Department of Geology and Petroleum Geology, University of Aberdeen, Aberdeen AB24 3UE, UK

Christopher Turnipseed
Coastal Studies Institute, Louisiana State University, Baton Rouge, Louisiana, USA

Dario Ventra
Department of Earth Sciences, University of Geneva, Geneva, Switzerland;
Faculty of Geosciences, Utrecht University, Utrecht, The Netherlands

Daniele P. Viero
Department of Civil, Environmental and Architectural Engineering, University of Padova, Padova, Italy

César Viseras
Sedimentary Reservoirs Workgroup,
Deptment of Stratigraphy and Palaeontology, University of Granada, Spain

Gary S. Weissmann
University of New Mexico, Department of Earth and Planetary Sciences, Albuquerque, New Mexico, USA

Brian J. Willis
Clastic Stratigraphy Team;
Earth Science Department, Chevron Energy Technology Company, Houston, Texas, USA

Clinton Willson
Department of Civil & Environmental Engineering, Louisiana State University, Baton Rouge, Louisiana, USA

Na Yan
Fluvial & Eolian Research Group, School of Earth and Environment, University of Leeds, Leeds, UK

Luis Miguel Yeste
Sedimentary Reservoirs Workgroup,
Department of Stratigraphy and Palaeontology, University of Granada, Spain

Shuyu Zhang
Department of Geoscience, University of Calgary, Calgary, Alberta, Canada;
Petroleum University of China (East China), Qingdao, Shandong, China

†Deceased.

Acknowledgements

The editors gratefully acknowledge all the reviewers for their constructive comments, which significantly contributed to the quality of this volume.

Int. Assoc. Sedimentol. Spec. Publ (2018) **48**, 1–14.

Sedimentology of meandering river deposits: advances and challenges

MASSIMILIANO GHINASSI*, LUCA COLOMBERA†, NIGEL P. MOUNTNEY† and ARNOLD JAN H. REESINK‡

* *Department of Geosciences, University of Padova, Padova, Italy*
† *Fluvial & Eolian Research Group, School of Earth and Environment, University of Leeds, Leeds, UK*
‡ *Lancing College, Lancing, West Sussex, UK*

INTRODUCTION

Understanding of the form and origin of river meander bends received relevant contributions between the end of the 19th century and the mid-20th century (Thompson, 1876; Tower, 1904; Sellards *et al.*, 1923; Fisk, 1944; Sundborg, 1956; Wright, 1959). In particular, two fundamental contributions provided insights on the morphodynamics of river bends: i) Thompson (1876) provided the first description of the helical secondary flow structure in river bends; and ii) Fisk (1944) highlighted the temporal evolution of the lower Mississippi River, mapping its bends as mutable elements in unprecedented detail. Subsequent research efforts sought to link the helical flow pattern with the lateral mobility of meanders and culminated in the facies models by Allen (1963) and Bernard & Major (1963). These models associated the lateral shift of river bends with the development of clinostratified, fining-upward point-bar deposits. These theories were promptly supported by studies of modern rivers (e.g. Bluck, 1971; Jackson, 1975, 1976a, b; Nanson, 1980, 1981), validated with observations from the rock record (e.g. Allen, 1965; Puigdefàbregas & Vliet, 1978) and were also strengthened by the first direct measurements of flow velocities in river bends (Bathurst *et al.*, 1977). In parallel, new morphometric studies linked metrics of meandering channels (e.g. width, depth) and hydraulic parameters (Schumm, 1972; Ethridge & Schumm, 1978), providing the basis for development of palaeohydraulic reconstructions (Hajek & Heller, 2012; Hampson *et al.*, 2013). The first ICFS (International Congress of Fluvial Sedimentology) meeting – held in 1977 in Calgary, Canada – contributed to disseminating, applying and refining these models.

During the 1980s, facies models were further improved, notably with the recognition and classification of 'Inclined Heterolithic Stratification' (Thomas *et al.*, 1987) and reinforced through increasingly detailed comparisons between modern and ancient systems (e.g. Nanson, 1980; Dietrich & Smith, 1983; Smith, 1988; Willis, 1989). Since the early 1990s, the implementation of new technologies, including ground penetrating radar, acoustic Doppler current profilers, 3D outcrop imaging (e.g. using LiDAR and photogrammetry), 3D reflection seismic, together with enhanced approaches to numerical and laboratory experimental modelling, promoted development of new approaches for understanding meandering rivers. These developments now make it increasingly possible to consider the subject from complementary points of view (Kleinhans *et al.*, 2010) and to investigate more complex dynamic flow-form interactions over larger spatial and temporal scales. Thus, recent developments help improve our understanding and enable us to challenge long-held beliefs about meandering rivers.

This IAS Special Publication has arisen in part from contributions to a Special Session titled 'Fluvial meanders and their sedimentary products in the fossil record', which was held during the 32nd IAS International Meeting (May 2016, Marrakech, Morocco). This introductory paper outlines the key advances made in the study of meandering rivers and their deposits, and frames the scientific contributions of this volume within specific research themes. The resulting holistic view on meandering rivers provides insight to outstanding issues, which we hope will become the focus of follow-on studies that will seek to advance the state-of-the-science yet further.

The articles that form this volume demonstrate the breadth of scope in the research that is currently being undertaken in fluvial sedimentology. The organisation of the volume seeks to reflect

Fluvial Meanders and Their Sedimentary Products in the Rock Record, First Edition.
Edited by Massimiliano Ghinassi, Luca Colombera, Nigel P. Mountney and Arnold Jan H. Reesink.

how the research contributions variably focus on geological controls, processes and products (Fig. 1). Collectively these articles demonstrate how several connected strands of research contribute to a more integrated understanding of the sedimentology of meandering rivers, which is leading to the advancement of both fundamental and applied science. Within this field of research, four themes have been identified as being particularly topical; these are discussed below.

ESTABLISHED MODELS AND FORTHCOMING WORKS

Four fundamental research themes that capture the breadth of contributions to this volume (Fig. 2) have fascinated fluvial sedimentologists and geomorphologists working on meandering rivers since the early 1970s: i) channel-bend growth and related point-bar facies distribution; ii) mechanisms of meander-bend cutoff; iii) meandering river channels and vegetation cover; and iv) geometries of meander-belt sedimentary bodies. For each of these themes, the main research advances and contributions in this volume are summarised herein.

Channel-bend growth and related point-bar facies distribution

Previous studies

The advent of GPR investigations of the shallow subsurface sedimentary record marked a revolutionary step in linking the planform evolution of braided rivers with stratal patterns in their deposits (e.g. Bristow & Best, 1993; Lunt & Bridge, 2004; Lunt *et al.*, 2004). Ground Penetrating Radar was also used to investigate meandering river deposits (Bridge *et al.*, 1995). However, the loss of the electromagnetic signal in bar-top mud deposits limits its application principally to relatively sand-prone point bars (Kostic & Aigner, 2007), and methods such as parametric echo-sounders may need to be deployed as an alternative (e.g. Sambrook Smith *et al.*, 2016). The majority of modern point-bar sedimentary facies – including mud-prone deposits – were investigated through vibracoring, following the pioneering work of Smith (1988), who identified commonalities between sedimentary features of some modern tidally influenced rivers and those of the Cretaceous McMurray Formation, which forms the Athabasca oil sands (Alberta, Canada). Development of the Athabasca oil sands – host of the largest heavy crude oil deposit in the world – strongly encouraged improved understanding of fluvial point-bar deposits, especially with regards to how sedimentary facies and architecture result from specific channel planform transformations.

Burge & Smith (1999) provided the first significant change to classical facies models by highlighting the common occurrence of translating meander bends (Daniel, 1971; Jackson, 1976a) and associated eddy-accretion deposits. This model was further refined by Smith *et al.* (2009, 2011), who investigated counter-point-bar and eddy-accretion deposits, and linked their development with specific conditions of outer bank erodibility. Despite their common occurrence in modern settings, translating (or 'downstream migrating', *sensu* Ghinassi *et al.*, 2016) point bars and related counter-point-bar and eddy-accretion deposits remain relatively poorly documented in the rock record (Ghinassi & Ielpi, 2015), except in rare cases for which high-resolution seismic data or planform exposures are available (Hubbard *et al.*, 2011; Ielpi & Ghinassi, 2014; Alqahtani *et al.*, 2015; Wu *et al.*, 2015). The noteworthy control of meander-bend planform transformations on spatial distribution of point-bar sedimentary facies has been recently highlighted through numerical simulations by Yan *et al.* (2017).

In the frame of understanding different styles of point-bar facies distribution, a special focus is often placed on deposits accumulated at the fluvial–marine transition zone, especially with the aim of unravelling the interaction between fluvial and tidal processes. Pioneering studies of Jones *et al.* (1993) and van den Berg *et al.* (2007) linked variations in fluvial discharge with sand-mud alternations in Inclined Heterolithic Stratification. Recent studies on the fluvial-tidal transition zone (see Ashworth *et al.*, 2015 for a review) have focussed their attention on the role of tidal currents in modulating fluvial point-bar sedimentation (Dalrymple & Choi, 2007; Martinius & Gowland, 2011; Shiers *et al.*, 2014; Carling *et al.*, 2015; Gugliotta *et al.*, 2016a, b) and have highlighted the different aspects of tidal signature on point-bar sedimentation. Choi *et al.* (2004) highlighted the spatial distribution of rhythmic tidal signatures in modern inclined heterolithic deposits. Jablonski & Dalrymple (2016) detected seasonality and climatic cyclicity

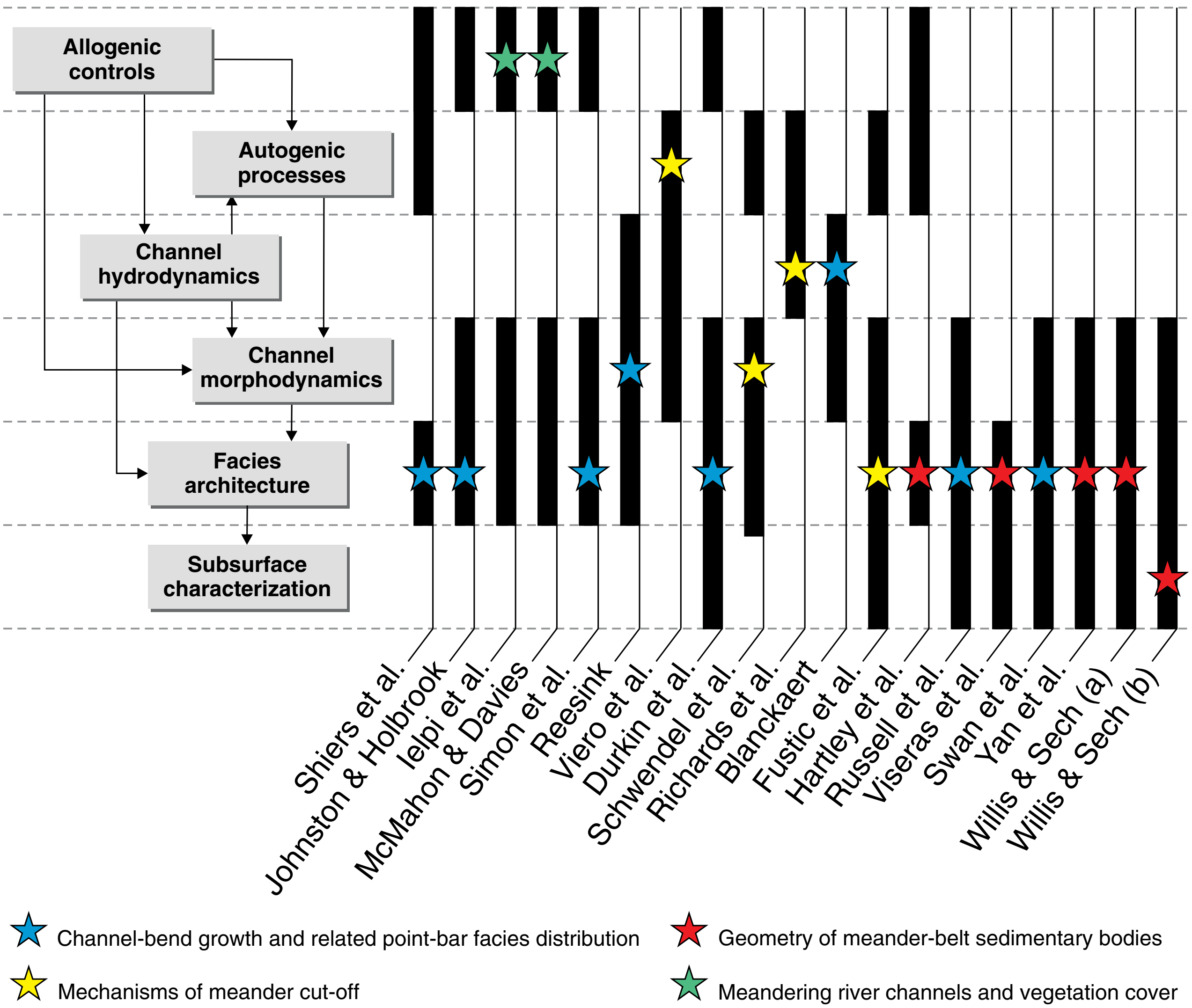

Fig. 1. Diagram that summarises the topics covered by each article in the volume. The flow chart on the left-hand side illustrates linkages between higher-order controls, processes, products and use of all related insight in applied contexts. For each article, as labelled, vertical black bars indicate which of these areas are covered and the position of stars indicates the primary focus of each. The four particular research themes discussed in more detail in the text are denoted by the coloured stars, as explained in legend. Allogenic controls (tectonics, eustatic sea-level changes, climate) are known to exert influence on fluvial systems over a range of timescales (e.g. through changes in sediment supply rate and calibre and in gradient). These factors are argued to affect fluvial systems through influences on both the behaviour of river systems and their long-term preservation in the stratigraphic record. Autogenic processes and river morphodynamics are distinguished, for convenience, because although certain processes will reflect the morphodynamic self-organisation of the river reach under study (e.g. neck cutoff), other processes might act independently (e.g. distant avulsions, shoreline progradation). Whereas studies of ancient successions allow consideration of what is ultimately preserved, studies of modern rivers permit observation of hydrodynamic processes and direct linkages of these to geomorphological and facies characteristics. It is therefore evident that integration is needed to obtain a more comprehensive understanding of the geological record of meandering rivers and to achieve improved predictions of subsurface fluvial successions. The order of articles in this volume largely follows the flow-chart in the figure and is indicated by the order in which the bars are laid out, from left to right.

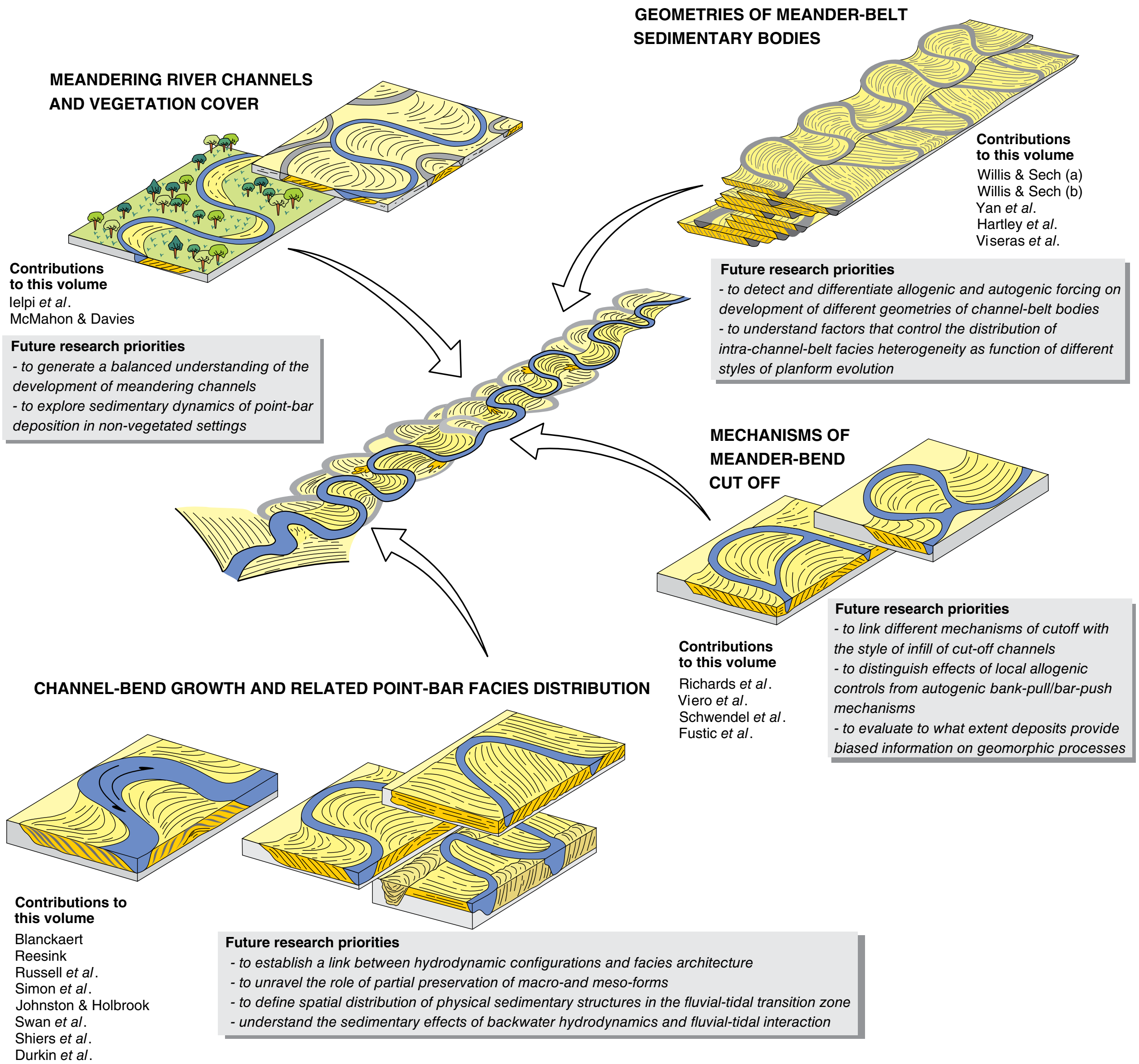

Fig. 2. Summary of the four main research themes and related future research priorities capturing the breadth of contributions to the present volume.

in tidally influenced point-bar deposits of the Cretaceous McMurray Formation. A spectrum of tidal influences spanning from the daily modulation of fluvial currents to the effects of tidal bores has been described by Martinius & Gowland (2011). The sedimentology of fluid muds in tide-dominated systems was investigated by Mackay & Dalrymple (2011). Olariu *et al.* (2015) highlighted the role of mutually evasive currents in modulating sedimentation in tidally influenced fluvial point bars.

Contributions to this volume

In this volume, contributions relating to point-bar sedimentary dynamics are provided by Blanckaert, Reesink, Russell *et al.*, Simon *et al.*, Johnston & Holbrook and Swan *et al.* Additionally, Shiers *et al.* and Durkin *et al.* focus on point-bar deposits accumulated in the distal part of alluvial plains, under the effects of processes that are characteristic of the fluvial-tidal transition zone.

Blanckaert reviews recent research on hydro-sedimentological processes and on their interaction in modern meandering rivers, highlighting and discussing the dominant controls on flow distribution. Reesink focuses on the bed-form scale and undertakes analyses of the preserved architecture of unit-bar cross strata in outcrops, highlighting how systematic measurements of these deposits may reveal valuable details of the formative fluvial palaeoenvironment. In seeking to address the discrepancy between the wide range of meander-bend planforms and the limited facies variability incorporated in facies models, Russell *et al.* present a new method to predict variable distribution of heterogeneities in point-bars, based on integration of meander-shape and meander scroll-bar pattern; the method is tested on Cretaceous deposits of the McMurray Formation (Alberta, Canada) and on Eocene deposits of the Montanyana Group (Spain). Mud-prone point-bar deposits are the focus of Simon *et al.* and Johnston & Holbrook. Simon *et al.* describe an exhumed point-bar element of the Permian upper Clear Fork Formation (Texas), highlighting the role of oblique accretion processes associated with suspended sediments plastering onto the steep inner channel bank. Johnston & Holbrook show mud-prone and sand-prone accretionary sets in a point-bar element of the Cretaceous Dinosaur Park Formation (Alberta, Canada) and link their formation with different styles of meander-bend transformations. Swan *et al.* illustrate the use of planform exposures of the Upper Jurassic Morrison Formation to reconstruct morphodynamic evolution of sandy fluvial point bars and to determine their internal facies distribution, highlighting how some sand-rich fluvial systems may previously have been interpreted incorrectly as deposits of braided rivers due to reliance on existing facies models of limited predictive capability. Focusing on the Campanian Neslen Formation (Utah, USA), Shiers *et al.* describe point-bar facies assemblages that only partially conform to those depicted in classical facies models and document and interpret substantial variability in point-bar architecture and internal facies distribution. Resultant models demonstrate how a range of interactions between allogenic (e.g. accommodation generation, fluvial discharge variations) and autogenic (e.g. backwater processes, presence of peat mires) processes can give rise to point-bar and related architectural elements with a variety of forms. Durkin *et al.* investigate transitions from point bars to counter-point bars along six modern river bends with varying channel scale, discharge and tidal influence. Results demonstrate downstream changes in net-to-gross ratio and provide criteria to detect counter-point bar deposits where a concave scroll pattern is not necessarily evident in planform.

Further developments

Although significant progress has been made in recent years in linking river-bend morphodynamics with related sedimentary products, there remains a need to improve our knowledge about how different hydrodynamic configurations are recorded in the facies architecture of point-bar deposits. Of particular importance is the role of partial preservation: most meander-belt deposits are lost to erosion and only a small portion of these deposits is ultimately preserved (Paola & Borgman, 1991; van de Lageweg *et al.*, 2013; Reesink *et al.*, 2015; Durkin *et al.*, 2017). The potential for deposition is linked to the sediment flux, which increases exponentially with discharge. Due to this exponential relationship, it is commonly assumed that sediment deposited by floods constitutes the majority of river-channel deposits. However, erosion and deposition are fundamentally controlled by the conservation of mass: along-stream changes in the transfer of sediment and not the absolute quantity of sediment transport, dictates the pattern of deposition. Consequently, erosion, deposition and sedimentary preservation must be affected greatly by increases in local gradients in water-surface slope and sediment transport, such as created by chute and neck cutoffs.

Furthermore, it is now known that the water-flow structure varies within the same meander bend at different flood stages (Kasvi *et al.* 2013; 2017), that overbank flood flows significantly modify the flow structure within bends (Loveless *et al.* 2000; Wormleaton *et al.* 2004) and that overbank deposition is a key control on the development of meanders (Van Dijk *et al.*, 2013a, b). Although the importance of these processes is widely acknowledged, the ways in which they are recorded in point-bar deposits and their ultimate preservation potential still needs to be further elucidated.

Although past research has offered notable insights into the detection of tidal influence in fluvial point-bar sedimentation at the bedform scale, less attention has hitherto been paid to understanding the role of tidal currents in shaping bar stratal architecture or controlling vertical and streamwise variations in sediment grain-size.

Assessment of these influences will require additional studies of modern meander bends, complemented with observations from tidal channels. Additionally, recognition of the location of channel deposits along the fluvial–marine transition zone (e.g. in terms of distance from a contemporaneous shoreline) is commonly attempted based on analysis of trace-fossil assemblages (e.g. Gingras *et al.*, 2012). A predictive tool that integrates knowledge of the spatial distribution of physical sedimentary structures is still lacking (Dalrymple *et al.*, 2015). Facies models developed for tidally influenced fluvial point bars should also be compared with those pertaining to muddy point bars formed far inland from tidal influence (Taylor & Woodyer, 1978; Jackson, 1981; Brooks, 2003). This comparison will contribute to the identification of distinctive features with which to detect tidally influenced fluvial point-bar deposits in the fossil record. In this context, the interference between backwater hydrodynamics and tidal–fluvial interaction was investigated in modern settings (Blum *et al.*, 2013) and efforts to detect their effects in terms of down-dip changes of architecture of distributary channel bodies were carried out by Colombera *et al.* (2016) and Fernandes *et al.* (2016). These studies provide a good starting point for further research into the diverse dynamics that characterise deposition in the zone of fluvial–marine transition.

Mechanisms of meander-bend cutoff

Previous studies

The process of abandonment of a channel reach, with the concomitant activation of a new river course (e.g. avulsion processes), has been widely documented in fluvial systems (Smith *et al.*, 1989; Slingerland & Smith., 1998, 2004; Morozova & Smith, 2000; Aslan *et al.*, 2005). In meandering rivers this process can occur at the bend scale and is known as meander-bend cutoff (Brice, 1974; Lewis & Lewin, 1983; Gagliano & Howard, 1984; Erskine *et al.*, 1992; Constantine & Dunne, 2008; Toonen *et al.*, 2012). The best-known of such processes is neck cutoff, whereby growing meanders intersect each other to cut off a meander loop (Lewis & Lewin, 1983). Less attention has been paid to chute cutoff, which occurs when a channel (i.e. chute channel) incises the inner side of the point bar (McGowen & Garner, 1970; Hooke, 2013). Chute channels can break through the upstream edge of a meander neck during major floods (Johnson & Paynter, 1967) but they can also form on the downstream side of the bar and step progressively upstream (Gay *et al.*, 1998). The latter mechanism recently received attention through laboratory experiments (van Dijk *et al.*, 2012) and outcrop studies (Ghinassi, 2011). Constantine *et al.* (2010) showed that these two processes can occur together. Zinger *et al.* (2011) highlighted the importance of cutoff processes in river dynamics, demonstrating that extreme sediment pulses are released to the main channel after occurrence of a cutoff. Such local dynamics of enhanced erosion and deposition have great potential to be preserved in the sedimentary record. Indeed, channel-fill deposits generated by cutoff events are important elements within channel-belt bodies; they give rise to significant lithological heterogeneities, which can control both the lateral channel mobility of active channels (Smith *et al.*, 2010; Güneralp *et al.*, 2011; Bogoni *et al.*, 2017) and fluid flow through channel-belt deposits (Colombera *et al.*, 2017, and references therein). In this context, different types of oxbow-lake infills (Toonen *et al.*, 2012) have been demonstrated to exert a notable control on connectivity between point-bar bodies (Donselaar & Overeem, 2008). This has important implications for reservoir development and groundwater management.

Contributions to this volume

In this volume, articles that discuss mechanisms of meander-bend cutoff are provided by Richards *et al.*, Viero *et al.*, Schwendel *et al.* and Fustic *et al.* Richards *et al.* present a dataset of measurements of the three-dimensional flow through neck cutoffs with complex configurations that includes valuable observations on helical flows, recirculation and zones with stagnated flow. Viero *et al.* present a numerical modelling approach applied to two case studies (Sacramento River, California; Cecina River, Italy) and highlight the role of channelised flow inertia and of topographic and sedimentary floodplain heterogeneities in promoting chute cutoff processes. Schwendel *et al.* investigate the infill of abandoned chute channels and of channel segments that were abandoned after neck cutoff, from meanders of the Rio Beni (Bolivian Amazon basin). Results demonstrate how patterns of infill vary in relation to hydrological connectivity and distance to the main active channel. Fustic *et al.* describe channelised deposits encased within a large-scale point-bar element exposed in the McMurray Formation type section (Athabasca River, Alberta, Canada). These deposits are interpreted as relics of the infill of larger channel incisions that represent unsuccessful channel cutoffs or avulsions.

Further developments

Although significant advances have been made in understanding cutoff processes, a detailed model that attempts to link different mechanisms of cutoff with the style of infill of cutoff channels is yet to be developed. This is of particular importance because chute cutoff processes enable the transition from meandering to braiding (Kleinhans & Van den Berg, 2011). The lack of more sophisticated interpretative models is one of the reasons why interpretations of the rock record commonly take on a binary meandering-versus-braiding view, rather than allowing for transitional systems with individual flow-form characteristics.

Furthermore, the increased water-surface gradients created by cutoff process promote periods of accelerated planform change, increases in local sediment transport gradients and generate bed-scale pulses of sediment with effects that propagate both downstream and upstream, then eventually dissipate (Zinger *et al.*, 2011). Similarly, the consequence of shifting patterns of bed shear and sediment transport at confluences during large changes in the relative discharge of the upstream branches ought to lead to significant pulses of sediment redistribution within rivers. It is reasonable to assume that such local dynamics are recorded and preserved in the rock record; yet no diagnostic criteria exist for the distinction of such local allogenic controls from the migration of meanders through autogenic bank-pull and bar-push mechanisms (Parker *et al.*, 2011; van de Lagweg *et al.*, 2014). Consequently, it also remains unclear as to whether there is preferential preservation of specific morphological elements, or events, and therefore to what extent the deposits of a river provide biased information on the formative geomorphology.

Meandering river channels and vegetation cover

Previous studies

The relationship between the presence of vegetation cover and the development of meandering river channels has been the focus of considerable study by fluvial sedimentologists in recent years. Davies & Gibling (2010) noted a parallel between appearance of riparian vegetation and an increase of occurrence of deposits indicative of sinuous rivers in the rock record. Such a notion was in agreement with observations from a number of field-based studies (Ielpi *et al.*, 2015) and laboratory experiments (van Dijk *et al.*, 2013b), which indicated that the presence of vegetation favours the development of sinuous channels (Tal & Paola, 2007, 2010) by acting to stabilise river banks both through rooting and by encouraging retention of pedogenic cohesive mud. These notions supported the idea that pre-vegetation channels were dominantly shallow and braided in planform. This form, designated the 'sheet-braided' river style by Cotter (1978), has been considered representative of Precambrian fluvial styles.

However, other geological evidence supports the presence of plan forms indicative of meandering in some non-vegetated settings; such evidence includes the documentation of laterally accreting channels in pre-Devonian deposits (Long, 2011; Ielpi & Rainbird, 2016; Santos & Owen, 2016) and the presence of sinuous fluvial channels draining arid, non-vegetated areas (Matsubara *et al.*, 2015). Laboratory experiments by Smith (1998), Peakall *et al.* (2007) and van de Lageweg *et al.* (2014) also showed that sinuous channels were able to be produced and maintained on a non-vegetated substratum. The occurrence of meandering channels on extra-terrestrial surfaces (Lorenz *et al.*, 2008) further challenges the notion of a paucity of meandering channels in non-vegetated settings.

Contributions to this volume

In the present volume, integrating a review of pre-existing literature with field evidence, the papers by McMahon & Davies and Ielpi *et al.* summarise the two main views on interaction between vegetation growth and development of meandering river channels. McMahon & Davies, supporting their claims with field data from the 1 Ga Torridon Group (Scotland), argue that meandering planforms were less frequent on pre-vegetation Earth and that there is a tangible shift in the physical nature of global alluvium, coincident with the evolution of land plants. Ielpi *et al.* show laterally accreting deposits from five sedimentary rock units deposited on Laurentia between 1.6 to 0.7 Ga. Undertaking detailed sedimentary, architectural and palaeoflow analyses, they recognise the presence of lateral-accretion sets, a feature that was previously thought to be rare or absent in these deposits.

Further developments

The uncertainty in interpretations arising from complexity in the relationships between products and processes ensure that the relative roles of factors controlling the evolution of sinuous channels, including vegetation, remain of considerable research interest (Davies, 2017; Santos *et al.*, 2017a,b). Further architectural studies are needed to assess morphodynamic feedbacks and adequately explain the dynamics and preservation of point-bar deposits in pre-vegetation and extra-terrestrial river systems. A combination of deduction based on laboratory and numerical experiments, induction based on field-based studies of modern rivers in different environments and abduction based on analysis of preserved deposits present in the geological record (cf. Kleinhans, 2010) is needed in order to generate a balanced understanding of the development of meandering channels that is applicable to the full range of boundary conditions within which meanders are found.

Geometries of meander-belt sedimentary bodies

Previous studies

Channel-belt deposits generated by the lateral shift and avulsion of sinuous channels represent sedimentary bodies of primary interest as hydrocarbon reservoirs and aquifers (Hajek *et al.*, 2010). The width-to-thickness aspect ratios of these sedimentary bodies have been compared with those of braid belts by Gibling (2006) and Colombera *et al.* (2013), who provide criteria to distinguish between these sedimentary bodies. Recently, the internal architecture of channel-belt bodies has received significant attention and has been the focus of several studies mainly based on numerical simulations and laboratory experiments. Using numerical simulations, Willis & Tang (2011) showed that different styles of point-bar planform transformations exert a remarkable control in shaping the basal surface of channel-belt bodies and distributing facies heterogeneities. These studies also highlight how a combination of different styles of planform behaviour with a variable aggradation rate strongly controls intra-channel-belt connectivity. Laboratory experiments by van de Lageweg *et al.* (2013) established a relationship between preserved set thickness and morphology formed by a meandering channel. Numerical simulation by van de Lageweg *et al.* (2016) quantified the effects of bed aggradation on the preservation of meandering channel morphologies and provided support to qualitative studies from the rock record (Ghinassi *et al.*, 2014).

Contributions to this volume

Geometries of meander-belt sedimentary bodies are analysed here by Willis & Sech (a, b), Yan *et al.*, Hartley *et al.* and Viseras *et al.* The two contributions by Willis & Sech are based on numerical simulations. Willis & Sech (a) predict the geometry and facies of channel belts by considering patterns of erosion and deposition during channel migration and underscore that facies models for channel belts need to better account for changes in the shape and position of channels, rather than present static views of river pattern. Willis & Sech (b) predict variations in fluid-flow patterns through subsurface hydrocarbon reservoirs and aquifers with improved consideration of 3D facies heterogeneity in channel-belt deposits. Yan *et al.* apply a 3D forward stratigraphic model, which is able to generate realistic architectural geometries and incorporate different types of facies heterogeneity, to a quantitative analysis of the static connectivity of point-bar sands based on data from geological analogues. Hartley *et al.* document amalgamated sandy meander belts from modern basins and the stratigraphic record, remarking that their recognition in the rock record is hindered by overlaps in facies characteristics between channel deposits of sandy meandering rivers and braided rivers. Viseras *et al.* present an outcrop/behind-outcrop multidisciplinary study of Triassic red beds from central Spain and make recommendations on how to identify and characterise poorly exposed ancient meander belts.

Further developments

Gaining improved understanding of intra-channel-belt facies heterogeneity has important applied implications, notably the characterisation of styles of compartmentalisation of sands by fine-grained deposits of different types (e.g. Colombera *et al.*, 2017; Yan *et al.*, 2017) and prediction of petrophysical heterogeneity (e.g. Burton & Wood, 2013; Nordahl *et al.*, 2014). At present, numerical modelling and laboratory experiments are the most powerful tools for understanding mechanisms controlling the internal architecture of channel-belt deposits formed by meandering channels, but improved remote sensing capabilities and the continuing efforts in capturing the variability in architectural styles from outcrop and modern analogues are also important sources of primary data. It is important that results from future research are translated to predictive tools that can be readily applied in subsurface studies.

A note on anthropogenic influences

Our future understanding of meandering rivers is contingent upon a multidisciplinary approach, which should be aimed at developing a new generation of quantitative fluvial facies models founded on datasets populated with information obtained from a broad range of investigations of modern and ancient rivers, laboratory experiments and numerical simulations. Although a comparison between these different datasets would be a fundamental step in advancing understanding in the discipline of fluvial sedimentology, it should be carried out considering the significance of anthropogenic effects on present-day fluvial systems. Nowadays, most rivers – whether they be considered to possess braided or meandering plan forms (or perhaps more usually combinations thereof) – are not hosted in pristine natural environments. The majority of present-day rivers are actively evolving under the influence of marked anthropogenic controls. Such controls have induced river behaviour and associated patterns of sediment erosion, transport and deposition that are difficult to predict. Therefore, understanding the continued evolution of meandering rivers in the Anthropocene represents an active and important field of research (e.g. Brooks *et al.*, 2003; Morais *et al.*, 2016; Munoz *et al.*, 2018). The effects of human-related activities (e.g. deforestation, loss of riparian vegetation, conversion of multi-channel systems to single-channel systems, channelisation [dredging] and bank revetments, flow regulation and damming, agricultural development, dispersion of pollutants, spreading of allochthonous aquatic faunas) need to be recognised in order to develop a new set of sedimentological models to assist with the management of rapidly evolving fluvial landscapes. Such models will enable valuable comparison of present-day fluvial deposits with the stratigraphic record and may, in turn, serve to predict the future effects of anthropogenic factors on river behaviour and patterns of erosion and sedimentation.

ACKNOWLEDGEMENTS

NPM and LC acknowledge FRG-ERG sponsors and partners AkerBP, Areva, BHPBilliton, Cairn India [Vedanta], ConocoPhillips, Murphy Oil, Nexen Energy, Petrotechnical Data Systems (PDS), Saudi Aramco, Shell, Tullow Oil, Woodside and YPF for financial support. LC has been supported by NERC (Catalyst Fund award NE/M007324/1; Follow-on Fund NE/N017218/1). MG has been supported by SID2016 project of Padova University (prot. BIRD168939). AR gratefully acknowledges the GSCO2 project for their support. We are grateful to Prof. Martin Gibling (Dalhousie University) for providing valuable comments that have helped improve this manuscript.

REFERENCES

Allen, J.R.L. (1963) The classification of cross-stratified units with notes on their origin. *Sedimentology*, **2**, 93–114.

Allen, J.R.L. (1965) The sedimentation and paleogeography of the Old Red Sandstone of Anglesy, North Wales. *Proceedings York. Geol. Soc.*, **35**, 139–185.

Alqahtani, F.A., **Johnson, H.D.**, **Jackson, C.A.L.** and **Som, M.R.B.** (2015) Nature, origin and evolution of a Late Pleistocene incised valley-fill, Sunda Shelf, Southeast Asia. *Sedimentology*, **62**, 1198–1232.

Ashworth, P.J., **Best, J.L.** and **Parsons, D.R.** (2015) *Fluvial-tidal sedimentology*. Dev. Sedimentol., **68**, Elsevier, Amsterdam.

Aslan, A., **Autin, W.J.** and **Blum, M.D.** (2005) Causes of river avulsion: insights from the late Holocene avulsion history of the Mississippi River, USA. *J. Sed. Res.*, **75**, 650–664.

Bathurst, J.C., **Thorne, C.R.** and **Hey, R.D.** (1977) Direct measurements of secondary currents in river bends. *Nature*, **269**, 504–506.

Bernard, H.A. and **Major Jr, C.F.** (1963) Recent Meander Belt Deposits of the Brazos River: An Alluvial. *AAPG Bull.*, **47**, 350–350.

Bluck, B.J. (1971) Sedimentation in the meandering River Endrick. *Scot. J. Geol.*, **7**, 93–138.

Blum, M., **Martin, J.**, **Milliken, K.** and **Garvin, M.** (2013) Paleovalley systems: insights from Quaternary analogs and experiments. *Earth-Sci. Rev.*, **116**, 128–169.

Bogoni, M., **Putti, M.** and **Lanzoni, S.** (2017) Modeling meander morphodynamics over self-formed heterogeneous floodplains. *Water Resour. Res.*, **53**, 5137–5157. https://doi.org/10.1002/2017WR020726

Brice, J.C. (1974) Evolution of Meander Loops. *Geol. Soc. Am. Bull.*, **85**, 581–586.

Bridge, J.S., **Alexander, J.A.N.**, **Collier, R.E.**, **Gawthorpe, R.L.** and **Jarvis, I.** (1995) Ground-penetrating radar and coring used to study the large-scale structure of point-bar deposits in three dimensions. *Sedimentology*, **42**, 839–852.

Bristow, C.S. and **Best, J.L.** (1993) Braided rivers: perspectives and problems. *Geol. Soc. London Spec. Publ.*, **75**, 1–11.

Brooks, A.P., **Brierley, G.J.** and **Millar, R.G.** (2003) The long-term control of vegetation and woody debris on channel and flood-plain evolution: insights from a paired catchment study in southeastern Australia. *Geomorphology*, **51**, 7–29.

Brooks, G.R. (2003) Alluvial deposits of a mud-dominated stream: the Red River, Manitoba, Canada. *Sedimentology*, **50**, 441–458.

Burge, L.M. and **Smith, D.G.** (1999) Confined meandering river eddy accretions: sedimentology, channel geometry and depositional processes. In: *Fluvial Sedimentology VI* (Eds N.D. Smith and J. Rogers), *Int. Assoc. Sedimentol. Spec. Publ.*, **28**, 113–130.

Burton, D. and **Wood, L.J.** (2013) Geologically-based permeability anisotropy estimates for tidally-influenced reservoirs using quantitative shale data. *Petrol. Geosci.*, **19**, 3–20.

Carling, P.A., **Chateau, C.C.**, **Leckie, D.A.**, **Langdon, C.T.**, **Scaife, R.G.** and **Parsons, D.R.** (2015) Sedimentology of a tidal point-bar within the fluvial–tidal transition: River Severn Estuary, UK. In: *Fluvial-Tidal Sedimentology* (Eds P. Ashworth, J. Best and D. Parsons), *Dev. Sedimentol.*, **68**, 149–189, Elsevier.

Choi, K.S., **Dalrymple, R.W.**, **Chun, S.S.** and **Kim, S.P.** (2004) Sedimentology of modern, inclined heterolithic stratification (IHS) in the macrotidal Han River delta, Korea. *J. Sed. Res.*, **74**, 677–689.

Colombera, L., **Mountney, N.P.** and **McCaffrey, W.D.** (2013) A quantitative approach to fluvial facies models: methods and example results. *Sedimentology*, **60**, 1526–1558.

Colombera, L., **Mountney, N.P.**, **Russell, C.E.**, **Shiers, M.N.** and **McCaffrey, W.D.** (2017) Geometry and compartmentalization of fluvial meander-belt reservoirs at the bar-form scale: Quantitative insight from outcrop, modern and subsurface analogues. *Mar. Petrol. Geol.*, **82**, 35–55.

Colombera, L., **Shiers, M.N.** and **Mountney, N.P.** (2016) Assessment of backwater controls on the architecture of distributary-channel fills in a tide-influenced coastal-plain succession: Campanian Neslen formation, USA. *J. Sed. Res.*, **86**, 476–497.

Constantine, J.A. and **Dunne, T.** (2008) Meander cutoff and the controls on the production of oxbow lakes. *Geology*, **36**, 23–26.

Constantine, J.A., **McLean, S.R.** and **Dunne, T.** (2010) A mechanism of chute cutoff along large meandering rivers with uniform floodplain topography. *Geol. Soc. Am. Bull.*, **122**, 855–869.

Cotter, E. (1978) The evolution of fluvial style, with special reference to the central Appalachians Paleozoic. In: *Fluvial Sedimentology* (Ed. A.D. Miall), *Mem. Can. Soc. Petrol. Geol.*, **5**, 361–384.

Dalrymple, R.W. and **Choi, K.** (2007) Morphologic and facies trends through the fluvial–marine transition in tide-dominated depositional systems: a schematic framework for environmental and sequence-stratigraphic interpretation. *Earth-Sci. Rev.*, **81**, 135–174.

Dalrymple, R.W., **Kurcinka, C.E.**, **Jablonski, B.V.J.**, **Ichaso, A.A.** and **Mackay, D.A.** (2015) Deciphering the relative importance of fluvial and tidal processes in the fluvial–marine transition. In: *Fluvial-Tidal Sedimentology* (Eds P. Ashworth, J. Best and D. Parsons), *Dev. Sedimentol.*, **68**, 3–45, Elsevier.

Daniel, J.F. (1971) *Channel movement of meandering Indiana streams. US Geol. Surv. Prof. Pap.*, **732-A**, 18 pp.

Davies, N.S. and **Gibling, M.R.** (2010) Cambrian to Devonian evolution of alluvial systems: the sedimentological impact of the earliest land plants. *Earth-Sci. Rev.*, **98**, 171–200.

Davies, N.S., **Gibling, M.R.**, **McMahon, W.J.**, **Slater, B.J.**, **Long, D.G.F.**, **Bashforth, A.R.**, **Berry, C.M.**, **Falcon-Lang, H.J.**, **Gupta, S.**, **Rygel, M.R.** and **Wellman, C.H.** (2017) Discussion on 'Tectonic and environmental controls on Palaeozoic fluvial environments: reassessing the impacts of early land plants on sedimentation'. *J. Geol. Soc. London*, **174**, 947–950. https://doi.org/10.1144/jgs2016-063. *J. Geol. Soc. London.*, doi: 10.1144/jgs2017-004.

Dietrich, W.E. and **Smith, J.D.** (1983) Influence of the point bar on flow through curved channels. *Water Resour. Res.*, **19**, 1173–1192.

Donselaar, M.E. and **Overeem, I.** (2008) Connectivity of fluvial point-bar deposits: An example from the Miocene Huesca fluvial fan, Ebro Basin, Spain. *AAPG Bull.*, **92**, 1109–1129.

Durkin, P.R., **Hubbard, S.M.**, **Holbrook, J.** and **Boyd, R.** (2017) Evolution of fluvial meander-belt deposits and implications for the completeness of the stratigraphic record. *Geol. Soc. Am. Bull.*, **130**, 721–739.

Erskine, W., **McFadden, C.** and **Bishop, P.** (1992) Alluvial cutoffs as indicators of former channel conditions. *Earth Surf. Proc. Land.*, **17**, 23–37.

Ethridge, F.G. and **Schumm, S.A.** (1978) Reconstructing paleochannel morphologic and flow characteristics: methodology, limitations and assessment. In: *Fluvial Sedimentology* (Ed. A.D. Miall), *Can. Soc. Petrol. Geol. Mem.*, **5**, 703–722.

Fernandes, A.M., **Törnqvist, T.E.**, **Straub, K.M.** and **Mohrig, D.** (2016) Connecting the backwater hydraulics of coastal rivers to fluvio-deltaic sedimentology and stratigraphy: *Geology*, **44**, 979–982.

Fisk, H.N. (1944) Geological Investigation of the Alluvial Valley of the Lower Mississippi River: U.S. Army Corps of Engineers Mississippi River Commission. 78 pp.

Gagliano, S.M. and **Howard, P.C.** (1984) The neck cutoff oxbow lake cycle along the Lower Mississippi River. In: *River Meandering* (Ed. C.M. Elliott). Proceedings of the Conference Rivers '83, American Society of Civil Engineers, 147–158.

Gay, G.R., **Gay, H.H.**, **Gay, W.H.**, **Martinson, H.A.**, **Meade, R.H.** and **Moody, J.A.** (1998) Evolution of cutoffs across meander necks in Powder River, Montana, USA. *Earth Surf. Process. Land.*, **23**, 651–662.

Ghinassi M. (2011) Chute channels in the Holocene high sinuosity-river deposits of the Firenze plain, Tuscany, Italy. *Sedimentology*, **58**, 618–642.

Ghinassi, M. and **Ielpi, A.** (2015) Stratal Architecture and Morphodynamics of Downstream-Migrating Fluvial Point Bars (Jurassic Scalby Formation, UK). *J. Sed. Res.*, **85**, 1123–1137.

Ghinassi, M., **Ielpi, A.**, **Aldinucci, M.** and **Fustic, M.** (2016) Downstream-migrating fluvial point bars in the rock record. *Sed. Geol.*, **334**, 66–96.

Ghinassi M., **Nemec W.**, **Aldinucci M.**, **Nehyba S.**, **Özaksoy V.** and **Fidolini, F.** (2014) Plan-form evolution of ancient meandering rivers reconstructed from longitudinal outcrop sections. *Sedimentology*, **61**, 952–977.

Gibling, M.R. (2006) Width and thickness of fluvial channel bodies and valley fills in the geological record: a literature compilation and classification. *J. Sed. Res.*, **76**, 731–770.

Gingras, M.K., **MacEachern, J.A.** and **Dashtgard, S.E.** (2012) Chapter 16: Estuaries. In: *Trace Fossils as Indicators of Sedimentary Environments* (Eds D. Knaust and R.G. Bromley), *Dev. Sedimentol.*, **64**, 471–514.

Gugliotta, M., **Flint, S.S.**, **Hodgson, D.M.** and **Veiga, G.D.** (2016a) Recognition criteria, characteristics and implications of the fluvial to marine transition zone in ancient deltaic deposits (Lajas Formation, Argentina). *Sedimentology*, **63**, 1971–2001.

Gugliotta, M., **Kurcinka, C.E.**, **Dalrymple, R.W.**, **Flint, S.S.** and **Hodgson, D.M.** (2016b) Decoupling seasonal fluctuations in fluvial discharge from the tidal signature in ancient deltaic deposits: an example from the Neuquén Basin, Argentina. *J. Geol. Soc.*, **173**, 94–107.

Güneralp, I. and **Rhoads, B.L.** (2011) Influence of floodplain erosional heterogeneity on planform complexity of meandering rivers. *Geophys. Res. Lett.*, **38**(14), https://doi.org/10.1029/2011GL048134

Hajek E.A. and **Heller, P.L.**, 2012, Flow-depth scaling in alluvial architecture and nonmarine sequence stratigraphy: example from the Castlegate Sandstone, central Utah, USA. *J. Sed. Res.*, **82**, 121–130.

Hajek, E.A., **Heller, P.L.** and **Sheets, B.A.** (2010) Significance of channel-belt clustering in alluvial basins. *Geology*, **38**, 535–538. https://doi.org/10.1130/G30783.1

Hooke, J.M. (2013) Rivermeandering. In: *Treatise on Geomorphology* (Ed. in Chief J. Shroder and Ed. E. Wohl), Academic Press, San Diego, CA, *Fluvial Geomorphology*, **9**, 260–288.

Hubbard, S.M., **Smith, D.G.**, **Nielsen, H.**, **Leckie, D.A.**, **Fustic, M.**, **Spencer, R.J.** and **Bloom, L.** (2011) Seismic geomorphology and sedimentology of a tidally influenced river deposit, Lower Cretaceous Athabasca oil sands, Alberta, Canada. *AAPG Bull.*, **95**, 1123–1145.

Ielpi, A. and **Ghinassi, M.** (2014) Planform architecture, stratigraphic signature and morphodynamics of an exhumed Jurassic meander plain (Scalby Formation, Yorkshire, UK). *Sedimentology*, **61**, 1923–1960.

Ielpi, A., **Gibling, M.R.**, **Bashforth, A.R.** and **Dennar, C.I.** (2015) Impact of Vegetation on Early Pennsylvanian Fluvial Channels: Insight From the Joggins Formation of Atlantic Canada. *J. Sed. Res.*, **85**, 999–1018.

Ielpi, A. and **Rainbird, R.H.** (2016) Highly variable Precambrian fluvial style recorded in the Nelson Head Formation of Brock Inlier (Northwest Territories, Canada). *J. Sed. Res.*, **86**, 199–216.

Jablonski, B.V. and **Dalrymple, R.W.** (2016) Recognition of strong seasonality and climatic cyclicity in an ancient, fluvially dominated, tidally influenced point bar: Middle McMurray Formation, Lower Steepbank River, north-eastern Alberta, Canada. *Sedimentology*, **63**, 552–585.

Jackson, R.G. (1976) a. Depositional model of point bars in the lower Wabash River. *J. Sed. Res.*, **46**, 579–594.

Jackson, R.G. (1976) b. Largescale ripples of the lower Wabash River. *Sedimentology*, **23**, 593–623.

Jackson, R.G. (1981) Sedimentology of muddy fine-grained channel deposits in meandering streams of the American middle west. *J. Sed. Petrol.*, **51**, 1169–1192.

Jackson, R.G. (1975) Velocity–bed-form–texture patterns of meander bends in the lower Wabash River of Illinois and Indiana. *Geol. Soc. Am. Bull.*, **86**, 1511–1522.

Johnson, R.H. and **Paynter, J.** (1967) The development of a cutoff on the River Irk at Chadderton, Lancashire. *Geography*, **52**, 41–49.

Jones, B.G., **Martin, G.R.** and **Senapti, N.** (1993) Riverine–tidal interactions in the monsoonal Gilbert River fan delta, northern Australia. *Sed. Geol.*, **83**, 319–337.

Kasvi, E., **Laamanen, L.**, **Lotsari, E.** and **Alho, P.** (2017) Flow patterns and morphological changes in a sandy meander bend during a flood—spatially and temporally intensive ADCP measurement approach: *Water*, **9**, 106.

Kasvi, E., **Vaaja, M.**, **Alho, P.**, **Hyyppä, H.**, **Hyyppä, J.**, **Kaartinen, H.** and **Kukko, A.** (2013) Morphological changes on meander point bars associated with flow structure at different discharges. *Earth Surf. Proc. Land.*, **38**, 577–590.

Kleinhans, M.G., **Buskes, C.** and **de Regt, H.** (2010) Philosophy of Earth Science, In: *Philosophies of the sciences* (Ed. F. Allhoff), Wiley-Blackwell, Chichester, UK, 213–236.

Kleinhans, M.G. and **Van den Berg, J.H.** (2011) River channel and bar patterns explained and predicted by an empirical and a physics-based method. *Earth Surf. Proc. Land.*, **36**, 721–738.

Kostic, B. and **Aigner, T.** (2007) Sedimentary architecture and 3D ground-penetrating radar analysis of gravelly meandering river deposits (Neckar Valley, SW Germany). *Sedimentology*, **54**, 789–808.

Lewis, G.W. and **Lewin, J.** (1983) Alluvial cutoffs in Wales and the Borderlands. In: *Modern and ancient fluvial systems* (Eds J.D. Collinson and J. Lewin), *Int. Assoc. Sedimentol. Spec. Publ.*, **6**, 145–154.

Long, D.G.F. (2011) Architecture and depositional style of fluvial systems before land plants: a comparison of Precambrian, early Paleozoic and modern river deposits. In: *From River to Rock Record: The Preservation of Fluvial Sediments and their Subsequent Interpretation* (Eds S. Davidson, S. Leleu and C.P. North), *SEPM Spec. Publ.*, **97**, 37–61.

Lorenz, R.D., **Lopes, R.M.**, **Paganelli, F.**, **Lunine, J.I.**, **Kirk, R.L.**, **Mitchell, K.L.**, **Soderblom, L.A.**, **Stofan, E.R.**, **Ori, G.**, **Myers, M.**, **Miyamoto, H.**, **Radebaugh, J.**, **Stiles, B.**, **Wall, S.D.**, **Wood, C.A.** and **The Cassini RADAR Team** (2008) Fluvial channels on Titan: initial Cassini RADAR observations. *Planet. Space Sci.*, **56**, 1132–1144.

Loveless, J.H., **Sellin, R.H.J.**, **Bryant, T.B.**, **Wormleaton, P.R.**, **Catmur, S.** and **Hey, R.** (2000) The effect of overbank flow in a meandering river on its conveyance and the transport of graded sediments. *Water and Environment Journal*, **14**, 447–455.

Lunt, I.A. and **Bridge, J.S.** (2004) Evolution and deposits of a gravely braid bar Sagavanirktok River, Alaska. *Sedimentology*, **51**, 1–18.

Lunt, I.A., **Bridge, J.S.** and **Tye, R.S.** (2004) A quantitative, three-dimensional depositional model of gravely braided rivers. *Sedimentology*, **51**, 377–414.

Mackay, D.A. and **Dalrymple, R.W.** (2011) Dynamic mud deposition in a tidal environment: the record of fluid-mud deposition in the Cretaceous Bluesky Formation, Alberta, *Canada. J. Sed. Res.*, **81**, 901–920.

Martinius, A.W. and **Gowland, S.** (2011) Tide-influenced fluvial bedforms and tidal bore deposits (late Jurassic Lourinhã Formation, Lusitanian Basin, Western Portugal). *Sedimentology*, **58**, 285–324.

Matsubara, Y., **Howard, A.D.**, **Burr, D.M.**, **Williams, R.M.E.**, **Dietrich, W.E.** and **Moore, J.M.** (2015) River meandering on Earth and Mars: A comparative study of Aeolis Dorsa meanders, Mars and possible terrestrial analogs of the Usuktuk River, AK and the Quinn River, NV. *Geomorphology*, **240**, 102–120.

McGowen, J.H. and **Garner, L.E.** (1970) Physiographic features and stratification types of coarse-grained point bars: modern and ancient examples. *Sedimentology*, **14**, 77–111.

Morais, E.S., **Rocha, P.C.** and **Hooke, J.** (2016) Spatiotemporal variations in channel changes caused by cumulative factors in a meandering river: The lower Peixe River, Brazil. *Geomorphology*, **273**, 348–360.

Morozova, G.S. and **Smith, N.D.** (2000) Holocene avulsion styles and sedimentation patterns of the Saskatchewan River, Cumberland Marshes, Canada. *Sed. Geol.*, **130**, 81–105.

Munoz, S.E., **Giosan, L.**, **Therrell, M.D.**, **Remo, J.W.**, **Shen, Z.**, **Sullivan, R.M.**, **Wiman, C.**, **O'Donnell, M.** and **Donnelly, J.P.** (2018) Climatic control of Mississippi River flood hazard amplified by river engineering. *Nature*, **556**, 95–98.

Nanson, G.C. (1981) New evidence of scroll-bar formation on the Beatton River. *Sedimentology*, **28**, 889–891.

Nanson, G.C. (1980) Point bar and floodplain formation of the meandering Beatton River, northeastern British Columbia, Canada. *Sedimentology*, **27**, 3–29.

Nordahl, K., **Messina, C.**, **Berland, H.**, **Rustad, A.B.** and **Rimstad, E.** (2014) Impact of multiscale modelling on predicted porosity and permeability distributions in the fluvial deposits of the Upper Lunde Member (Snorre Field, Norwegian Continental Shelf). In: *Sediment-body Geometry and Heterogeneity: Analogue Studies for Modelling the Subsurface* (Eds A.W. Martinius, J.A. Howell and T.R. Good), *Geol. Soc. London Spec. Publ.*, **387**, 85–109.

Olariu, C., **Steel, R.J.**, **Olariu, M.I.** and **Choi, K.** (2015) Facies and architecture of unusual fluvial–tidal channels with inclined heterolithic strata: Campanian Neslen Formation, Utah, USA. In: *Fluvial-Tidal Sedimentology* (Eds P. Ashworth, J. Best and D. Parsons), *Dev. Sedimentol.*, **68**, 353–394, Elsevier.

Paola, C. and **Borgman, L.** (1991) Reconstructing random topography from preserved stratification. *Sedimentology*, **38**, 553–565.

Parker, G., **Shimizu, Y.**, **Wilkerson, G. V.**, **Eke, E. C.**, **Abad, J. D.**, **Lauer, J. W.**, **Paola, C.** and **Voller, V. R.** (2011) A new framework for modeling the migration of meandering rivers. *Earth Surf. Proc. Land.*, **36**, 70–86.

Peakall, J., **Ashworth, P.J.** and **Best, J.L.** (2007) Meander-bend evolution, alluvial architecture and the role of cohesion in sinuous river channels: a flume study. *J. Sed. Res.*, **77**, 197–212.

Puigdefàbregas, C. and **Van Vliet, A.** (1978) Meandering stream deposits from the Tertiary of the Southern Pyrenees. In: *Fluvial Sedimentology* (Ed. A.D. Miall), *Can. Soc. Petrol. Geol. Mem.*, **5**, 469–485.

Reesink A.J.H., **Parsons D.R.**, **Van den Berg J.**, **Amsler M.L.**, **Best J.L.**, **Hardy R.J.**, **Lane, S.N.**, **Orfeo, O.** and **Szupiany, R.** (2015) Extremes in dune preservation; controls on the completeness of fluvial deposits. *Earth-Sci. Rev.*, **150**, 652–665.

Sambrook Smith, G.H., **Best, J.L.**, **Leroy, J.Z.** and **Orfeo, O.** (2016) The alluvial architecture of a suspended sediment dominated meandering river: the Rio Bermejo, Argentina. *Sedimentology*, **63**, 1187–1208.

Santos, M.G.M., **Mountney, N.P.** and **Peakall, J.** (2017a) Tectonic and environmental controls on Palaeozoic fluvial environments: reassessing the impacts of early land plants on sedimentation, *J. Geol. Soc.*, **174**, 393–404.

Santos, M.G.M., **Mountney, N.P.**, **Peakall, J.**, **Thomas, R.E.**, **Wignall, P.B.** and **Hodgson, D.M.** (2017b) Reply to Discussion on 'Tectonic and environmental controls on Palaeozoic fluvial environments: reassessing the impacts of early land plants on sedimentation', *J. Geol. Soc. London*, **174**, 950–952. https://doi.org/10.1144/jgs2016-063.

Santos, M.G.M. and **Owen, G.** (2016) Heterolithic meandering-channel deposits from the Neoproterozoic of NW Scotland: Implications for palaeogeographic reconstructions of Precambrian sedimentary environments. *Precambrian Res.*, **272**, 226–243.

Schumm, S.A. (1972) Fluvial paleochannels. In: Recognition of Ancient Sedimentary Environments (Eds J.K. Rigby and W.K. Hamblin), *SEPM Spec. Publ.*, **16**, 98–107).

Sellards, E.H., **Tharp, B.C.** and **Hill, R.T.** (1923) Investigation on the Red River made in connection with the Oklahoma-Texas boundary suit. *Texas Bulletin*, **2327**, 174.

Shiers, M.N., **Mountney, N.P.**, **Hodgson, D.M.** and **Cobain, S.L.** (2014) Depositional controls on tidally influenced fluvial successions, Neslen Formation, Utah, USA. *Sed. Geology*, **311**, 1–16.

Slingerland, R. and **Smith, N.D.** (1998) Necessary conditions for a meandering-river avulsion. *Geology*, **26**, 435–438.

Slingerland, R. and **Smith, N.D.** (2004) River avulsions and their deposits. *Ann. Rev. Earth Planet. Sci.*, **32**, 257–285.

Smith, C.E. (1998) Modeling high sinuosity meanders in a small flume. *Geomorphology*, **25**, 19–30.

Smith D.G. (1988) Modern point bar deposits analogous to the Athabasca oil sands, Alberta, Canada. In: *Tide-influenced sedimentary environments and facies* (Eds P.L. deBoer, A. VanGelder and S.D. Nio), D Reidel Publishing Company, 417–432 (530p).

Smith, D.G., **Hubbard, S.M.**, **Lavigne, J.**, **Leckie, D.A.** and **Fustic, M.** (2011) Stratigraphy of counter-point-bar and eddy-accretion deposits in low-energy meander belts of the peace-Athabasca Delta, Northeast Alberta, Canada. In: *From River to Rock Record: The Preservation of Fluvial Sediments and Their Subsequent Interpretation* (Eds S.K. Davidson, S. Leleu and C.P. North), *SEPM Spec. Publ.*, **97**, 143–152.

Smith, D.G., **Hubbard, S.M.**, **Leckie, D.** and **Fustic, M.** (2009) Counter point bars in modern meandering rivers: recognition of morphology, lithofacies and reservoir significance, examples from Peace River, AB, Canada. *Sedimentology*, **56**, 1655–1669.

Smith, N.D., **Cross, T.A.**, **Dufficy, J.P.** and **Clough, S.R.** (1989) Anatomy of an avulsion. *Sedimentology*, **36**, 1–23.

Sundborg, Å. (1956). The river Klarälven a study of fluvial processes. *Geogr. Ann.*, **38**, 125–316.

Tal, M. and **Paola, C.** (2007) Dynamic single-thread channels maintained by the interaction of flow and vegetation. *Geology*, **35**, 347–350.

Tal, M. and **Paola, C.** (2010) Effects of vegetation on channel morphodynamics: results and insights from laboratory experiments. *Earth Surf. Proc.*, **35**, 1014–1028.

Taylor, G. and **Woodyer, K.D.** (1978) Bank deposition in suspended-load streams. In: *Fluvial Sedimentology* (Ed. A.D. Miall). *Can. Soc. Petrol. Geol. Mem.*, **5**, 257–275.

Thomas, R.G., **Smith, D.G.**, **Wood, J.M.**, **Visser, J.**, **Calverley-Range, E.A.** and **Koster, E.H.** (1987) Inclined heterolithic stratification and terminology, description, interpretation and significance. *Sed. Geol.*, **53**, 123–179.

Thomson, J. (1876) On the windings for rivers in alluvial plains, with remarks on the flow of water round bends in pipes. *Proc. Roy. Soc. London*, **25**, 5–8.

Toonen, W.H., **Kleinhans, M.G.** and **Cohen, K.M.** (2012) Sedimentary architecture of abandoned channel fills. *Earth Surf. Proc. Land.*, **37**, 459–472.

Tower, W.S. (1904) The Development of Cut-Off Meanders. *Bull. Am. Geogr. Soc.*, **36**, 589–599.

van de Lageweg, W.I., **Van Dijk, W.M.**, **Baar, A.W.**, **Rutten, J.** and **Kleinhans, M.G.** (2014) Bank pull or bar push: what drives scroll-bar formation in meandering rivers? *Geology*, **42**, 319–322.

van de Lageweg, W.I., **Dijk, W.M.** and **Kleinhans, M.G.** (2013) Channel belt architecture formed by a meandering river. *Sedimentology*, **60**, 840–859.

van de Lageweg, W.I., **Schuurman, F.**, **Cohen, K.M.**, **Dijk, W.M.**, **Shimizu, Y.** and **Kleinhans, M.G.** (2016) Preservation of meandering river channels in uniformly aggrading channel belts. *Sedimentology*, **63**, 586–608.

Van den Berg, J.H., **Boersma, J.R.** and **Van Gelder, A.** (2007) Diagnostic sedimentary structures of the fluvial–tidal transition zone. Evidence from deposits of the Rhine Delta. *Neth. J. Geosci.*, **86**, 253–272.

van Dijk, W.M., **Lageweg, W.I.** and **Kleinhans, M.G.** (2012) Experimental meandering river with chute cutoffs. *J. Geophys. Res.: Earth Surf.*, **117**(F3).

van Dijk, W.M., **Lageweg, W.I.** and **Kleinhans M.G.** (2013b) Formation of a cohesive floodplain in a dynamic experimental meandering river. *Earth Surf. Proc. Land.*, **38**, 1550–1565.

van Dijk, W.M., **Teske, R.**, **van de Lageweg, W.I.** and **Kleinhans, M.G.** (2013a) Effects of vegetation distribution on experimental river channel dynamics. *Water Resour. Res.*, **49**, 7558–7574.

Willis, B.J. (1989) Palaeochannel reconstructions from point bar deposits: a three-dimensional perspective. *Sedimentology*, **36**, 757–766.

Willis, B.J. and **Tang, H.** (2011) Three-dimensional connectivity of point-bar deposits. *J. Sed. Res.*, **80**, 440–454.

Wormleaton, P.R., **Sellin, R.H.J.**, **Bryant, T.**, **Loveless, J.H.**, **Hey, R.D.** and **Catmur, S.E.** (2004) Flow structures in a two-stage channel with a mobile bed: *J. Hydraul. Res.*, **42**, 145–162.

Wright, M.D. (1959) The formation of cross-bedding by a meandering or braided stream. *J. Sed. Petrol.*, **29**, 610–615.

Wu, C., **Bhattacharya, J.P.** and **Ullah, M.S.** (2015) Paleohydrology and 3D facies architecture of ancient point bars, Ferron Sandstone, Notom Delta, south-central Utah, USA. *J. Sed. Res.*, **85**, 399–418.

Yan, N., **Mountney, N.P.**, **Colombera, L.** and **Dorrell, R.M.** (2017) A 3D forward stratigraphic model of fluvial meander-bend evolution for prediction of point-bar lithofacies architecture. *Comput. Geosci.*, **105**, 65–80.

Zinger, J.A., **Rhoads, B.L.** and **Best, J.L.** (2011) Extreme sediment pulses generated by bend cutoffs along a large meandering river. *Nature Geoscience*, **4**, 675.

Int. Assoc. Sedimentol. Spec. Publ (2018) **48**, 15–46.

Controls on the depositional architecture of fluvial point-bar elements in a coastal-plain succession

MICHELLE N. SHIERS[†‡], NIGEL P. MOUNTNEY[†], DAVID M. HODGSON[†] and LUCA COLOMBERA[†]

[†] *School of Earth and Environment, University of Leeds, Leeds, UK*
[‡] *CASP, West Bldg, Madingley Rise, Madingley Road, Cambridge, UK*

ABSTRACT

The architecture and lithofacies organisation of fluvial point-bar elements record the spatio-temporal evolution of river channels. This study discusses the factors that control facies distributions and geometries of point-bar elements present in a fluvial succession that accumulated on a low-gradient coastal plain on the western margin of the Western Interior Seaway (Campanian Neslen Formation, eastern Utah, USA). Forty outcropping point-bar elements located within an established sequence stratigraphic framework have been examined through facies, architectural and palaeocurrent analyses. Point-bar elements increase in width-to-thickness aspect ratio vertically through the succession. Four point-bar element types are identified based upon their lithofacies assemblages and geometry. Two point-bar types conform to those depicted in traditional facies models; they are dominated by cross-bedded sandstone, with subordinate amounts of ripple-laminated and horizontally laminated sandstone. In contrast, the other two point-bar types exhibit unusually low proportions of cross-bedded sandstone and higher proportions of massive sandstone, horizontally laminated sandstone and ripple-laminated sandstone. The occurrence of these atypical point-bar assemblages is restricted to the marine-influenced lower and middle parts of the Neslen Formation. An up-succession increase in aspect ratio and degree of amalgamation of point-bar elements through the Neslen Formation may reflect a decrease in the rate of accommodation generation, an increase in the rate of sediment supply, or autogenic processes that operated on an overall prograding coastal plain. The accumulation of point-bar elements with lower proportions of cross-bedded sandstone in the lower Neslen Formation can be attributed to decreased stream power. Database-assisted analysis has been undertaken to compare the lithofacies and architecture of point-bar elements from the Neslen Formation to those in other humid-climate, coastal-plain successions. This comparison reveals that the geometry and facies observed in point-bar elements of the Neslen Formation might record an unusual set of combined allogenic (accommodation generation and fluvial discharge variations) and autogenic (backwater processes and presence of peat mires) process interactions.

Keywords: Fluvial, point-bar, Neslen Formation, marine influence, backwater

INTRODUCTION

Studies of point-bar elements in both fluvial and tidal environments (e.g. Visher, 1965; Allen, 1965; 1983; 1991; McGowen & Garner, 1970; Harms *et al.*, 1975; Barwis, 1977; Jackson II, 1976; 1978; Miall, 1977; 1985; 1988; Nanson, 1980; Nanson & Page, 1983; Smith, 1987; Cloyd *et al.*, 1990; Nio & Yang, 1991; Rasanen *et al.*, 1995; Galloway & Hobday, 1996; Fenies & Faugères, 1998; Leeder, 1999; Ghazi & Mountney, 2009, 2011; Brekke & Couch, 2011; Johnson & Dashtgard, 2014) have identified associations of commonly occurring bodies with predictable lithofacies and geometric arrangements. Such facies and architectural relationships are commonly summarised as facies

Fluvial Meanders and Their Sedimentary Products in the Rock Record, First Edition.
Edited by Massimiliano Ghinassi, Luca Colombera, Nigel P. Mountney and Arnold Jan H. Reesink.

models (Fig. 1; e.g. Cant & Walker, 1978; Nanson, 1980; Walker, 1984; Miall, 1985; Thomas *et al.*, 1987; Miall, 1988; Ghazi & Mountney, 2009; Smith *et al.*, 2009; Colombera *et al.*, 2013; Labrecque *et al.*, 2011; Fustic *et al.*, 2012; Musial *et al.*, 2012). There is a documented variability in the lithofacies assemblage of point-bar elements with a wide range of width-to-thickness aspect ratios (cf. Gibling 2006; Colombera *et al.*, 2017); this means that no single facies model can account for the known range of stratigraphic complexity in fluvial point-bar deposits.

The evolution of point-bar elements is controlled by the interplay of allogenic and autogenic parameters (Hampson, 2016). From an applied standpoint, understanding controls on point-bar evolution is important to enhance understanding of the distribution of facies (Russell *et al.*, this volume), including the occurrence of inclined heterolithic stratification (IHS; Fig. 1B) within point-bar elements (Weimer *et al.*, 1982; Demowbray, 1983; Thomas *et al.*, 1987; Shanley *et al.* 1992; Turner & Eriksson, 1999; Choi *et al.*, 2004; 2011a; 2011b; Dalrymple & Choi, 2007; Hovikoski *et al.*, 2008; Brekke & Couch, 2011; Sisulak & Dashtgard, 2012; Johnson & Dashtgard, 2014). Inclined heterolithic stratification has been observed in many fluvial successions (e.g. Cretaceous McMurray Formation, Alberta, Canada, Jablonski *et al.*, 2012; Fairlight Clay and Ashdown Beds Formation, Stewart, 1983; Cretaceous Wessex Formation, UK, Stewart, 1983) and is commonly associated with tidal processes (e.g. Weimer *et al.*, 1982; Thomas *et al.*, 1987; Shanley *et al.*, 1992; Choi *et al.*, 2004; Dalrymple & Choi, 2007; Hovikoski *et al.*, 2008; Sisulak & Dashtgard, 2012; Johnson & Dashtgard, 2014; Yan *et al.*, 2017), or with secondary or counter currents, notably during the development of counter point bars in exclusively fluvial settings (e.g. Smith *et al.*, 2009). The proportion and distribution of heterogeneities within fluvial successions exerts a major control on hydrocarbon reservoir behaviour and on water flow and contaminant transport in groundwater aquifers. Fine-grained deposits may act as baffles or even barriers to fluid flow (mesoscopic heterogeneity: Tyler & Finley, 1991; Miall, 2013; Colombera *et al.*, 2017). Recently, database approaches have proved to be a valuable tool to compare heterogeneity distribution, point-bar element geometries and internal facies arrangements from many studied successions. The Fluvial Architecture Knowledge Transfer System (FAKTS) is one such relational database that describes the anatomy of fluvial successions including lithofacies proportions and geometries of fluvial deposits from a wide variety of successions (Colombera *et al.*, 2012a, b; 2013).

The aim of this study is to discuss the controls that give rise to a range of facies distributions within point-bar elements present in a fluvial succession that accumulated on a low-gradient and low-relief coastal plain. To achieve this aim, a detailed outcrop-based study of point-bar elements in the Campanian Neslen Formation, Utah, USA, has been undertaken. This approach permits integration of detailed sedimentological data of multiple point-bar elements distributed laterally and vertically through a succession for which an established sequence stratigraphic framework is well constrained. Specific objectives of this study are as follows: (i) to describe the typical facies arrangements of point-bar elements within the Neslen Formation; (ii) to establish the stratigraphic and spatial distribution of point-bar elements through the formation; (iii) to use a quantitative database approach to compare and contrast the architecture and facies distributions of point-bar elements in the Neslen Formation to both previously proposed facies models and to other comparable successions; and (iv) to develop an understanding of the controls on the internal lithofacies within point-bar elements, the external geometry of the elements and their vertical stacking and connectivity.

GEOLOGICAL SETTING

The Campanian Neslen Formation accumulated in a low-gradient (Colombera *et al.*, 2016), low-relief (Cole & Cumella, 2003), lower coastal plain setting on the western margins of the Cretaceous Western Interior Seaway (WIS; Fig. 2A). The seaway formed in a foreland basin that was infilled with a wedge of siliciclastic strata shed from the Sevier Orogenic Belt to the west (Armstrong, 1968; Jordan, 1981). The seaway was characterised by relatively shallow water depths along its length, rarely exceeding 100 m, and by low gradient margins (Kauffman 1977). The climatic regime of Utah during the Cretaceous was humid and subtropical (Fillmore, 2010) with potentially monsoonal conditions (Fricke *et al.*, 2010; Foreman *et al.*, 2015).

The sequence stratigraphic framework of the Neslen Formation has been established previously

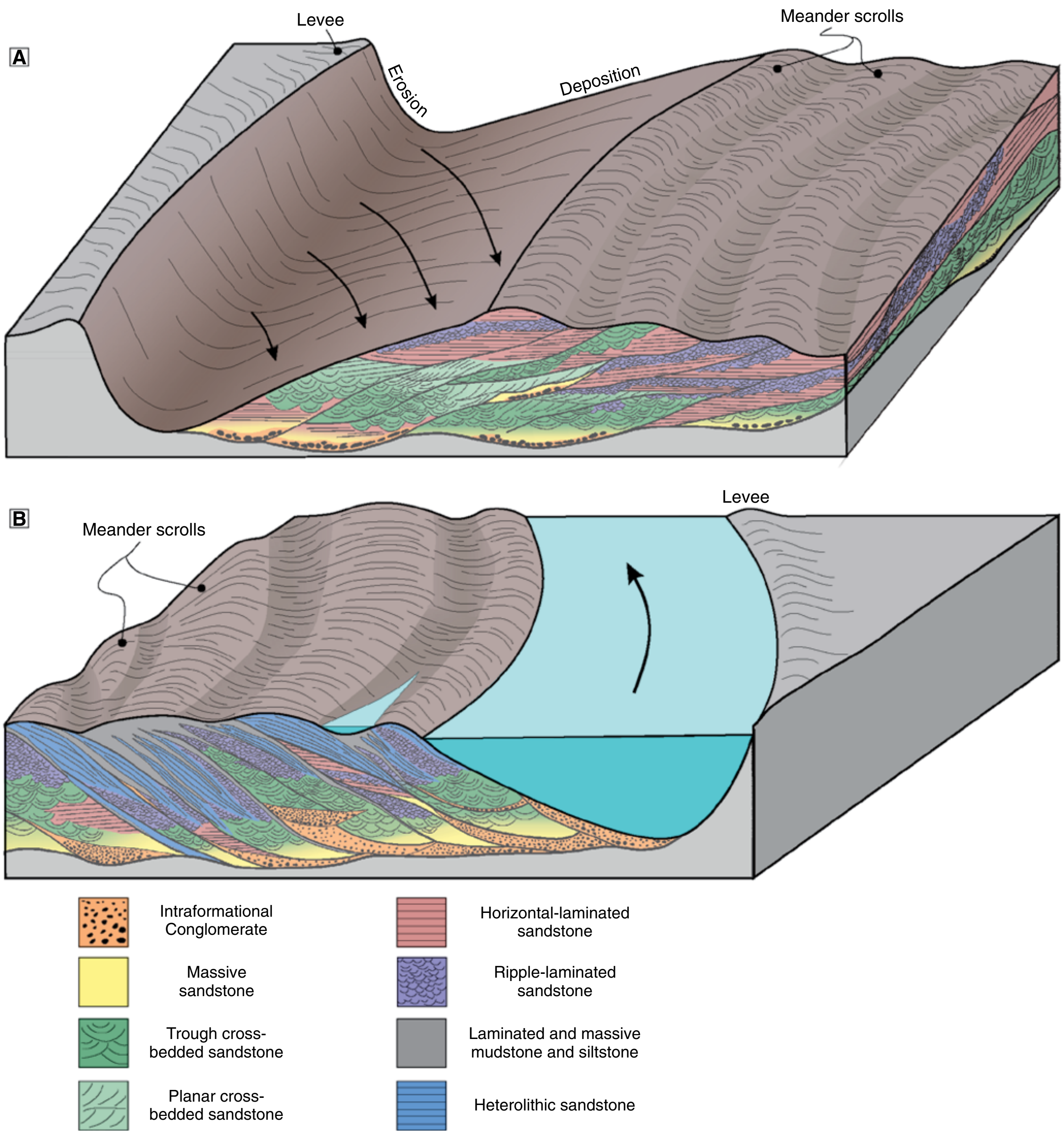

Fig. 1. Conceptual model of point-bar elements. (A) Three-dimensional depositional model of facies and architecture of a sandstone-dominated point-bar element (adapted after Allen, 1970; Cant & Walker, 1978; Nanson, 1980; Walker, 1984; Miall, 1985; Miall, 1988; Ghazi & Mountney, 2009; Colombera *et al.*, 2013). (B) Three-dimensional depositional model of facies and architecture of a heterolithic point-bar element (adapted in part from Thomas *et al.*, 1987; Smith *et al.*, 2009; Labrecque *et al.*, 2011; Fustic *et al.*, 2012; Musial *et al.*, 2012).

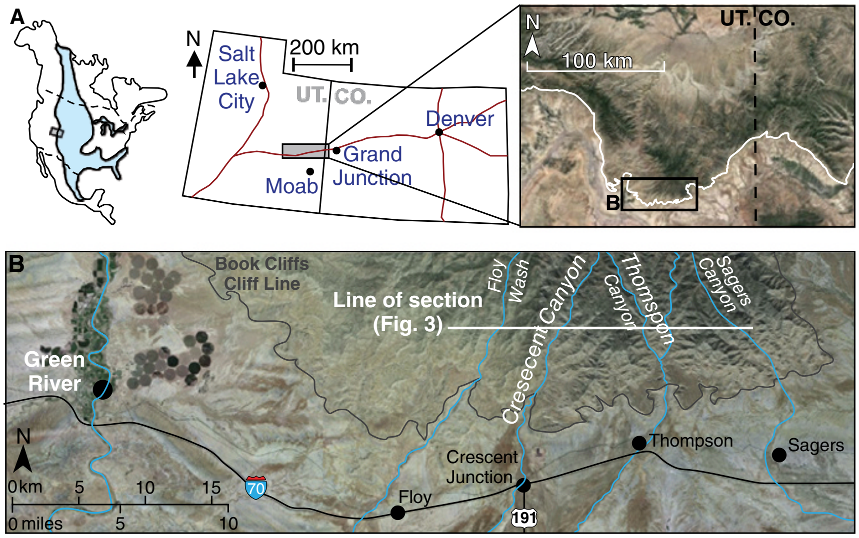

Fig. 2. Study location map. (A) Map of Western Interior Seaway (blue) with location of the study area in the Book Cliffs. (B) Location of the studied stratigraphy between Floy Canyon and Sagers Canyon. GoogleEarth ©. UT = Utah, CO = Colorado.

(Yoshida *et al.*, 1996; McLaurin & Steel, 2000; Hettinger & Kirschbaum, 2003; Shiers *et al.*, 2014; 2017; Fig. 3A). This framework has allowed each of the point-bar elements described here to be located within a specific systems tract, such that differences in point-bar internal facies distributions can be related to different accommodation settings (as described below).

The Neslen Formation comprises sandstones encased within argillaceous, commonly coal-bearing strata (Young, 1957; Fisher *et al.*, 1960; Willis, 2000; Cole, 2008; Colombera *et al.* 2016; Shiers *et al.*, 2014; 2017). The succession is interpreted as the accumulated sedimentary record of coastal delta-plain palaeoenvironments (Kirschbaum & Hettinger, 2004; Aschoff & Steel, 2011a; Shiers *et al.*, 2014; 2017). An overall westward transition from paralic to fluvial deposits across the coeval Neslen Formation and adjacent upper Castlegate Sandstone is associated with a lateral coarsening of lithologies toward the Sevier orogenic belt.

The lower Neslen Formation accumulated in brackish and fresh-water environments in a coastal-plain setting, which was characterised by various sub-environments including tidal flats, lagoons, bays, marshes and oyster reefs (Pitman *et al.* 1987; Chan & Pfaff, 1991; Shiers *et al.*, 2014; 2017) and is interpreted to represent a 4th order Transgressive Systems Tract (TST; Shiers *et al.*, 2017). Within the lower Neslen Formation, tidal and brackish-water influence is expressed by bioturbation and ichnospecies common to brackish water, single and double drapes of fine-grained sediment on sandstone ripple foresets, laminations that show evidence of rhythmicity and sedimentary indicators of current reversal including successive sets in which ripple foresets show opposing dip directions (Shiers *et al.*, 2017). The upper Neslen Formation accumulated in an upper coastal-plain and lower alluvial-plain setting that was characterised by meandering rivers that traversed extensive floodplains (Pitman *et al.*, 1987) as part of a Highstand Systems Tract (HST).

Some tabular sandstone bodies within the Neslen Formation (Fig. 3) are interpreted be formed of wave reworked sandstone as part of a backstepping barrier system (Shiers *et al.*, 2017) and provide important correlation datums within the succession. One example, the Thompson Canyon Sandstone Bed (TCSB) separates the lower and upper Neslen Formation (Shiers *et al.*, 2014; 2017). The base of the TCSB can be mapped for at least 45 km in an east-west oriented depositional dip direction (Gualtieri, 1991) and it shows a marked facies dislocation that is interpreted to define a Maximum Flooding Surface (MFS). The Basal Ballard Sandstone Bed (BBSB) is a similar example, with a continuity of at least 18 km (Shiers *et al.*, 2017).

Laterally extensive coal beds are also present in the Neslen Formation (Cole, 2008; Shiers *et al.*, 2014; 2017). In the study region, the tabular

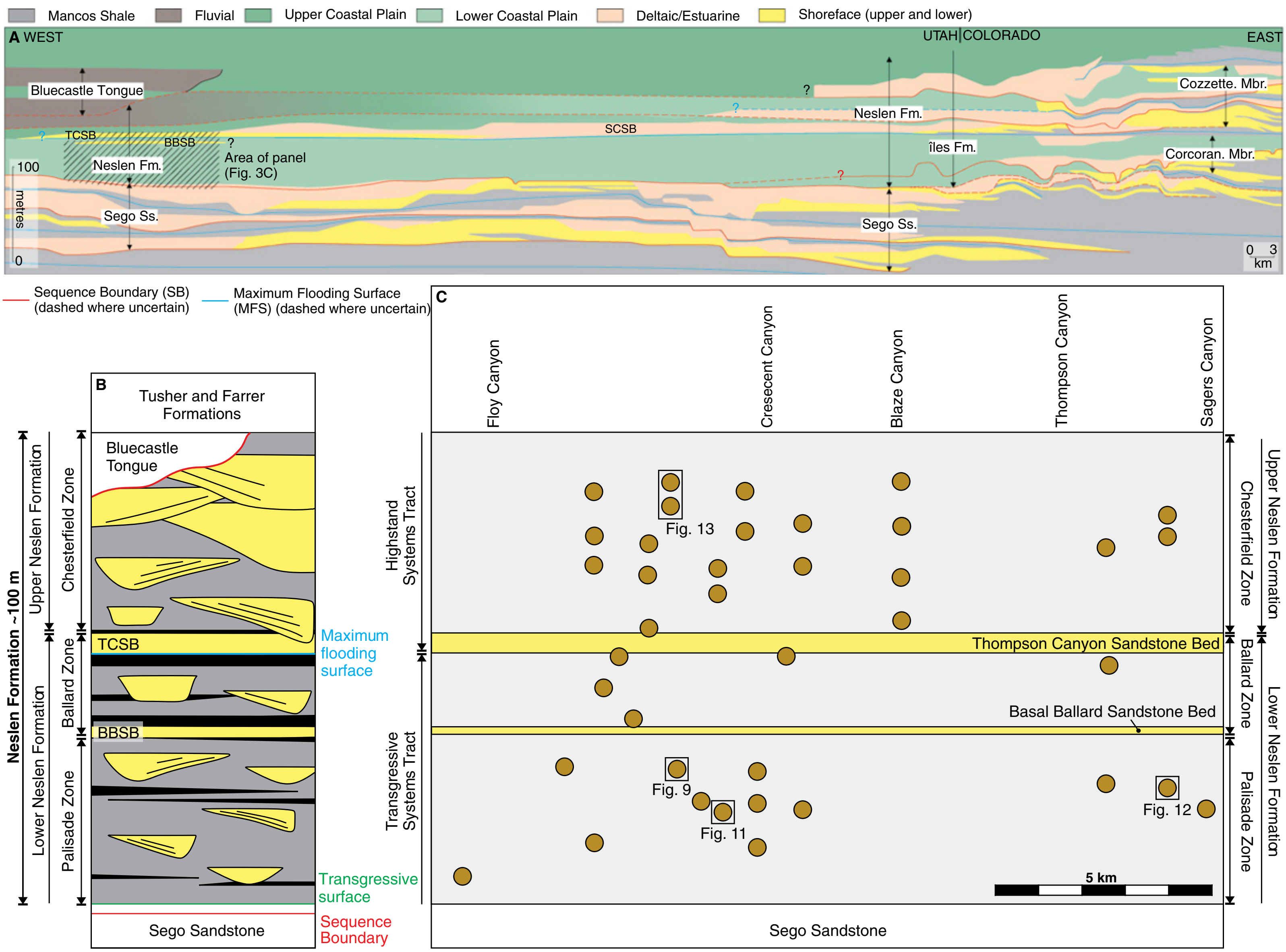

Fig. 3. (A) Stratigraphy of the upper Mesaverde Group in the Book Cliffs; study area is indicates (B) Simplified stratigraphy of the Neslen Formation (cf. Shiers *et al.*, 2014; 2017) and (C) the stratigraphic position of outcrops with studied point-bar elements. TCSB = Thompson Canyon Sandstone Bed. BBSB = Basal Ballard Sandstone Bed. SCSB = Sulphur Canyon Sandstone Bed. Part A based in part on Kirschbaum & Hettinger (2004).

sandstone bodies and the coal-bearing intervals collectively provide the basis for an informal subdivision of the Neslen Formation into 3 zones (Shiers *et al.*, 2014): from base to top, the Palisade Zone, the Ballard Zone and the Chesterfield Zone. The Palisade and Ballard Zones together make up the lower Neslen Formation, the Chesterfield Zone is the upper Neslen Formation (Fig. 3).

Three different types of channel-related element have been previously identified in the Neslen Formation: distributary-channel elements (or ribbon channel-fill elements) (Shiers *et al.*, 2014; 2017; Colombera *et al.*, 2016), sandstone-dominated point-bar elements, alternatively referred to as fluvial-channel sandstones (Willis, 2000; Kirschbaum & Hettinger, 2004; Cole, 2008; Shiers *et al.*, 2014; 2017; Colombera *et al.*, 2016), and heterolithic point-bar elements, alternatively referred to as inclined heterolithic strata or tidally influenced channel deposits (Willis, 2000; Kirschbaum & Hettinger, 2004; Shiers *et al.*, 2014; Olariu *et al.*, 2015; Colombera *et al.*, 2016). The point-bar elements are the focus of this study.

METHODS

Data have been collected from 40 ancient point-bar elements identified in the Neslen Formation, (Fig. 2). Point-bar elements were characterised at outcrop by their facies associations (Table 1), fining-upwards grain-size trends, occurrence of internal inclined surfaces and lenticular external geometry (Fig. 4), and by analysis of palaeocurrent indicators. These characteristics are used to interpret these sedimentary bodies as the product of meandering rivers, in accordance with previous interpretations for the Neslen Formation (Yoshida *et al.*, 1996; McLaurin & Steel, 2000; Hettinger & Kirschbaum, 2003; Willis, 2000; Kirschbaum & Hettinger, 2004; Cole, 2008; Shiers *et al.*, 2014; 2017; Burns *et al.*, 2017) and analogue deposits of modern meandering rivers. The lithological character of infill of fluvial channels by point-bar architectural elements is represented by 14 lithofacies (Fig. 5; Table 1). The facies are interpreted in terms of depositional or post-depositional processes.

Field study has focused on the identification and facies characterisation of sandbodies interpreted to have accumulated as point bars in response to the evolution of meandering fluvial channels. The stratigraphic position of studied point-bar elements was determined in relation to the top of the underlying Sego Sandstone, as well as their position relative to the marker beds (see also Colombera *et al.*, 2016).

The studied point-bar elements are distributed laterally and vertically throughout the studied interval of the Neslen Formation (Fig. 3): of the 16 located in the lower Neslen Formation, 13 are in the Palisade Zone and 3 are in the Ballard Zone (Fig. 3C). Of the 24 examples located in the upper Neslen Formation, 4 are in the lower Chesterfield Zone and 20 are in the upper Chesterfield Zone (Fig. 3C).

Measurements collected from the studied point-bar elements include the external geometry (length, width and thickness; cf. Colombera *et al.*, 2012b), internal lithofacies and bounding-surface orientations (Fig. 4). The relationship of point-bar elements to surrounding elements (e.g. the vertical and lateral relationship of point-bar elements with peat-mire and overbank elements; Table 1) was determined through the construction of measured architectural-element panels. Internal lithofacies distributions were described and logged in detail at one of more locations along the outcrops (the 40 studied elements were analysed using 65 measured logs in total with a cumulative measured section length of 400 m).

Trace fossils were ascribed to ichnological assemblages (Pemberton *et al.*, 1982; Bromley, 1996; Gingras *et al.*, 2012). Palaeocurrent readings (n = 1021) were determined from the dip direction of foresets of cross bedding and ripple lamination. The palaeocurrent database was augmented by the collection of 400 dip azimuths of bounding surfaces of lateral-accretion sets, from which bar-growth trajectories were determined. These data are displayed in rose diagrams which show both palaeocurrent and bar-growth trajectory indicators for individual point-bar elements. Note, however, that the rose diagrams do not express the spatial variability of palaeocurrents around the point bar, which is expected to arise due to the meandering nature of the formative river channels, for example in relation to potential secondary circulation. Channelised sandbodies in the upper Chesterfield Zone (Fig. 3) are highly amalgamated (Shiers *et al.*, 2014) and analysis of these bodies was restricted to single vertical logs and photographic stratigraphic panels because of the cliff-forming nature of the outcrop.

Table 1. Descriptions and interpretation of the facies observed in point-bar elements of the Neslen Formation.

Facies	Bed thickness (m)	Description	Interpretation
Massive mottled mudstone/ siltstone (Fsm)	0.01–0.10	Massive silt/mud, grey to black in colour, often with roots and bioturbation, wood fragments and coal clasts.	Low-energy deposits by suspension settling, probably in the distal parts of crevasse splays (Collinson *et al.*, 2006; Burns *et al.*, 2017).
Laminated mudstone/ siltstone (Fl)	0.01–0.50	Laminated and interbedded mudstone and siltstone, some ripples.	Overbank, abandoned-channel and/or waning-flood deposit
Massive-faintly laminated sandstone (Sm)	0.03–0.30	Fine-grained to medium-grained sandstone with lack of sedimentary structures, except occasional horizontal laminations. Bioturbation is commonly observed.	Deposits of sediment gravity flows or hyperconcentrated flows (Jones & Rust, 1983). Bioturbation may mask original sedimentary structures to produce a massive appearance.
Symmetrical ripple-laminated sandstone (Sw) Draped (Swd)	0.05–0.15	Observed on top surfaces and in cross section. Co-sets form thicknesses of decimetres to a few metres. Single and double drapes of mud are common, carbonaceous and detrital drapes are also observed.	Ripples formed as a product of either oscillatory flows or combined flows in a restricted marine environment, e.g. from waves (Collinson *et al.*, 2006). Double drapes, often rhythmic, indicate a tidal influence.
Current ripple-laminated sandstone (Sr) Draped (Srd)	0.03–0.40	Observed on top surfaces and in cross section. Co-sets form thicknesses of decimetres to a few metres. Single and double drapes of mud are common, carbonaceous and detrital drapes are also observed.	Ripples formed in fluvial channels or bars with a unidirectional current. Drapes indicate periods of reduced energy in the system, possibly due to tidal fluctuations (Shanley *et al.*, 1992).
Trough cross-stratified sandstone (St)	0.10–2.0	Very fine-grained to medium-grained sandstone, commonlyassociated with a lag and occasionally showing aligned intraformational clasts to cross-bedding sets. Commonly preserved stacked with reactivation surfaces.	Trough cross-bedding formed from migrating three-dimensional dunes under uni-directional currents in fluvial channels (Collinson *et al.*, 2006).
Planar cross-stratified sandstone (Sp)	0.15–0.90	Very fine-grained to medium-grained sandstone with flat upper and lower bounding surfaces and approximately parallel cross-bedding	Formed from migrating two-dimensional dunes under uni-directional currents in fluvial channels (Collinson *et al.*, 2006).
Horizontally bedded sandstone (Sh)	0.05–0.70	Interlaminated fine-grained to medium-grained sandstone.	Upper flow-regime plane bed conditions (Miall, 1992).
Low-angle cross-stratified sandstone (Sl)	0.20–0.60	Laminations within fine-grained to medium-grained sandstone dipping at < 15°.	Formed from sediment under unidirectional flow which is transitional to upper flow-regime within the fluvial environment (Bridge, 1993).
Deformed sandstone (Sd)	0.10–1.0	Soft-sediment deformation in fine-grained to medium-grained sandstone beds. The most common expression is convolute lamination.	Loading and rapid deposition on water-logged sediment (Allen, 1977).
Interbedded sandstone and siltstone (Si)	0.10–0.50	Horizontally laminated beds exhibiting an alternation of mm-thick laminae of sandstone and siltstone (often carbonaceous). Alternations show occasionally rhythmic alternations in thickness.	Formed due to alternating current energies in the upper flow regime; siltstone deposited under low flow energy, possibly due to tidal forcing (Shanley *et al.*, 1992).
Lenticular/wavy/flaser bedded sandstone (H)	0.05–0.50	Inter-laminated mud and sand arranged such that lenses of sand and mud can be preserved as lenticular, wavy, or flaser bedding.	Unidirectional currents producing ripples, which were draped in mud at slackwater due to fluctuations in flow energy, possibly of tidal origin (Reineck & Wunderlich, 1968; Shanley *et al.*, 1992).
Intraformational conglomerate	0.05–0.30	Gravel-sized clasts generally a few centimetres in diameter, commonly occur in lags at the base of channels, lining scour surfaces or aligned to cross-bed surfaces. Clasts can occur in the form of mud-chip conglomerate or are composed of sideritised mudstone or sandstone.	Channel lags or scour fills of sediment which was reworked from nearby floodplain deposits (Bridge, 1993).

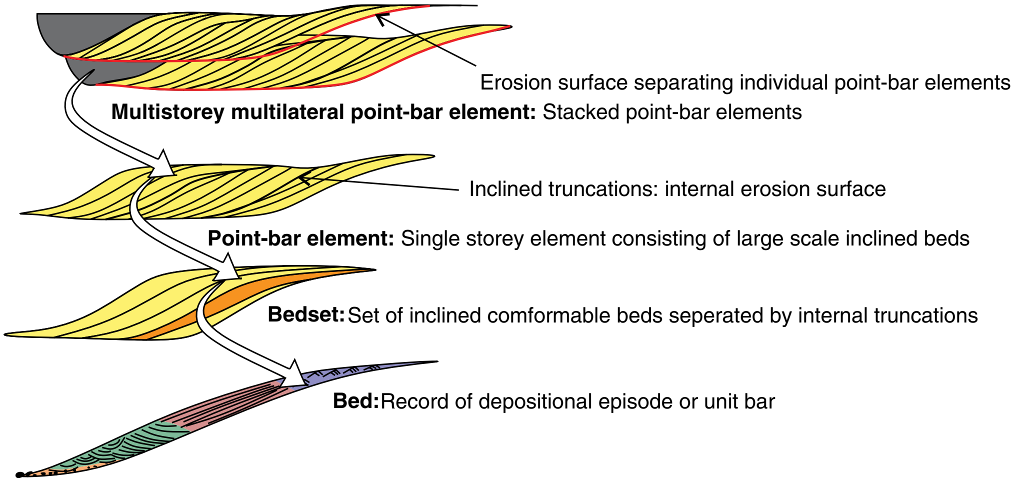

Fig. 4. Descriptive terminology for point-bar elements (cf. Bridge 1993); facies colours correspond to Fig. 6.

Quantitative analysis

The lithofacies and geometries for each studied point-bar element were quantified by coding collated data using the Fluvial Architecture Knowledge Transfer System (FAKTS; Colombera *et al.*, 2012a, b; 2013). Bespoke database queries allow analysis of facies characteristics and point-bar dimensions. Calculation of facies proportions within point-bar elements are recorded as a fraction of the logged sections within point-bar elements (Fig. 6), where the base and top of the element is well defined. Within sand-rich point-bar elements, lithological heterogeneity is defined as the thickness proportion of fine-grained lithofacies (silt and finer) relative to the total logged thickness. Point-bar elements with less than 10% fine material (mudstone and siltstone) are defined as being low heterogeneity; moderate-heterogeneity elements have 10 to 20% mudstone and siltstone; high-heterogeneity elements have > 20% mudstone and siltstone (Fig. 6A). Statistical techniques (ANOVA) are used to analyse the statistical significance of observed facies and geometry variations.

The aspect ratio of point-bar elements is calculated as a ratio between the minimum known width of the bar (measured at outcrop) and the maximum logged thickness (Fig. 6C). The true cross-stream width of the element was inferred where possible from 3D reconstructions through multiple exposures along spurs and re-entrants in the hillsides. An apparent width is defined where an outcrop lacked sufficient palaeocurrent indicators to establish the true width (cf. Geehan & Underwood, 1993).

Coding of studied examples within the FAKTS database facilitates quantitative comparison of similarities and differences between individual point-bar elements and has enabled the construction of quantitative facies models (cf. Colombera *et al.*, 2013). Moreover, the FAKTS database has additionally enabled point-bar elements from different systems to be compared to those studied in the Neslen Formation, as presented in the Discussion.

Dimensions of point-bar elements were used to extrapolate channel depth and estimates of fluvial discharge. Point-bar thickness measured at the outcrop is used as a proxy for the maximum bankfull channel depth. There is uncertainty using this method because any inference of maximum bankfull depth derived from bar thickness is a local estimate, due to changes in the geometry of a channel around a bend, from pool to riffle, and as the river sinuosity increases during channel migration (Willis & Tang, 2010).

RESULTS

Comparison of the average internal facies proportions and width-to-thickness aspect ratio of point-bar elements within the Neslen Formation (Figs 7 and 8) to other systems with similar climatic regimes and/or environmental settings analysed using FAKTS (Colombera *et al.*, 2012a; 2012b; 2013) exhibits overall similarity. However, our quantitative investigation allows us to separate the observed elements into four types based on their facies proportions and aspect ratio (Table 2).

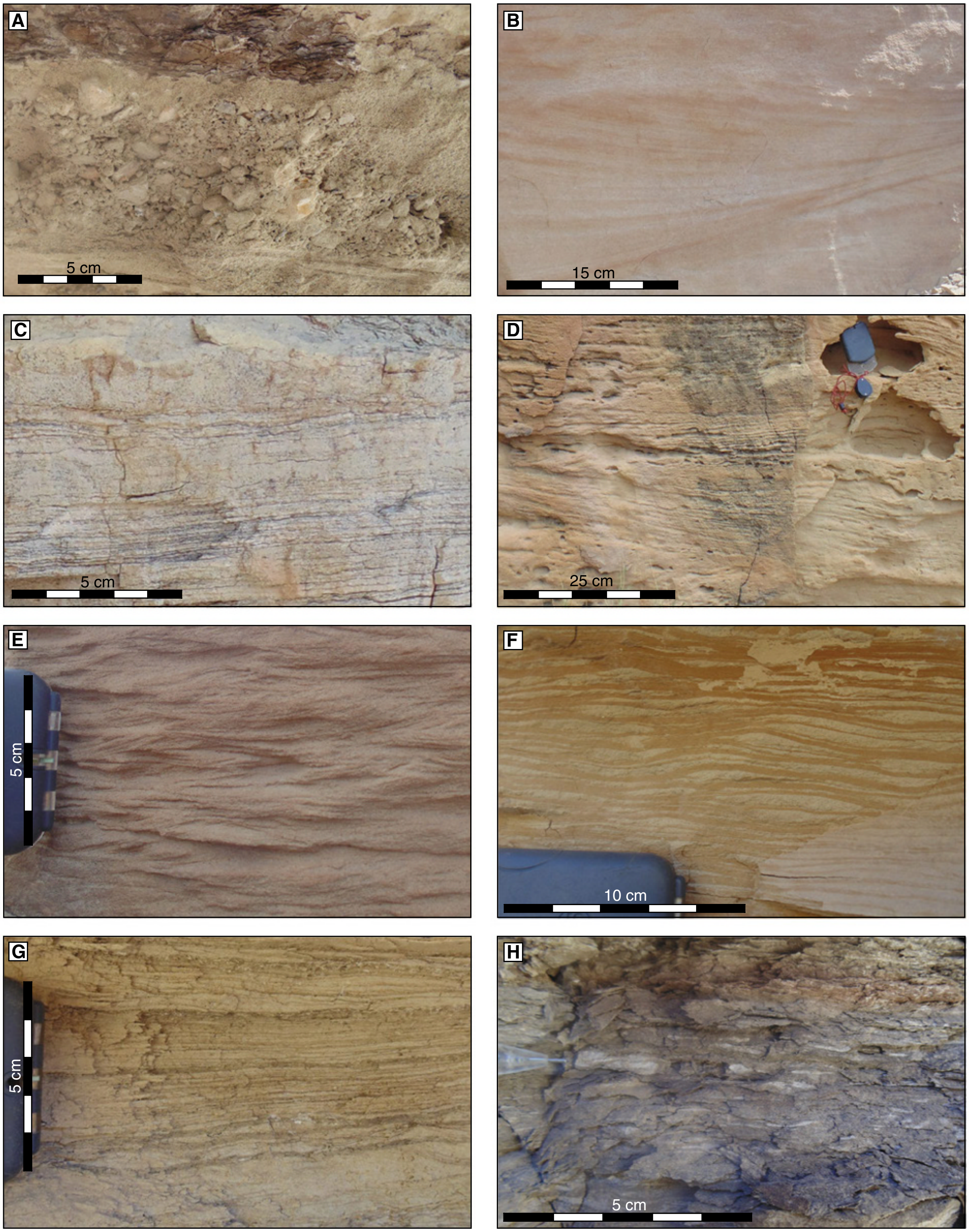

Fig. 5. Representative photographs of sedimentary facies observed within point-bar elements of the Neslen Formation. (A) Intraformational conglomerate (Gh) found at the base of elements and on erosional surfaces. (B) Trough cross-bedded sandstone (Sx). (C) Horizontally laminated sandstone (Sh). (D) Low-angle laminated sandstone (Sl). (E) Ripple cross-laminated sandstone (Sa). (F) Lenticular and wavy sandstone with intervening siltstone laminations (H). (G) Horizontally interbedded sandstone and siltstone (Si). H) Massive (Fsm) and laminated (Fl) mudstone and siltstone.

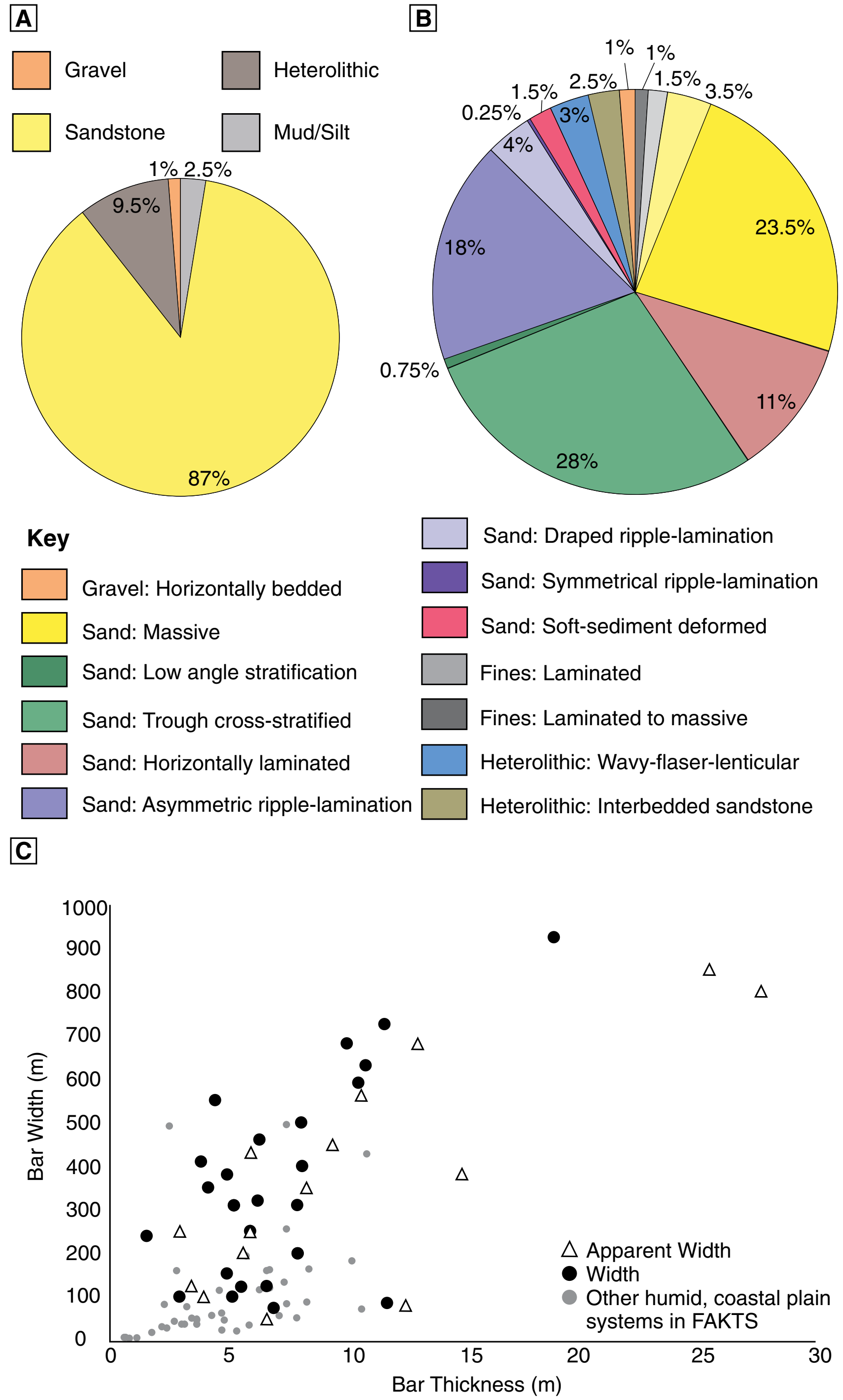

Fig. 6. Quantitative analysis of facies of point-bar elements of the Neslen Formation carried out using the FAKTS database. (A) Lithology of all studied point-bar elements in the Neslen Formation. (B) Facies proportions of all studied point-bar elements within the Neslen Formation. (C) Graph showing aspect ratio of all studied point-bar elements in the Neslen Formation in comparison to other bars analysed in the FAKTS database interpreted to have been deposited in successions accumulated in humid-climate and/or lower coastal-plain settings.

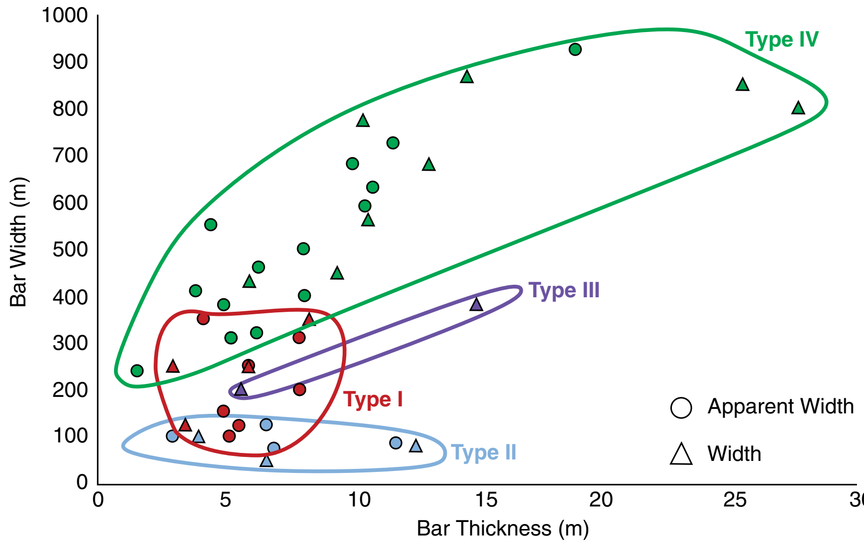

Fig. 7. Graph showing the aspect ratio of the different point-bar element types in the Neslen Formation.

Type I

Description

Type I point-bar elements (Table 2; Fig. 9) are characterised by high proportions of well-sorted ripple-laminated sandstone, mud, silt and carbonaceous draped ripple-laminated sandstone (17.6 to 68%; Fig. 9D). No cross-bedding is observed (Fig. 8). Thirteen elements of this type are identified. Elements are 3 to 12 m-thick and exhibit a wide range of width-to-thickness ratios (between 1:10 and 1:83; Table 2; Fig. 7). The proportion of horizontally laminated sandstone in these types of elements is 8 to 24%. The dip of point-bar accretion surfaces is 10 to 20°. Heterogeneity within this type of element is generally low (0 to 3.6%); two instances of higher heterogeneity also occur (16.7%, 17.6%).

Commonly, the lowermost 0.5 m of the fill exhibits wood fragments and intraformational conglomerate (Gh) within massive, fine-grained and medium-grained sandstone. *Teredolites* and *Thalassinoides* are observed in channel-lag deposits at the base of the elements. Ripples are dominantly asymmetrical (Fig. 5E) and are commonly draped by mud, silt or carbonaceous material; both single and double drapes are observed. Vertically, the changes in facies are subtle; ripple lamination gives way upwards to draped ripple lamination and heterolithic deposits of wavy and flaser bedding (H) and then interbedded siltstone and sandstone laminae (Si) with thin beds of massive and horizontally laminated sandstone (Fig. 9B). The facies proportions and their vertical and lateral transitions can be collated to produce a semi-quantitative depositional model for type I point-bar elements (Fig. 10A). There is a high angle between the palaeoflow direction indicated by ripple cross-laminae dip directions and the accretion direction of the bar-form elements demonstrated by the dip azimuth of inclined bar surfaces (Fig. 9F).

Interpretation

The dominantly lateral direction of accretion within these point-bar elements is demonstrated by the palaeocurrents (Fig. 9F). Rippled sandstone is the product of deposition by migrating asymmetrical ripples (Collinson *et al.*, 2006) under waning traction flows (Simons *et al.*, 1960; Visher, 1965). Thick stacks of rippled sandstone such as that observed in this type of point-bar element can also be indicative of sharp hydrographic variations and rapidly waning floods (cf. Ielpi *et al.*, 2014). Abundant drapes on ripple fore-sets indicate rapid fluctuations in current velocity, possibly influenced by tides (Table 1). Double drapes are specifically diagnostic of tidally influenced environments (Shanley *et al.*, 1992).

Point-bar elements that exhibit a large proportion of ripple-laminated sandstone include those within the Clear Fork Formation (Simon & Gibling 2017a; b). Horizontal laminated sandstone (Sh; Table 1; Fig. 5C) with primary current lineation was deposited from traction flows on the upper

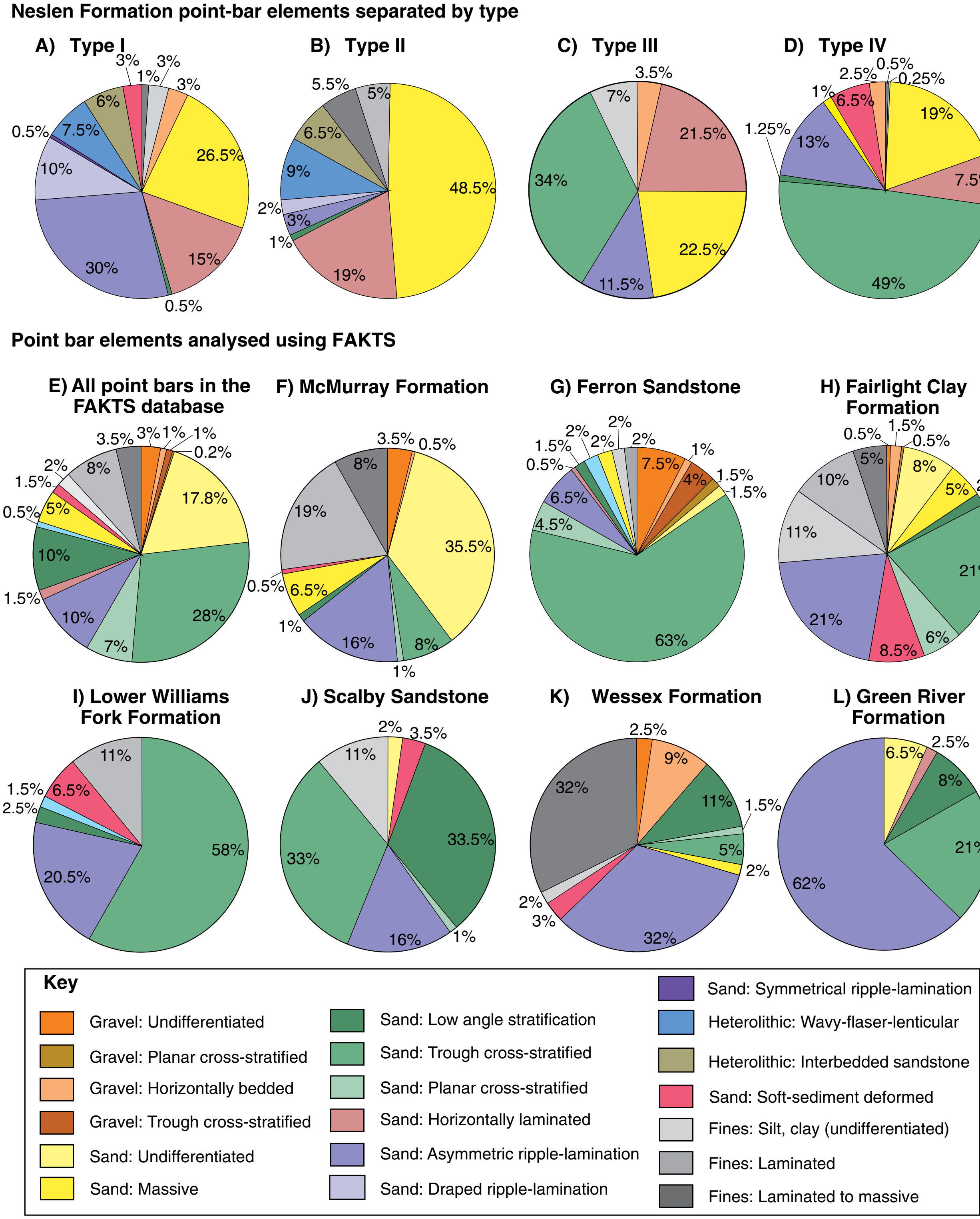

Fig. 8. Quantitative proportions of point-bar element facies within the Neslen Formation separated into interpreted types (A to D): (A) type I; (B) type II; (C) type III; (D) type IV. (E) Cumulative average constituent facies within all point-bar elements analysed in the FAKTS database B to H. Average facies proportions within point-bar elements for other modern and ancient successions (F to L) analysed using data present in the FAKTS database: (F) McMurray Formation facies proportions (Jablonski *et al.*, 2012); (G) Ferron Sandstone (Corbeanu *et al.*, 2004); (H) Fairlight Clay and Ashdown Beds Formation (Stewart, 1983); (I) Lower Williams Fork Formation (Pranter *et al.*, 2007); (J) Scalby Sandstone (Ielpi & Ghinassi, 2014), (K) Wessex Formation (Stewart, 1983); and (L) Green River Formation (Keighley *et al.*, 2003).

Table 2. Key variables for the interpretation of different point-bar element types within the Neslen Formation. Sm = massive sandstone, Sh = horizontally laminated sandstone, Sx = trough cross-bedded sandstone, Sa = asymmetrical laminated sandstone, H = heterolithic sandstone, Si = interbedded sandstone and siltstone, Gh = intraformational conglomerate. Te = *Teredolites*, Me = *Medousichnus*, Th = *Thalassinoides*, Ar = *Arenicolites*.

		Type I	Type II	Type III	Type IV
Number of elements		13	4	2	22
Thickness range (m) (average)		3–12.6 (6.4)	3.5–12.6 (5.8)	5.7–15 (10.35)	4–25 (10.6)
Aspect ratio range (average)		7–83 (36)	30–40 (20)	25–40 (30)	33–150 (71)
Lateral accretion angle (°)		10–20	5–10	10–15	<10
Heterogeneity range/% (average/%)		0–17.6 (7)	0.5–23.5 (10.5)	0.5–9 (4)	0–12.5 (0.75)
Average Facies proportions (%)	Sm	26.5	48.5	22.5	19
	Sh	15	19	21.5	7.5
	Sx	0.5	1	34	50.25
	Sa	40	5	11.5	13
	H	7.5	9	0	0
	Si	6	6.5	0	0
	Gh	3	0	3.5	2.5
Bioturbation		Ar, Te, Th throughout	Te and Th prevalent	Minor Te, Me at base	Minor Te at base of lowermost elements

flow-regime plane-beds. Finer-grained laminations (Si; Table 1) reflect minor energy fluctuations (Simons *et al.*, 1960; Visher, 1965; Fielding, 2006). Horizontally laminated sand deposits are characteristic of rivers subject to seasonal palaeoclimates and flashy discharge, (Fielding *et al.* 2006; Gulliford *et al.*, 2014; Plink-Björklund 2015). Horizontal lamination can also form in bar-top areas during waning river stage. Heterolithic facies (H) indicates deposition under fluctuating flow energies (potentially modulated by tidal influence). There is a balance between deposition of mud from suspension and sand deposition either from suspension or as saltating bedload via migrating unidirectional ripples (Miranda *et al.*, 2009). Strong seasonal differences in river discharge and flashy river floods would be anticipated for the study area during the Campanian, in connection with the inferred dominance of a tropical, monsoonal climate (Fricke *et al.*, 2010).

The occurrence of heterolithic facies and the presence of *Teredolites* and *Thalassinoides* trace fossils can be used to infer marine influence in these deposits (Bromley, 1996).

Type II

Description

Type II point-bar elements (Table 2; Fig. 11) are classified based upon the dominance of massive sandstone (30 to 68%; Fig. 11G) and the small proportion of ripple-laminated sandstone (<12%). Four examples of this element are identified; they are 3.5 to 12.6 m-thick and have width-to-thickness ratios of 1:30 to 1:40 (Table 2). The dip of point-bar accretion surfaces is 5 to 10°. Examples of this type of point-bar element have a high proportion of mudstone and siltstone present compared to sandstone (up to 23.5%; Fig. 11G), arranged in heterolithic packages (Fig. 11B and E). These elements have the highest proportion of preserved fines (Figs 8B and 11G).

The proportion of horizontally laminated sandstones (Sh; Table 1) varies from 6 to 32%. Sandstone beds in these elements thin upward, from 0.2 to 0.8 m-thick at the base to 0.05 to 0.5 m-thick in the upper parts of the elements; however, sandstone beds do not exhibit strong fining-upward trends (Fig. 11B). The thickness of fine-grained beds increases upwards. Towards the base of an element, fine-grained beds are mm-thick to cm-thick beds. In the upper parts of elements individual fine-grained beds are up to 0.5 m-thick. Interbedded sandstone and siltstone beds (Si) and heterolithic sandstones (H) commonly exhibit subtle rhythmicity of lamina thicknesses. Massive sandstone occurs in beds, commonly with scoured bases. Trace fossils such as *Teredolites* and *Thalassinoides* are present in the basal-most deposits of some examples (e.g. Fig. 11C) as mono-specific assemblages. The semi-quantitative depositional model for these types of point-bar element (Fig. 10B) reflects the vertical successions and facies proportions observed.

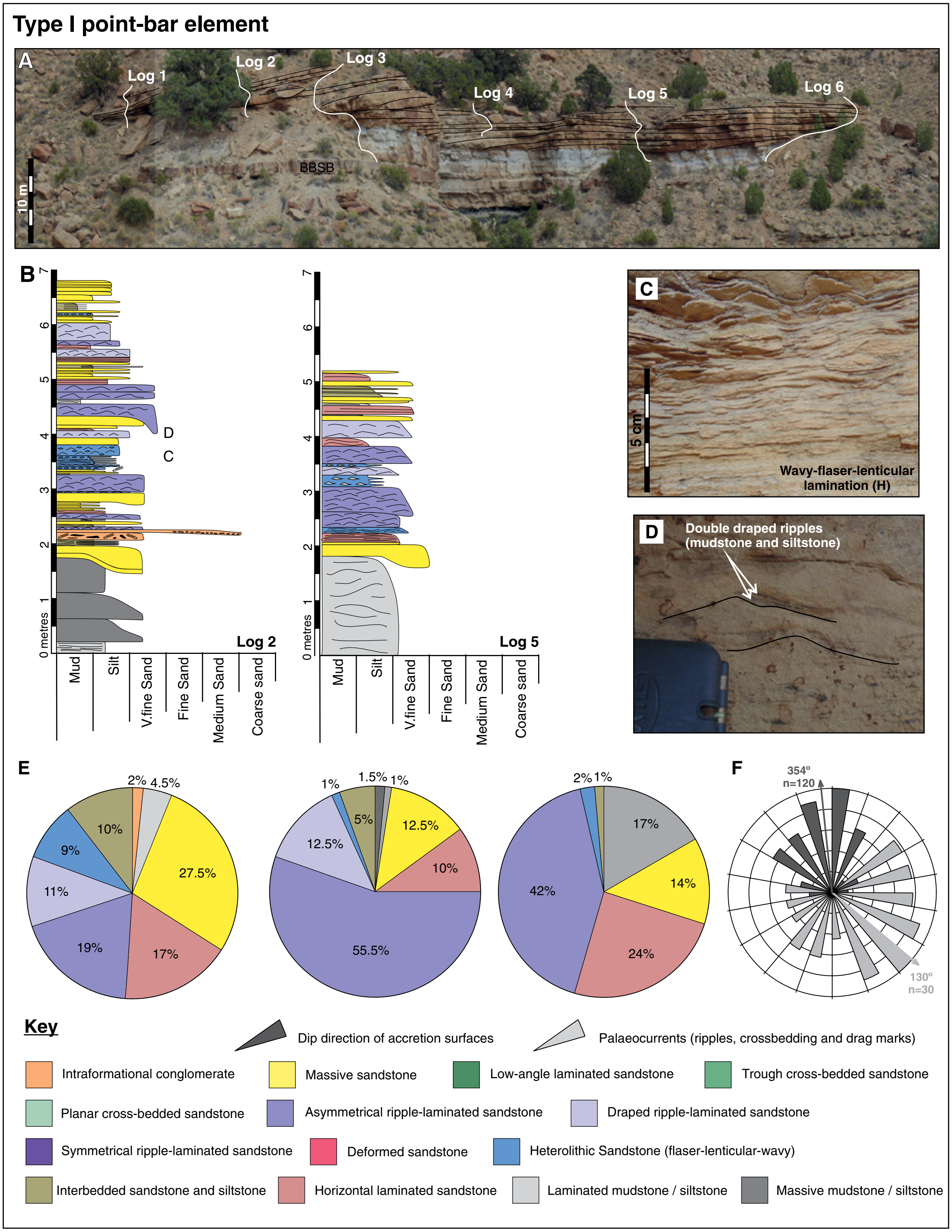

Fig. 9. Example of a type I point-bar element within the Neslen Formation. (A) Photograph panel of a representative type I point-bar element located at Crescent Canyon (Fig. 3); inclined surfaces dip at 10 to 15°. (B) Representative logged sections through the type I point-bar element in (A); location of logs are indicated. (C) Wavy-flaser-lenticular laminated sandstone (H), base shows horizontally interbedded sandstone and siltstone (Si). (D) Double draped ripple lamination. (E) Representative facies proportions within separate examples of type I point-bar elements. (F) Palaeocurrent data for the studied example shown in (A).

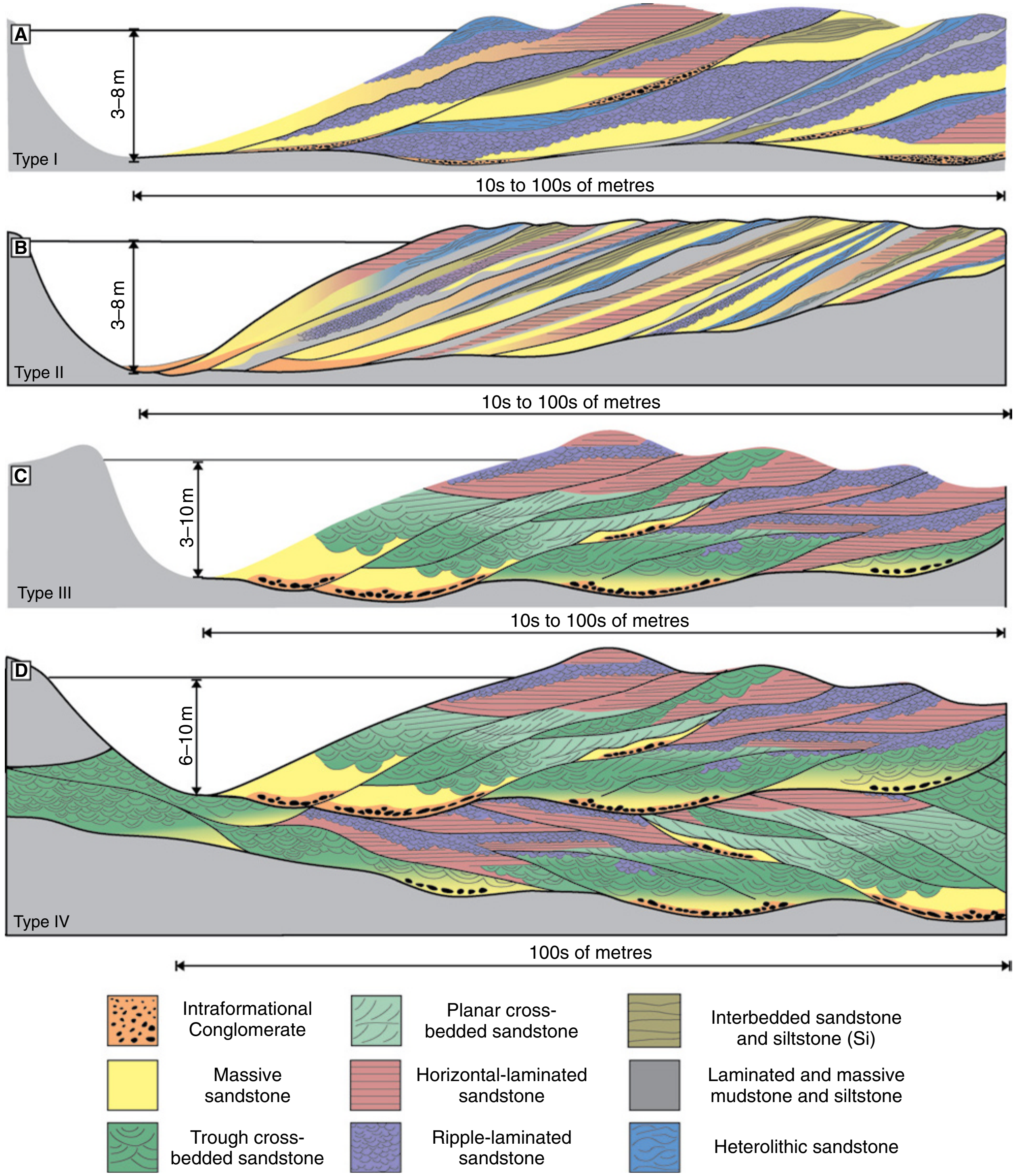

Fig. 10. Semi-quantitative depositional models for point-bar element types in the Neslen Formation; models are based upon accurate width-to-thickness ratios, facies proportions and observed vertical and spatial facies transitions: (A) type I; (B) type II; (C) type III; (D) type IV.

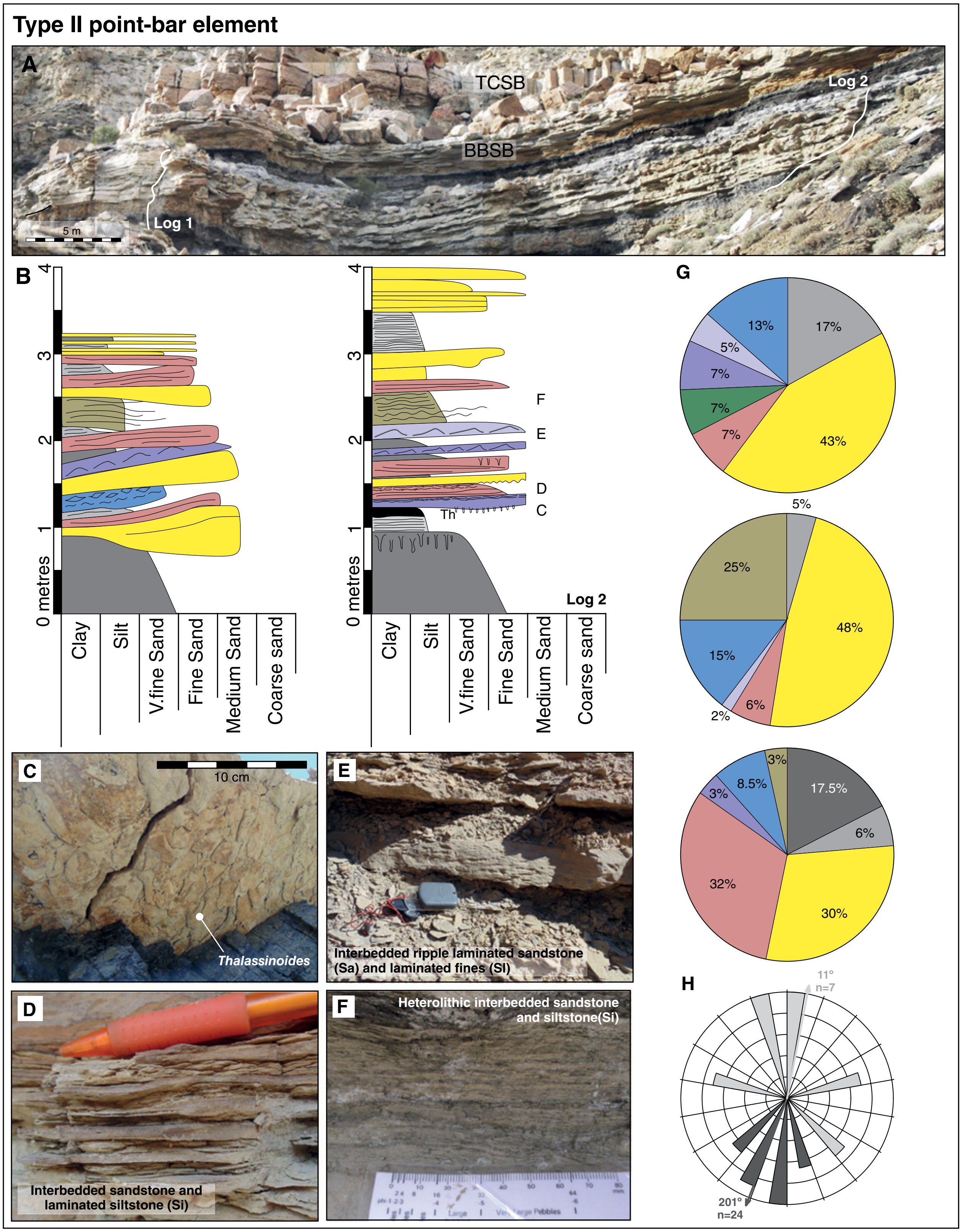

Fig. 11. Example of a type II point-bar element within the Neslen Formation. (A) Photograph panel of a type II point-bar element; inclined surfaces dip at 5 to 10° (Fig. 3) TCSB = Thompson Canyon Sandstone Bed, BBSB = Basal Ballard Sandstone Bed; location of logs are indicated. (B) Logged sections through type II point-bar element with alternating sandstone and siltstone beds. (C) Abundant Thalassinoides on the base of the point-bar element. (D) Horizontally laminated sandstone with interbedded siltstone (Sh and Si). (E) Ripple-laminated sandstone beds (Sa) with intervening laminated siltstones (Fl). (F) Pinstriped interbedded siltstone and sandstone (Si) within which sandstone laminae thicken upwards. (G) Constituent facies proportions for separate examples of type II point-bar elements. (H) Palaeocurrent data for the studied example shown in (A); there is a high angle between the azimuth of dip direction of accretion surfaces and that of ripple lamination indicating the dominance of lateral accretion. For key for facies colours refer to Fig. 9.

Interpretation

Similar to type I point-bar elements, these bodies are interpreted as laterally accreting point bars (Fig. 11H). The proportion of mudstone and siltstone, which occur alternating with sandstone beds in inclined packages within the elements, defines them as IHS. Although IHS is sometimes interpreted as the product of tidal influence (Shanley *et al.*, 1992; Dalrymple & Choi, 2007), such deposits can also occur in perennial and ephemeral fluvial systems (Thomas *et al.*, 1987; Lynds & Hajek, 2006; Archer, 1995; Kvale *et al.*, 1990; Kvale, 2011). Here, tidal influence is supported by the presence of mono-specific assemblages of trace fossils interpreted to reflect brackish or saline depositional environments (Bromley, 1996). Sedimentological evidence of tidal influence includes the presence of interbedded sandstone and siltstone (Si, H; Fig. 11D and E), repeating beds of which show subtle rhythmicity. The high proportion of massive sandstone (Sm; Figs 8B and 11) is interpreted to reflect rapid deposition of sediment with a narrow grain-size range, from concentrated flows, locally filling scours (Collinson *et al.*, 2006). Massive sandstone could also be the result of post-depositional modification through fluidisation, although no deformation structures commonly associated with fluidisation have been observed. Alternatively, intense burrowing could also result in a similar massive fabric. Low proportions of cross-bedding may be due to finer grain-size or a lower flow velocity than is required for sandstone to accumulate as dune-scale bedforms (Harms *et al.*, 1975).

The facies association of these bodies demonstrates that the sediment accumulated under fluctuating energy conditions, which may be due to marine influence.

Type III

Description

Type III point-bar elements (Table 2; Fig. 12) in the Neslen Formation are characterised by relatively high proportions of cross-bedded sandstone (over 30%) and low to medium heterogeneity (0.5 to 9% fines; Figs 8C and 12G). The two examples of this type have aspect ratios of 25 and 40, and element thicknesses of 5.7 m and 15 m. Beds have tangential geometries at the base, wedging out laterally over 3 to 5 m (Fig. 12A). The dip of point-bar accretion surfaces is 10 to 15°.

Beds thin and fine upwards from fine-grained and medium-grained sandstone at the base, to very fine-grained sandstone at the top (Fig. 10B). The basal deposits are gravel to pebble mud clasts (Figs 5A and 12B to C) and trace fossils (*Teredolites* and *Medousichnus*). Massive or cross-bedded sandstone beds (Sm/Sx) are common in the lowermost parts, with sets typically partitioned by erosion surfaces or multiple reactivation surfaces. Higher within the elements, cross-bedded sandstone dominates (Fig. 12B and D). The thickness of cross-bedded sandstone beds decreases upward (from ~ 0.5 m-thick beds towards the base to 0.2 m-thick in the upper parts of elements) and ripple laminated (Sr; Fig. 12B and E), massive (Sm) and horizontally laminated (Sh) sandstone facies become more common (Fig. 12G). These facies trends are shown in a semi-quantitative depositional model (Fig. 10C).

Interpretation

The high angle between the palaeoflow direction indicated by cross-laminae dip directions and the accretion direction in bar-form elements demonstrated by the azimuth of dipping bar surfaces supports a dominantly lateral direction of accretion (Fig. 12H; Bridge, 2006). Large proportions of trough cross-bedding (St; Fig. 5B) are interpreted as the record of deposition by migrating subaqueous dunes or unit bars (Table 1). Where cross-bedded sandstones exhibit multiple reactivation surfaces, they are interpreted as indicating variations in flow energy and/or direction, due to changes in river discharge or tidal processes (Shanley *et al.*, 1992). The presence of *Medousichnus* can indicate tidal influence (Howard & Frey, 1984; Gingras *et al.*, 2012) and *Teredolites* (bored wood) is typical of both marine and brackish environments. However, individual logs can be pushed (rafted) upstream within the fluvial-to-marine transition zone (Savrda, 1991). The proportion of trough and planar cross-bedded sandstone (26%) is similar to the amount preserved in all lateral-accretion elements recorded in the FAKTS database (35%; Fig.8E). The amount of ripple lamination in type III point-bar elements is 11% (Fig. 12D) and in all point-bar elements in the FAKTS database is 9% (Fig. 8E).

This element is interpreted as the preserved product of lateral accretion formed from fluvially dominated meandering channels that traversed the coastal plain (Kirschbaum & Hettinger, 2004; Aschoff & Steel, 2011b).

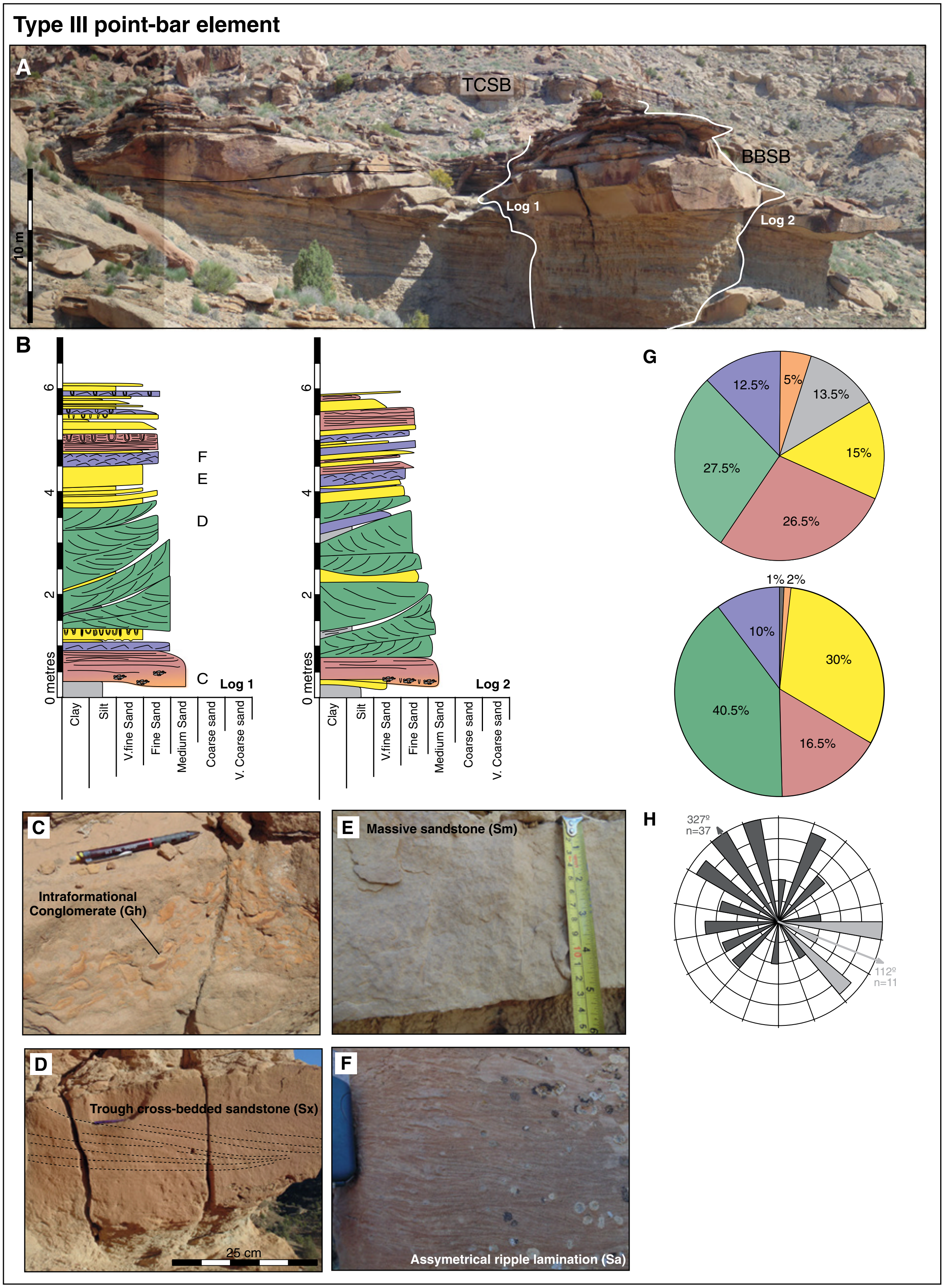

Fig. 12. Example of a type III point-bar element within the Neslen Formation. (A) Photograph panel of a point-bar element showing the sigmoidal shape of beds (Fig. 3), TCSB = Thompson Canyon Sandstone Bed; location of logs are indicated. (B) Logged sections through a type III point-bar element. (C) Photograph of intraformational conglomerate (Gh) found at the base of a type III point-bar element. (D) Trough cross-bedded sandstone (Sx). (E) Massive sandstone bed (Sm). (F) Asymmetrical ripple-laminated sandstone (Sa). (G) Constituent facies proportions for separate examples of type III point-bar elements. (H) Palaeocurrent data for the studied example shown in (A); there is a high angle between the azimuth of dip direction of accretion surfaces and that of ripple lamination indicating the dominance of lateral accretion. Key for facies colours refer to Fig. 9.

Type IV

Description

Type IV point bars (Table 2; Fig. 13) exhibit a high proportion of cross-bedded sandstone (49%). Twenty point-bars of this type are identified within the upper Chesterfield Zone. Elements are 4 to 25 m-thick (average: 10.2 m). The thickness of individual point-bar elements may be overestimated where the nature of the outcrop does not permit the identification of the thickest part of each individual point-bar element and possess high aspect ratios: 33 to 150 (average is 71; Fig. 7). Inclined accretion surfaces are less defined than in other point-bar types but where observed dip at moderate angles, up to 10° (Fig. 13A; Table 2). Where measurement has been possible, there is a high relative angle between lateral-accretion surfaces and the orientation of cross-bedding. Type IV elements generally have low heterogeneity; on average < 0.75%, with one example of 12.5% (Figs 8D and 13E; Table 2). Elements of this type are commonly vertically and laterally amalgamated, forming extensive sandstone belts (400 to 1000 m) in the upper Chesterfield Zone (Fig. 13; *sensu* Shiers *et al.*, 2014).

Erosion surfaces separating individual channel elements are commonly observed; with metre-scale relief and intraformational conglomerate preserved in the lowermost beds (Fig. 13B). Cross-bedded sandstone and massive sandstone dominates, passing upwards to ripple laminated and horizontally laminated sandstone (Fig. 13B); these relationships are shown in Fig. 10D. Bioturbation is not observed in these elements.

Interpretation

The facies assemblage within these bodies is similar to type III point-bar elements; however, they are distinguished by their thickness and aspect ratio (Table 2; Fig. 7), as well as the degree of amalgamation (Fig. 13A; Shiers *et al.*, 2014).

The high relative angle (80 to 150°) between the cross-bedding and lateral-accretion surfaces indicates a dominance of lateral accretion. The vertical succession of facies reflects lower velocity flows developing progressively through filling of the channel (Visher, 1965). The amalgamated nature of these point-bar elements is interpreted to reflect high energy channels eroding underlying floodplain and earlier channelised deposits (Leeder, 1977; Allen, 1978; Bridge & Leeder, 1979; Heller & Paola, 1996; Shiers *et al.*, 2014). The absence of marine indicators in these bodies might indicate deposition in a fully fluvial setting.

Distribution of point-bar element types

Type I point-bar elements are abundant throughout the Palisade, Ballard and lower Chesterfield zones. Type II elements are restricted to the Palisade Zone. Type III elements occur towards the middle of the formation (upper Palisade and lower Chesterfield zones). Type IV point bars occur exclusively within the upper Chesterfield Zone. The upward stratigraphic increase in width-to-thickness ratio of the point-bar elements (Fig. 14) means that the sandstone bodies are increasingly wide for a given thickness. Channel bodies become increasingly amalgamated upwards. The detailed analysis of the external geometry and internal facies character of each point-bar element type allows for the construction of semi-quantitative depositional models (Fig. 12).

The proportions of facies and the observed vertical transitions preserved in type III and IV point-bar elements (Figs 8C and D, 10, 12 and 13) are similar to many other point-bar elements that accumulated in humid subtropical settings, such as those of the Jurassic Scalby Formation (Nami & Leeder, 1977; Ielpi & Ghinassi, 2014; Fig. 8J) and the lower Williams Fork Formation (Pranter *et al.*, 2007; Fig. 8I). Type III and IV point-bar elements (Fig. 8C and D) have similar facies proportions to those elements analysed within the FAKTS database (Fig. 8E) and presented in published facies models (Fig. 1). The vertical transition of facies (Figs 12B and 13B) demonstrates that, as the point bar progressively developed, the preserved facies reflect vertically decreasing flow velocities on the inner bend of the migrating channel element.

Type I and II point-bar elements (Fig. 10A and B) are dissimilar to models presented in the literature (Fig. 1), as well as to the facies proportions of most successions analysed and stored in the FAKTS database (Fig. 8E). Examples exposed in the Wessex and Green River Formations (Fig. 8K, L; Keighley *et al.*, 2003; Stewart, 1983) also exhibit a dominance of ripple-laminated sandstone, although these elements also contain significant proportions of cross-bedded sandstone. Point-bar elements that are dominated by ripple strata are described by Miall (1985; his model 7) and are interpreted in that study as representative of

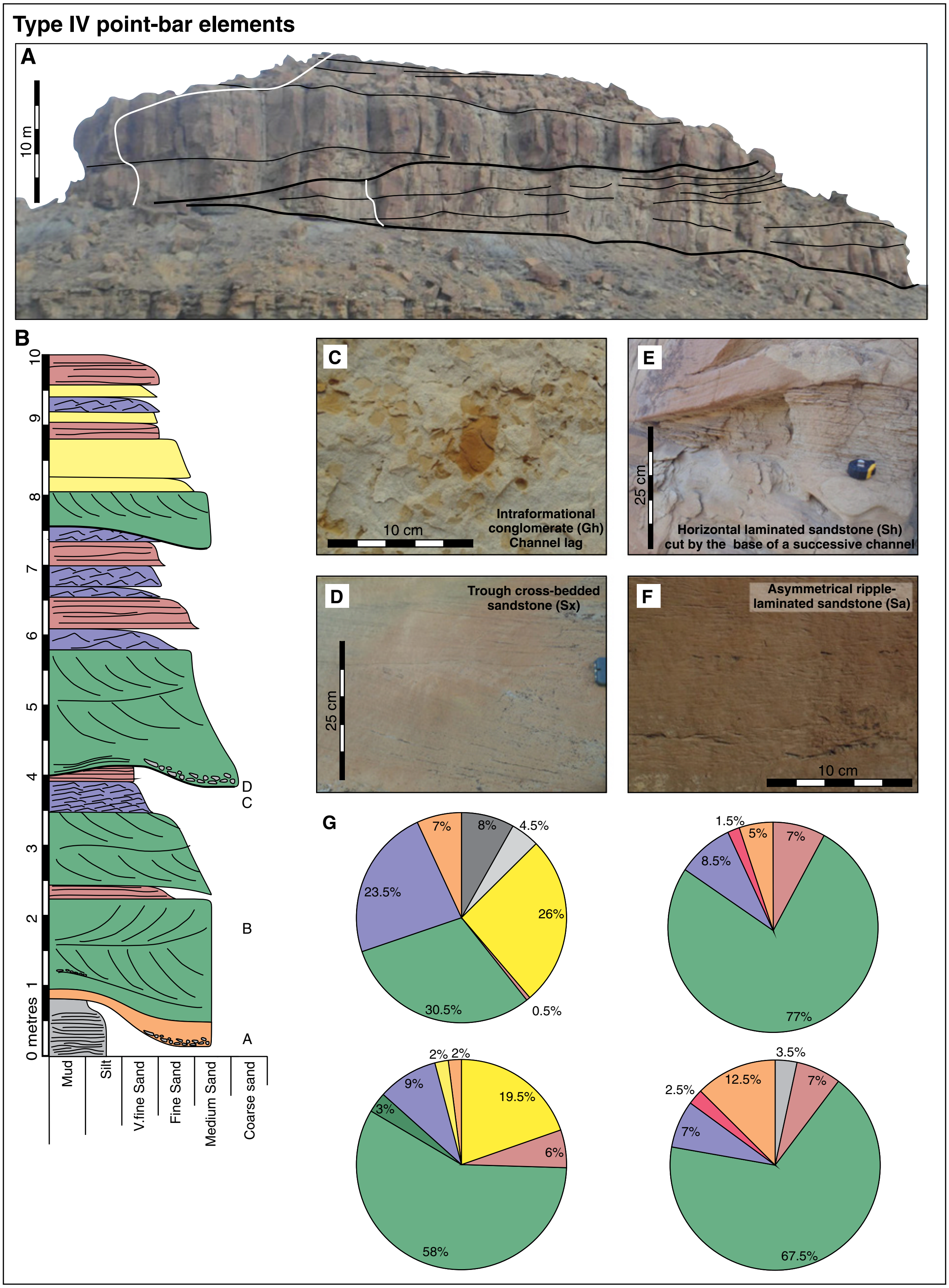

Fig. 13. Example of a type IV point-bar element within the Neslen Formation. (A) Photograph panel of representative type IV point-bar elements; thicker lines show the basal incision surface of individual point-bar elements (location shown in Fig. 3). (B) Representative logged section through typical type IV point-bar elements showing erosive surfaces at the base of each point-bar element and the vertical transition from cross-bedded to ripple laminated sandstone. (C) Intraformational conglomerate (Gh). (D) Trough cross-bedded sandstone (Sx). (E) Horizontally laminated sandstone (Sh) cut it into by an overlying point-bar element. (F) Asymmetrical ripple-laminated sandstone (Sa). (G) Representative facies proportions within separate examples of type IV point-bar elements. Key for facies colours refer to Fig. 9.

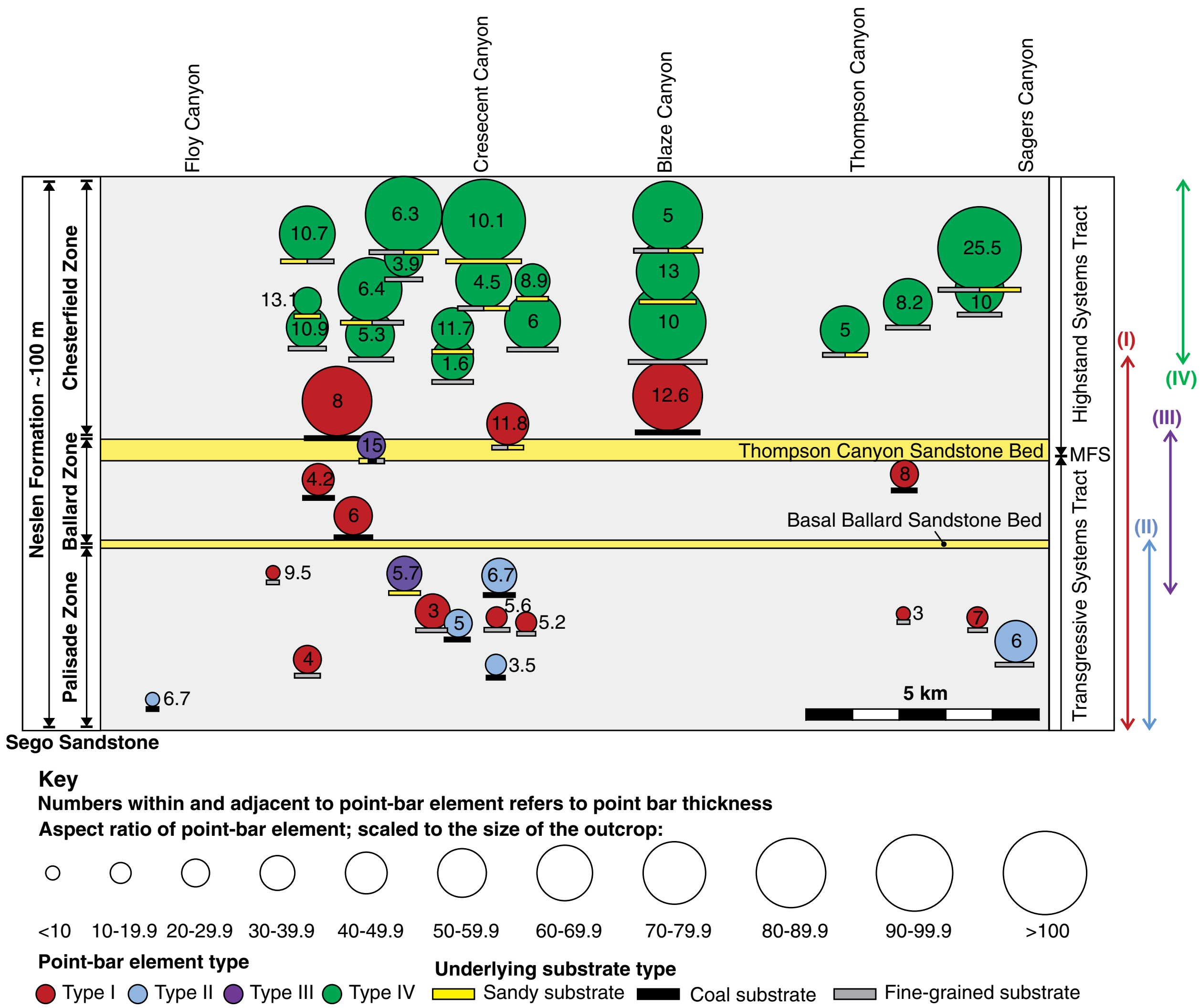

Fig. 14. Schematic panel showing the location of each point-bar element examined in this study in relation to the interpreted sequence stratigraphic framework. Each point-bar element is coloured to represent the point-bar element type (I, II, III or IV) and is shown in relation to underlying substrate, as well as scaled in proportion to the aspect ratio of the outcrop. Numbers within examples refer to the maximum logged thickness of the point-bar element in metres.

deposition from highly sinuous, suspended-load dominated rivers.

In the studied examples from the Neslen Formation, there is an increase in the amalgamation of sandstone bodies upwards. The aspect ratios of type I, II and III point-bar elements are similar to those of other point-bar elements in the FAKTS database (Fig. 7). The aspect ratio of type IV point-bar elements is higher than that of other systems. There is a statistically significant increase in the aspect ratio of point-bar elements from the lower to upper Neslen Formation with an abrupt increase across the TCSB (tested using ANOVA: significance level = 0.05, p value = 0.001). This is probably due to the highly amalgamated nature of these sandbodies and their development on a substrate with limited cohesion. Therefore, the thickness of individual point-bar elements might be overestimated where the nature of the outcrop does not permit the identification of the base of each individual point-bar element. This uncertainty has been minimised as far as possible through the careful combined use of stratigraphic panels and sedimentary logs.

DISCUSSION

The presented results are discussed in two ways: (i) in terms of the vertical changes of point-bar character (geometry, facies and amalgamation); and (ii) in terms of the occurrence of atypical point-bar assemblages in the lower Neslen Formation.

Tectonism, climate change and eustasy influence point-bar lithofacies (Cecil *et al.*, 1993; Blum & Törnqvist, 2000; Hampson *et al.*, 2012; Shiers *et al.*, 2014), geometry and stacking patterns (Leeder, 1977; Bridge & Leeder, 1979; Bristow & Best, 1993; Mackey & Bridge, 1995; Heller & Paola, 1996).

Controlling Factors in the Neslen Formation

Vertically through the Neslen Formation, there is a systematic change in point-bar element type (Fig. 14). The controls on the stacking and facies assemblage of the point-bar elements are varied, encompassing allogenic and autogenic processes, as discussed below. The possibility that a range of these controls are responsible for the point-bar character observed in the Neslen Formation is considered below and further examined in relation to other successions that have been analysed using the FAKTS database.

Accommodation generation rate

In the lower Neslen Formation, interpreted as a TST (Shiers *et al.*, 2017), point-bar elements are predominantly type I and II elements. In the upper Neslen Formation, interpreted as the highstand systems tract (HST), there is a change from type I elements to type IV elements upwards. This change in element type is concurrent with an increase in amalgamation of the sandstone bodies. These changes reflect the interplay of eustasy, tectonics, sediment supply and compaction, which collectively control the stacking of accumulated fluvial sandbodies (cf. Leeder, 1977; Allen, 1978; Bridge & Leeder, 1979; Aitken & Flint, 1995; Heller & Paola, 1996; Currie, 1997; Sønderholm & Tirsgaard, 1998; Huerta *et al.*, 2011; Foix *et al.*, 2013). During periods of increased accommodation generation, a high proportion of overbank material is preserved, and reworking of fluvial deposits is limited (Wright & Marriott, 1993; Legarreta & Uliana, 1998). Periods of low accommodation generation promote extensive reworking of fine-grained overbank material due to lateral channel migration or avulsion (Posamentier & Vail, 1988; Holbrook, 1996), increasing stacking density of channel elements, and hence net:gross and connectivity. Although changes in the rate of accommodation generation can explain the change in aspect ratio and amalgamation of point-bar elements upwards through the Neslen Formation (Shiers *et al.*, 2014) it is difficult to reconcile this interpretation with the change in facies observed within point-bar elements.

Marine influence

Element types II, I, III, and IV exhibit progressively less marine influence and are inferred to have been deposited farther from the contemporaneous shoreline (Fig. 15).

Point-bar elements in the lower Neslen Formation (mostly types I, II and III) show moderate marine influence (Lawton, 1986; Pitman *et al.*, 1987; Kirschbaum & Hettinger, 2004; Gualtieri, 1991; Karaman, 2012; O'Brien 2015; Gates & Scheetz, 2015; Burton *et al.*, 2016; Shiers *et al.*, 2017). The overall regressive trend of the Neslen Formation through time is recorded by a shift in facies belts eastward (Shiers *et al.*, 2017). The upper Neslen Formation is interpreted to represent an environment up-dip of any discernible influence of marine or backwater processes (Shiers *et al.*, 2014; Fig. 15). Channel fills that might bear a record of the influence of backwater hydrodynamics (cf. ribbon channel fills of Colombera *et al.*, 2016) are recognised in stratigraphic proximity to the maximum flooding surface (the base of the TCSB; Fig. 3B). The stratigraphic location of ribbon channel fills is coincident with the change from isolated (types I, II and III) to amalgamated point-bar elements (type IV) and may correlate with the change in hydrodynamics of the channels through and out of the backwater zone, i.e. the part of the fluvial system downstream of the point where the streambed elevation drops below contemporary sea-level (Fig. 15). A reduction in the rate of lateral migration of fluvial channels is expected in a down-dip direction (through the backwater zone towards the shoreline) due to backwater control on sediment flux (Lamb *et al.*, 2012; Nittrouer *et al.*, 2012; Blum *et al.*, 2013). The decrease in point-bar heterogeneity and increase in bar width-to-thickness ratio through the overall progradational stratigraphy of the Neslen Formation can therefore be interpreted in

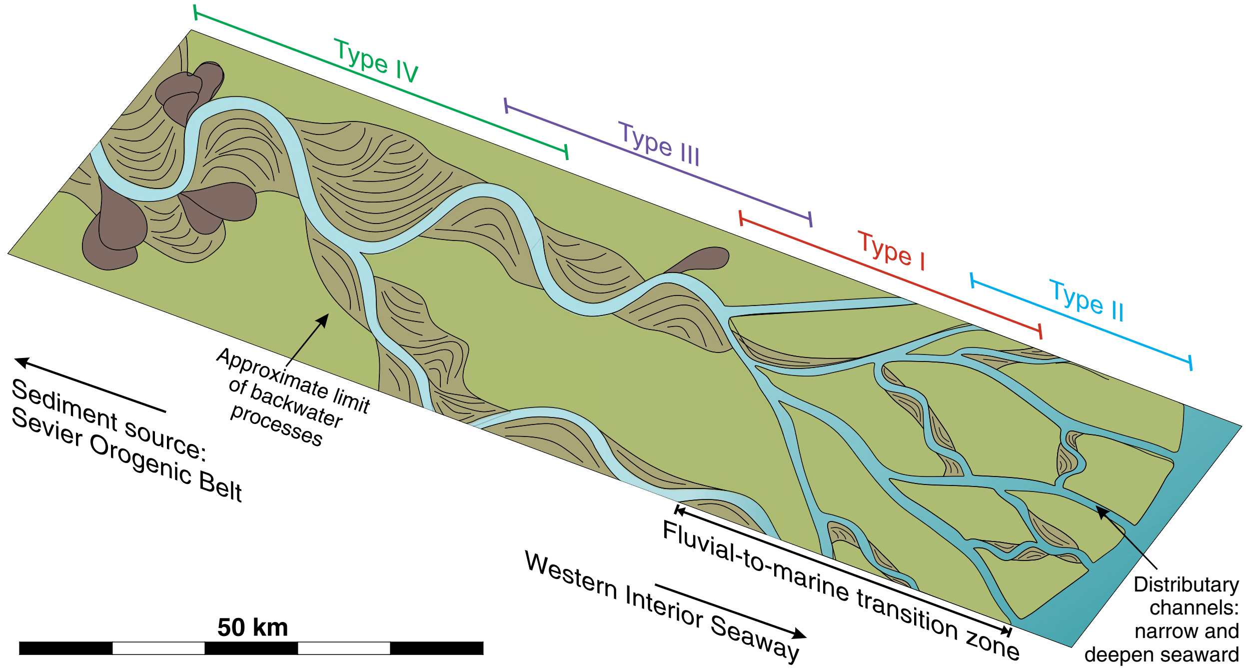

Fig. 15. Schematic diagram showing the possible spatial zones for deposition of the different type of point-bar elements with relation to the limit of marine influence (tidal and backwater processes).

terms of a progressive evolution of hydrodynamics and channel kinematics away from the shoreline, as recognised in some modern systems (cf. Blum *et al.*, 2013; Fernandes *et al.*, 2016).

The upstream end of the backwater zone is recognised as an area with increased avulsion frequency due to the change in hydrodynamics and its effect on streambed aggradation (cf. Chatanantavet *et al.*, 2012; Nittrouer *et al.*, 2012). Increased avulsion rate due to a shifting backwater zone is an autogenic explanation for the observed increase in point-bar amalgamation of type IV point-bar elements (Fig. 15). Alternatively, the change from dominantly type III to type IV point-bar elements in the upper Neslen Formation might be associated with a decrease in the rate of relative sea-level rise (or increase in sediment supply) from the TST to HST.

The influence of marine processes on facies assemblages within point-bar elements is well-documented (Weimer *et al.*, 1982; Thomas *et al.*, 1987; Shanley *et al.*, 1992; Choi *et al.*, 2004; Dalrymple & Choi, 2007; Hovikoski *et al.*, 2008; Sisulak & Dashtgard, 2012; Johnson & Dashtgard, 2014). Type I and II point-bar elements are interpreted to have been subject to marine influence. A greater marine influence is evident within type II point-bar elements. Type I and II elements also exhibit abundant trace fossils indicative of deposition in a stressed, brackish water environment (Table 2; Bromley, 1996; Gingras *et al.*, 2012).The relative position of the deposition of the different types of point-bar elements on the floodplain can therefore be established (Fig. 15). Minor evidence of brackish water ichnofacies at the base of type III point-bar elements indicates that they might have accumulated at a site closer to the palaeo-coastline than type IV point-bar elements, which themselves apparently accumulated up-dip of the zone of marine and backwater influence (Fig. 15). The vertical changes in occurrence of point-bar element types could have originated through shifting of these facies belts through time according to Walther's Law.

Presence of coal beds

There is a decrease in the occurrence and quality of coal beds up-section in the Neslen Formation (Fig. 3). Changes in coal beds and point-bar element type may be related to the same allogenic changes. Alternatively, peat abundance may have been a causative factor influencing point-bar element type.

Laterally extensive, ombrotrophic mires in the lower Neslen Formation (Shiers *et al.*, 2017) was facilitated by an overall increase in the rate of accommodation generation such that it was balanced by the accumulation rate of peat (see discussions in Speiker, 1949; Young, 1955; Bloom, 1964; Rampino & Sanders, 1981; Tissot & Welte, 1984; Courel, 1989). The rapid compaction of peat can also generate localised topographic lows following accumulation (Bohacs & Suter, 1997), for channels located within these topographic lows, channel avulsion frequency would be limited.

Point-bar elements underlain by coal (type I or II elements; Fig. 14) have low aspect ratios and are associated with narrower channels than those with sandstone, siltstone or mudstone substrates (Fig. 14). Therefore, it is possible that channel evolution (through incision and accretion) was controlled by the presence of mires either adjacent to or underlying the channel. Incision and accretion of these narrower channels would have been limited by the higher relief of ombrotrophic mires (Shiers *et al.*, 2017) and their ability to withstand erosion (McCabe, 1985). The presence of a bounding mire would therefore potentially control the geometry of point-bar elements, as well as influence the morphodynamics of the river and hence the internal lithofacies character of the developing point bars.

Flow velocity

Stream power is directly proportional to discharge and gradient, and inversely proportional to the channel width (Flint, 1974). Higher stream power (i.e. flow velocity) may result in the preferential accumulation of sediment into dunes rather than ripple-scale features for a given grain size (Harms *et al.*, 1975). At finer grain-sizes it is not possible for sediment to accumulate into dune-sized features and ripples preferentially form. The palaeoflow velocity within the channels associated with ancient point-bar elements is difficult to determine. Numerous equations relate channel dimensions to sinuosity, water discharge and gradient (e.g. Leopold & Wolman, 1960; Schumm, 1963; 1972; Williams, 1986; Bridge & Mackey, 1993; Table 3). Although these relationships commonly ignore short-term discharge variations (e.g. single flood events), collectively they are a widely accepted approach to relate changes in hydraulic geometry to element thickness (e.g. Bridge & Tye 2000; Bridge *et al.*, 2000; Gouw & Autin 2008; Tewari *et al.*, 2012; Famubode & Bhattacharya 2016; Chakraborty *et al.*, 2017). Generally, the calculated flow velocity (Table 3) for the channels associated with Neslen Formation point-bar elements increase upwards through the Neslen Formation. Moreover, the calculated annual discharge for type I and II point-bar elements (87.7 and 62.4 $m^3 s^{-1}$) is significantly lower than those calculated for type III and IV elements (470 and 510.8 $m^3 s^{-1}$).

The inferred low flow velocities of channels in the lower Neslen Formation, compared to the upper Chesterfield Zone and other units deposited on the margins of the WIS (Table 3), may be attributed to river deceleration in its backwater zone, or to allogenic controls, themselves linked to low floodplain gradients, or to times of very low river flow during a period of reduced water discharge (be it seasonal or longer term). There is no link between the proportion of preserved fines within the point bars and the flow velocity: the calculated flow velocities are time and depth averaged and fine-grained sediments are attributed to periods of low river flow.

An estimated floodplain gradient for the Neslen Formation of $\sim 2.5 \times 10^{-4}$ m/m (Colombera *et al.*, 2016) is inferred (subject to uncertainties in compaction and correlation) from the gradient of transgressive surfaces traced in the coastal-plain deposits (Aschoff & Steel, 2011a). This low basin gradient may have resulted from the interference between Sevier-style and Laramide-style tectonics (Armstrong 1968) and dynamic subsidence. No broad scale changes in tectonics (e.g. faulting or thinning) are recognised through the deposition of the Neslen Formation to account for any large changes in floodplain gradient.

A monsoonal climate is inferred to have operated during accumulation of the Neslen Formation (Fricke *et al.*, 2010); this would cause seasonal changes of flow within the channels of the Neslen Formation. The overall reduction in the presence, thickness, extent and continuity of coals from the lower to middle parts of the Neslen Formation to the upper part of the Neslen Formation may have arisen in response to a less humid climate (i.e. lower annual rainfall) through time. However, this is counter to what is suggested by the fluvial discharge variations determined throughout the Neslen Formation, as calculated from reconstructed channel dimensions (Table 3).

Type I and type II point-bar elements are attributed to channels within which the stream power was reduced (hence carrying a fine-grained sediment load) and hence sediment was not

Table 3. Quantitative analysis of channels in the Neslen Formation separated by element type, compared to other systems on the margins of the Western Interior Seaway (green) and humid-climate successions generally (orange). Maximum bankfull depth is interpreted from the average point-bar thickness assuming no compaction. Sources for equations: (1) Bridge & Mackey, 1993; (2) Williams, 1986; (3) Williams, 1986; (4) Leopold & Wolman, 1960; (5) Schumm, 1963; (6, 7, 8) Schumm, 1972.

	Unit	Equation		Neslen Fm.	Type I	Type II	Type III	Type IV	McMurray Fm.	Ferron Ss.	Lower Williams Fork Fm.	Scalby Ss.	Wessex Fm.	Green River Fm
Maximum bankfull depth (d)	m	Measured		8.8	6.4	5.8	10.35	10.6						
Mean bankfull depth (D)		D = 0.57d	(1)	5.02	3.65	3.31	5.9	6.04	30–40	7	6.65	6.65	3.24	6.5
Bankfull width (W)	m	Or measured $8.88 \times D^{1.82}$	(2)	167.38	93.71	78.43	224.58	234.37	500–548	290	281	165	100	74
Channel belt width (Wm)	m	Or measured $148 \times D^{1.52}$	(3)	1719	1059	913	2198	2277	40,308	2850	2636	2636	883	2546
W:D (F)	/	W/D	(4)	33.3	25.7	23.7	38.1	38.8	13.9–18.3	41.4	42.3	24.8	30.86	11.4
Wavelength (λ)	m	$10.9 \times W^{1.01}$	(5)	1920	1069	893	2584	2698	5500-6400	3345	3241	1892	1141	842
Sinuosity (P)	/	$3.5F^{-0.27}$	*(6)*	1.36	1.46	1.49	1.31	1.3	1.6–2.4	1.3	1.2	1.5	1.4	1.8
Mean annual discharge (Qm)	$m^3 s^{-1}$	$\frac{W^{2.43}}{18 \times F^{1.13}}$	(7)	267.9	87.7	62.4	470	510.8	10,978	796	719	361	83.5	123
Mean annual flood (Qma)	$m^3 s^{-1}$	$16\left(\frac{W^{1.56}}{F^{0.66}}\right)$	(9)	4659	2236	1787	6743	7121	43,994	9511	8927	5534	2193	2645

capable of accumulating into dune-sized bed forms (Fig. 10). This situation could have arisen in channels located away from the main trunk channel belt, or within distributive channel splitting (Fig. 15). The increase in channel size and grain-size up-section can be explained by an increase in discharge. However, the equations used in determining the discharge of ancient river channels negate discharge variability; this means that any seasonality within the rivers is obscured. A change between seasonal and perennial discharges may explain the difference between type I and II point bar elements and type III and IV elements respectively. Type I and II point-bar elements might be related to a seasonal climate, due to the dominance of horizontally laminated sandstone (cf. Fielding *et al.*, 2009).

Comparison of the Neslen Formation to other similar depositional systems

Analysis shows that trends in point-bar element facies and their vertical stacking density through the Neslen Formation may be due to the increasing accommodation (influenced by the presence of coal and marine processes) and declining flow velocity towards the coast. Analysis has been undertaken using the FAKTS database to test if these trends can be observed in other ancient successions of humid-climate, coastal-plain settings.

Marine influenced successions

The change in the aspect ratio and amalgamation of point-bar elements within the Neslen Formation, as demonstrated above, can be attributed to their position on the floodplain in relation to the limit of backwater processes as part of the fluvial-to-marine transition zone. However, the link between point bar elements interpreted to have been modified by tidal processes and the lack of cross-bedded sandstone (but high proportion of ripple-laminated and horizontally laminated sandstone) is not observed within other formations (e.g. Weimer *et al.*, 1982; Thomas *et al.*, 1987; Shanley *et al.*, 1992; Bose & Chakraborty, 1994; Choi *et al.*, 2004; Dalrymple & Choi, 2007; van den Berg *et al.*, 2007; Hovikoski *et al.*, 2008; Matinius & Gowland, 2011; Sisulak & Dashtgard, 2012; Johnson & Dashtgard, 2014; Legler *et al.*, 2014). None of the successions interpreted as having been laid down in environments proximal to the marine realm show similar facies assemblages to the Neslen Formation. This indicates that, although marine processes may have been responsible for the introduction of significant heterogeneities within point-bar elements, they cannot be shown to have been the dominant control on the occurrence of cross-bedding within these elements.

Successions containing appreciable amounts of coal

Other coal-bearing systems analysed using FAKTS do not exhibit similar facies assemblages to type I or II point-bar elements of the Neslen Formation. Other coal-bearing systems documented in the literature (e.g. Ferron Sandstone, Ryer, 1981; Raniganj coal measures, Casshyap & Kumar, 1987; Straight Cliffs Formation, Shanley *et al.*, 1992; Weisselster Basin, Halfar *et al.*, 1998; Lopingian coal measures, Wang *et al.*, 2011) do not display instances of facies assemblages similar to those in the type I or II point-bar elements of the Neslen Formation. This indicates that, although there is a strong relationship between the presence of coal substrates and the occurrence of type I and II facies assemblages (Fig. 14), this relationship has not hitherto been established in other successions.

Calculated discharge values within other successions

Systems associated with low mean annual discharge values ($<150\,m^3\,s^{-1}$; Table 3) have greater proportions of ripple-laminated sandstone within associated point-bar elements (e.g. Green River Formation: Keighley *et al.*, 2003; Wessex Formation: Stewart, 1983; Fig. 8). No other studied successions documented in the literature have a similarly low proportion of cross-bedded sandstone as the type I or II point-bar elements studied here. The high proportion of ripple-laminated and horizontally laminated sandstone are probably a product of sharp hydrographic variations and rapidly waning floods (Ielpi *et al.*, 2014), such as within tropical, monsoonal climates where rivers are subject to seasonal discharge variations (e.g. Fielding, 2006; Gugliotta *et al.*, 2015).

CONCLUSIONS

Quantitative analysis of 40 point-bar elements from the Cretaceous Neslen Formation has allowed four point-bar element types to be distinguished based on their internal facies types, proportions and geometry. Type I and II point-bar elements are characterised internally by a distinctive lack of cross-bedding and are instead dominated by ripple-laminated sandstone and massive and horizontally laminated sandstone, respectively. Type III and IV point-bar elements are similar to many examples from other successions, based on analysis undertaken using the FAKTS database; these types conform to traditional point-bar models.

Upwards through the Neslen Formation, passing from a transgressive systems tract to a highstand systems tract, there are a series of changes in the character of point-bar elements: (i) an increase in the width-to-thickness aspect ratio of point-bar elements; (ii) an increase in the thickness and amalgamation of point-bar elements; (iii) a decrease in internal heterogeneity (mud and silt content); (iv) a change from dominantly type I and II point-bar elements in the lower Neslen Formation to type III and IV point-bar elements in the upper part.

A vertical increase in sediment supply or a decrease in the rate of accommodation generation might have been the dominant controls on the vertical changes in channel-body stacking density. Similar changes might produce the upward decrease in the occurrence of coal beds. In the lower Neslen Formation, point-bar elements that exhibit an abundance of ripple and horizontally laminated and massive sandstone, and a corresponding absence of cross-bedded sandstone, are recognised. The deposition of these less common types of point-bar elements (i.e. types I and II) can be attributed to a combination of marine influence with inferred low stream power of autogenic (e.g. backwater-driven) or allogenic (e.g. climate-driven). Other important considerations in the deposition of unusual point-bar assemblages include the fine-grained nature of the sediment and the presence of mire deposits. This study emphasises the complicated interplay of depositional processes in channels within the fluvial-to-marine transition zone, the discernment of which requires a high-resolution sequence stratigraphic framework.

ACKNOWLEDGEMENTS

This research was funded by AkerBP, Areva, BHPBilliton, Cairn India (Vedanta), ConocoPhillips, Murphy Oil, Nexen, Petrotechnical Data Systems, Saudi Aramco, Shell, Tullow Oil, Woodside and YPF through their sponsorship and support of the Fluvial & Eolian Research Group at the University of Leeds. LC was supported by NERC (Catalyst Fund award NE/M007324/1; Follow-on Fund NE/N017218/1). Luke Beirne and Camille Dwyer are thanked for their help and assistance in the field. Catherine Russell and Howard Johnson are thanked for many helpful discussions. Reviews by Brian Willis and Alessandro Ielpi, and advice from Series Editor Mark Bateman have greatly improved the manuscript.

REFERENCES

Aitken, J.F. and **Flint, S.S.** (1995) The application of high-resolution sequence stratigraphy to fluvial systems: a case study from the Upper Carboniferous Breathitt Group, eastern Kentucky, USA. *Sedimentology*, **42**, 3–30.

Allen, G.P. (1991) Sedimentary processes and facies in the Gironde Estuary: a recent model for macrotidal estuarine systems. In: *Clastic Tidal Sedimentology* (Eds D.G. Smith, G.E. Reinson, B.A. Zaitlin and R.A. Rahmani), *Mem. Can. Soc. Petrol. Geol.*, **16**, 29–40.

Allen, J. (1970) Physical processes of sedimentation. Earth Science Series 1, Unwin University Books, George Allen and Unwin, 248pp.

Allen, J. (1978) Studies in fluviatile sedimentation: an exploratory quantitative model for the architecture of avulsion-controlled alluvial suites. *Sed. Geol.*, **21**, 129–147.

Allen, J. (1977) The possible mechanics of convolute lamination in graded sand beds. *J. Geol. Soc.*, **134**, 19–31.

Allen, J.R. (1965) A review of the origin and characteristics of recent alluvial sediments. *Sedimentology*, **5**, 89–191.

Allen, J.R. (1983) Studies in fluviatile sedimentation: bars, bar-complexes and sandstone sheets (low-sinuosity braided streams) in the Brownstones (L. Devonian), Welsh Borders. *Sed. Geol.*, **33**, 237–293.

Archer, A.W. and **Greb, S.F.** (2012) Hypertidal Facies from the Pennsylvanian Period: Eastern and Western Interior Coal Basins, USA. In: *Principles of Tidal Sedimentology*, 421–436. Springer.

Armstrong, R.L. (1968) Sevier orogenic belt in Nevada and Utah. *Geol. Soc. Am. Bull.*, **79**, 429–458.

Aschoff, J.L. and **Steel, R.J.** (2011a) Anatomy and development of a low-accommodation clastic wedge, upper Cretaceous, Cordilleran Foreland Basin, USA. *Sed. Geol.*, **236**, 1–24.

Aschoff, J. and **Steel, R.** (2011b) Anomalous clastic wedge development during the Sevier-Laramide transition, North American Cordilleran foreland basin, USA. *Geol. Soc. Am. Bull.*, **123**, 1822–1835.

Barwis, J.H. (1977) Sedimentology of some South Carolina tidal-creek point bars and a comparison with their fluvial counterparts. In: *Fluvial Sedimentology: Bedforms and Bars* (Ed. A.D. Miall). *Mem. Can. Soc. Petrol. Geol.*, **5**, 129–160.

Bloom, A.L. (1964) Peat accumulation and compaction in a Connecticut coastal marsh. *J. Sed. Res.*, **34**, 599–603.

Blum, M., **Martin, J.**, **Milliken, K.** and **Garvin, M.** (2013) Paleovalley systems: insights from Quaternary analogs and experiments. *Earth-Sci. Rev.*, **116**, 128–169.

Blum, M.D. and **Törnqvist, T.E.** (2000) Fluvial responses to climate and sea-level change: a review and look forward. *Sedimentology*, **47**, 2–48.

Bohacs, K. and **Suter, J.** (1997) Sequence stratigraphic distribution of coaly rocks: fundamental controls and paralic examples. *AAPG Bull.*, **81**, 1612–1639.

Brekke, H. and **Couch, A.** (2011) Use of image logs in differentiating point bar and tidal bar deposits in the Leismer area: implications for SAGD reservoir definition in the Athabasca oilsands. In: *Extended Abstract, CSPG CSEG CWLS Convention*.

Bridge, J.S. and **Tye, R.S.** (2000) Interpreting the dimensions of ancient fluvial channel bars, channels, and channel belts from wireline-logs and cores. *AAPG Bull.*, **84**, 1205–1228.

Bridge, J.S., **Jalfin, G.A.** and **Georgieff, S.M.** (2000) Geometry, lithofacies, and spatial distribution of Cretaceous fluvial sandstone bodies, San Jorge Basin, Argentina: outcrop analog for the hydrocarbon-bearing Chubut Group. *J. Sed. Res.*, **70**, 341–359.

Bromley, R. (1996) *Trace Fossils: Biology, Taphonomy and Applications*. Chapman Hall. London, 361 pp.

Bridge, J.S. (1993) Description and interpretation of fluvial deposits: a critical perspective. *Sedimentology*, **40**, 801–810.

Bridge, J.S. and **Leeder, M.R.** (1979) A simulation model of alluvial stratigraphy. *Sedimentology*, **26**, 617–644.

Bridge, J. and **Mackey, S.** (1993) A theoretical study of fluvial sandstone body dimensions. In: *The geological modelling of hydrocarbon reservoirs and outcrop analogues* (Ed. I.D Bryant). *Int. Assoc. Sedimentol.*, Blackwell, 213–236.

Bridges, P.H. and **Leeder, M.R.** (1976) Sedimentary model for intertidal mudflat channels, with examples from the Solway Firth, Scotland. *Sedimentology*, **23**, 533–552.

Bristow, C. and **Best, J.** (1993) Braided rivers: perspectives and problems. *Geol. Soc. London Spec. Publ.*, **75**, 1–11.

Burns, C.E., **Mountney, N.P.**, **Hodgson, D.M.** and **Colombera, L.** (2017) Anatomy and dimensions of fluvial crevasse-splay deposits: Examples from the Cretaceous Castlegate Sandstone and Neslen Formation, Utah, U.S.A. *Sed. Geol.*, **351**, 21–35.

Burton, D., **Flaig, P.P.** and **Prather, T.J.** (2016) Regional Controls On Depositional Trends In Tidally Modified Deltas: Insights From Sequence Stratigraphic Correlation and Mapping of the Loyd And Sego Sandstones, Uinta and Piceance Basins of Utah and Colorado, USA. *J. Sed. Res.*, **86**, 763–785.

Cant, D.J. and **Walker, R.G.** (1978) Fluvial processes and facies sequences in the sandy braided South Saskatchewan River, Canada. *Sedimentology*, **25**, 625–648.

Casshyap, S. and **Kumar, A.** (1987) Fluvial architecture of the Upper Permian Raniganj coal measure in the Damodar basin, Eastern India. *Sed. Geol.*, **51**, 181–213.

Cecil, C.B., **Dulong, F.T.** and **Cobb, J.C.** (1993) Allogenic and autogenic controls on sedimentation in the Central Sumatra Basin as an analogue for Pennsylvanian coal-bearing strata in the Appalachian Basin. *Geol. Soc. Am. Spec. Pap.*, **286**, 3–22.

Chakraborty, P. P., **Saha, S.** and **Das, K.** (2017) Record of continental to marine transition from the Mesoproterozoic Ampani basin, Central India: An exercise of process-based sedimentology in a structurally deformed basin. *J. Asian Earth Sci.*, **143**, 122–140.

Chatanantavet, P., **Lamb, M.P.** and **Nittrouer, J.A.** (2012) Backwater controls of avulsion location on deltas. *Geophys. Res. Lett.*, **39**, L01402.

Choi, K.S. (2011a) External controls on the architecture of inclined heterolithic stratification (IHS) of macrotidal Sukmo Channel: Wave versus rainfall. *Marine Geology*, **285**, 17–28.

Choi, K.S. (2011b) Tidal rhythmites in a mixed-energy, macrotidal estuarine channel, Gomso Bay, west coast of Korea. *Mar. Geol.*, **280**, 105–115.

Choi, K.S., **Dalrymple, R.W.**, **Chun, S.S.** and **Kim, S.P.** (2004) Sedimentology of Modern, Inclined Heterolithic Stratification (IHS) in the Macrotidal Han River Delta, Korea. *J. Sed. Res.*, **74**, 677–689.

Cloyd, K.C., **Demicco, R.V.** and **Spencer, R.J.** (1990) Tidal channel, levee and crevasse-splay deposits from a Cambrian tidal channel system: a new mechanism to produce shallowing-upward sequences. *J. Sed. Res.*, **60**, 78–83.

Cole, R. (2008) Characterization of fluvial sand bodies in the Neslen and lower Farrer formations (Upper Cretaceous), Lower Sego Canyon, Utah. In: *Hydrocarbons Systems and Production in the Uinta Basin, Utah* (Eds M.W. Longman and C.D. Morgan). *RMAG-UGA Publication*, **37**, 81–100.

Cole, R. and **Cumella, S.** (2003) Stratigraphic architecture and reservoir characteristics of the Mesaverde Group, southern Piceance Basin, Colorado. In: *Piceance Basin 2003 guidebook* (Eds K.M. Petersen, T.M. Olsen and D.S. Anderson). Rocky Mountain Association of Geologists, 385–442.

Collinson, J.D., **Mountney, N.** and **Thompson, D.** (2006) *Sedimentary Structures*. Terra Publishing, Hertfordshire.

Colombera, L., **Felletti, F.**, **Mountney, N.P.** and **McCaffrey, W.D.** (2012a) A database approach for constraining stochastic simulations of the sedimentary heterogeneity of fluvial reservoirs. *AAPG Bull.*, **96**, 2143–2166.

Colombera, L., **Mountney, N.P.** and **McCaffrey, W.D.** (2013) A quantitative approach to fluvial facies models: methods and example results. *Sedimentology*, **60**, 1526–1558.

Colombera, L., **Mountney, N.P.** and **McCaffrey, W.D.** (2015) A meta-study of relationships between fluvial channel-body stacking pattern and aggradation rate: Implications for sequence stratigraphy. *Geology*, **43**, 283–286.

Colombera, L., **Mountney, N.P.** and **McCaffrey, W.D.** (2012b) A relational database for the digitization of fluvial architecture concepts and example applications. *Petrol. Geosci.*, **18**, 129–140.

Colombera, L., **Mountney, N.P.**, **Russell, C.E.**, **Shiers, M.N.** and **McCaffrey, W.D.** (2017) Geometry and compartmentalization of fluvial meander-belt reservoirs at the bar-form scale: Quantitative insight from outcrop, modern and subsurface analogues. *Mar. Petrol. Geol.*, **82**, 35–55.

Colombera, L., **Shiers, M.** and **Mountney, N.** (2016) Assessment of backwater controls on the architecture of distributary channel fills in a tide-influenced coastal-plain succession: Campanian Neslen Formation, USA. *J. Sed. Res.*, **86**, 476–497.

Corbeanu, R.M., **Wizevich, M.C.**, **Bhattacharya, J.P.**, **Zeng, X.** and **McMechan, G.A.** (2004) Three-dimensional architecture of ancient lower delta-plain point bars using ground-penetrating radar, Cretaceous Ferron Sandstone, Utah. Regional to Wellbore Analog for Fluvial–Deltaic Reservoir Modeling, The Ferron of Utah. *AAPG Stud. Geol.*, **50**, 427–449.

Courel, L. (1987) Stages in the compaction of peat; examples from the Stephanian and Permian of the Massif Central, France. *J. Geol. Soc.*, **144**, 489–493.

Currie, B.S. (1997) Sequence stratigraphy of nonmarine Jurassic–Cretaceous rocks, central Cordilleran foreland-basin system. *Geol. Soc. Am. Bull.*, **109**, 1206–1222.

Dalrymple, R.W. and **Choi, K.** (2007) Morphologic and facies trends through the fluvial-marine transition in tide-dominated depositional systems: A schematic framework for environmental and sequence-stratigraphic interpretation. *Earth-Sci. Rev.*, **81**, 135–174.

Demowbray, T. (1983) The genesis of lateral accretion deposits in recent intertidal mudflat channels, Solway Firth, Scotland. *Sedimentology*, **30**, 425–435.

Famubode, O. and **Bhattacharya, J.** (2016) Hierarchical organization of strata within a high-frequency Milankovitch-scale fluvial sequence, cretaceous Ferron Notom delta, south central Utah, USA. In International Conference and Exhibition, Barcelona, Spain, 3-6 April 2016. *Society of Exploration Geophysicists and American Association of Petroleum Geologists*.

Fenies, H. and **Faugères, J.-C.** (1998) Facies and geometry of tidal channel-fill deposits (Arcachon Lagoon, SW France). *Mar. Geol.*, **150**, 131–148.

Fernandes, A.M., **Törnqvist, T.E.**, **Straub, K.M.** and **Mohrig, D.** (2016) Connecting the backwater hydraulics of coastal rivers to fluvio-deltaic sedimentology and stratigraphy. *Geology*, **44**, 979–982.

Fielding, C.R. (2006) Upper flow regime sheets, lenses and scour fills: Extending the range of architectural elements for fluvial sediment bodies. *Sed. Geol.*, **190**, 227–240.

Fielding, C.R., **Allen, J.P.**, **Alexander, J.** and **Gibling, M.R.** (2009) Facies model for fluvial systems in the seasonal tropics and subtropics. *Geology*, **37**, 623–626.

Fillmore, R. (2010) Geological Evolution of the Colorado Plateau of Eastern Utah and Western Colorado, Including the San Juan River, Natural Bridges, Canyonlands, Arches, and the Book Cliffs. University of Utah Press.

Fisher, D.J., **Erdmann, C.E.** and **Reeside, J.B.J.** (1960) Cretaceous and Tertiary formations of the Book Cliffs, Carbon, Emery and Grand Counties, Utah and Garfield and Mesa Counties, Colorado. *Geol. Surv. Prof. Pap.*, **332**, 1–79.

Flint, J.J. (1974) Stream gradient as a function of order, magnitude and discharge. *Water Resour. Res.*, **10**, 969–973.

Foix, N., **Paredes, J.M.** and **Giacosa, R.E.** (2013) Fluvial architecture variations linked to changes in accommodation space: Río Chico Formation (late Paleocene), Golfo San Jorge basin, Argentina. *Sed. Geol.*, **294**, 342–355.

Foreman, B. Z., **Roberts, E. M.**, **Tapanila, L.**, **Ratigan, D.** and **Sullivan, P.** (2015) Stable isotopic insights into paleoclimatic conditions and alluvial depositional processes in the Kaiparowits Formation (Campanian, south-central Utah, USA). *Cretaceous Res.*, **56**, 180–192.

Fricke, H.C., **Foreman, B.Z.** and **Sewall, J.O.** (2010) Integrated climate model-oxygen isotope evidence for a North American monsoon during the Late Cretaceous. *Earth Planet. Sci. Lett.*, **289**, 11–21.

Fustic, M., **Hubbard, S.M.**, **Spencer, R.**, **Smith, D.G.**, **Leckie, D.A.**, **Bennett, B.** and **Larter, S.** (2012) Recognition of down-valley translation in tidally influenced meandering fluvial deposits, Athabasca Oil Sands (Cretaceous), Alberta, Canada. *Mar. Petrol. Geol.*, **29**, 219–232.

Galloway, W.E. and **Hobday, D.K.** (1996) Fluvial Systems. In: *Terrigenous Clastic Depositional Systems*, pp. 60–90. Springer.

Gates, T.A. and **Scheetz, R.** (2015) A new saurolophine hadrosaurid (Dinosauria: Ornithopoda) from the Campanian of Utah, North America. *J. Systematic Palaeontology*, **13**, 711–725.

Geehan, G. and **Underwood, J.** (2009) The use of length distributions in geological modelling. In: *The Geological Modelling of Hydrocarbon Reservoirs and Outcrop Analogues* (Eds S.S. Flint and I.D. Bryant). *Int. Assoc. Sedimentol.*, Blackwell Publishing Ltd., Oxford, UK. doi: 10.1002/9781444303957.ch13.

Ghazi, S. and **Mountney, N.P.** (2009) Facies and architectural element analysis of a meandering fluvial succession: The Permian Warchha Sandstone, Salt Range, Pakistan. *Sed. Geol.*, **221**, 99–126.

Ghazi, S. and **Mountney, N.P.** (2011) Petrography and provenance of the Early Permian Fluvial Warchha Sandstone, Salt Range, Pakistan. *Sed. Geol.*, **233**, 88–110.

Gibling, M.R. (2006) Width and thickness of fluvial channel bodies and valley fills in the geological record: a literature compilation and classification. *J. Sed. Res.*, **76**, 731–770.

Gingras, M.K., **MacEachern, J.A.** and **Dashtgard, S.E.** (2012) The potential of trace fossils as tidal indicators in bays and estuaries. *Sed. Geol.*, **279**, 97–106.

Gouw, M. J. and **Autin, W. J.** (2008) Alluvial architecture of the Holocene Lower Mississippi Valley (USA) and a comparison with the Rhine–Meuse delta (The Netherlands). *Sed. Geol.*, **204**, 106–121.

Gualtieri, J.L. (1991) Map and cross sections of coal zones in the Upper Cretaceous Neslen Formation, North-Central part of the Westwater 30’ * 60’ quadrangle, Grand and Uintah counties, Utah, 133. *U.S. Geol. Surv.*

Gugliotta M.; **Kurcinka C.E.**, **Dalrymple R.W.**, **Flint S.S.** and **Hodgson D.M.** (2016) Decoupling seasonal fluctuations in fluvial discharge from the tidal signature in ancient deltaic deposits: An example from the Neuquén Basin, Argentina, *J. Geol. Soc.*, **173**, 94–107.

Gulliford A.R., **Flint S.S.** and **Hodgson D.M.** (2014) Testing applicability of models of distributive fluvial systems or trunk rivers in ephemeral systems: Reconstructing 3-D fluvial architecture in the Beaufort Group, South Africa, *J. Sed. Res.*, **84**, 1147–1169.

Halfar, J., **Riegel, W.** and **Walther, H.** (1998) Facies architecture and sedimentology of a meandering fluvial system: a Palaeogene example from the Weisselster Basin, Germany. *Sedimentology*, **45**, 1–17.

Hampson, G.J., **Royhan Gani, M.**, **Sahoo, H.**, **Rittersbacher, A.**, **Irfan, N.**, **Ranson, A.**, **Jewell, T.O.**, **Gani, N.D.**, **Howell, J.A.** and **Buckley, S.J.** (2012) Controls on large-scale patterns of fluvial sandbody distribution in alluvial to coastal plain strata: Upper Cretaceous Blackhawk Formation, Wasatch Plateau, Central Utah, USA. *Sedimentology*, **59**, 2226–2258.

Harms, J., **Southard, J.B.**, **Spearing, D.R.** and **Walker, R.G.** (1975) Stratification produced by migrating bed forms. In: *Depositional Environments as Interpreted from Primary Sedimentary Structures and Stratification Sequences* (Eds J. Harms, J. Southard, D. Spearing and R. Walker), **2**, pp. 45–61. *SEPM.*

Heller, P.L. and **Paola, C.** (1996) Downstream changes in alluvial architecture: an exploration of controls on channel-stacking patterns. *J. Sed. Res.*, **66**, 297–306.

Hettinger, R.D. and **Kirshbaum, M.A.** (2003) Stratigraphy of the Upper Cretaceous Mancos Shale (Upper Part) and Mesaverde Group in the Southern Part of the Uinta and Piceance Basins, Utah and Colorado. In: *Petroleum Systems and Geologic Assessment of Oil and Gas in the Uinta-Piceance Province, Utah and Colorado* (Ed. U.U.-P.A. Team), *U.S Geol. Surv.*, DDS-69-B, pp. 1–16.

Holbrook, J.M. (1996) Complex fluvial response to low gradients at maximum regression: A genetic link between smooth sequence-boundary morphology and architecture of overlying sheet sandstone. *J. Sed. Res.*, **66**, 713–722.

Hovikoski, J., **RÄSÄNen, M.**, **Gingras, M.**, **Ranzi, A.** and **Melo, J.** (2008) Tidal and seasonal controls in the formation of Late Miocene inclined heterolithic stratification deposits, western Amazonian foreland basin. *Sedimentology*, **55**, 499–530.

Howard, J.D. and **Frey, R.W.** (1984) Characteristic trace fossils in nearshore to offshore sequences, Upper Cretaceous of east-central Utah. *Can. J. Earth Sci.*, **21**, 200–219.

Huerta, P., **Armenteros, I.** and **Silva, P.G.** (2011) Large-scale architecture in non-marine basins: the response to the interplay between accommodation space and sediment supply. *Sedimentology*, **58**, 1716–1736.

Ielpi, A. and **Ghinassi, M.** (2014) Planform architecture, stratigraphic signature and morphodynamics of an exhumed Jurassic meander plain (Scalby Formation, Yorkshire, UK). *Sedimentology*, **61**, 1923–1960.

Ielpi, A., **Gibling, M.R.**, **Bashforth, A.R.**, **Lally, C.**, **Rygel, M.C.** and **Al-Silwadi, S.** (2014) Role of vegetation in shaping Early Pennsylvanian braided rivers: architecture of the Boss Point Formation, Atlantic Canada. *Sedimentology*, **61**, 1659–1700.

Jablonski, B.V. and **Dalrymple, R.W.** (2016) Recognition of strong seasonality and climatic cyclicity in an ancient, fluvially dominated, tidally influenced point bar: Middle McMurray Formation, Lower Steepbank River, north-eastern Alberta, Canada. *Sedimentology*, **63**, 552–585.

Jackson II, R.G. (1976) Depositional model of point bars in the lower Wabash River. *J. Sed. Res.*, **46**, 579–594.

Jackson II, R.G. (1978) Preliminary evaluation of lithofacies models for meandering alluvial streams. In: *Fluvial Sedimentology: Fluvial Facies Models* (Ed. A.D. Miall). *Mem. Can. Soc. Petrol. Geol.*, **5**, 543–576.

Johnson, S.M. and **Dashtgard, S.E.** (2014) Inclined heterolithic stratification in a mixed tidal-fluvial channel: Differentiating tidal versus fluvial controls on sedimentation. *Sed. Geol.*, **301**, 41–53.

Jones, B.G. and **Rust, B.R.** (1983) Massive sandstone facies in the Hawkesbury Sandstone, a Triassic fluvial deposit near Sydney, Australia. *J. Sed. Res.*, **53**, 1249–1259.

Jordan, T.E. (1981) Thrust loads and foreland basin evolution, Cretaceous, western United States. *AAPG Bull.*, **65**, 2506–2520.

Kauffman, E.G. (1977) Geological and biological overview: Western Interior Cretaceous basin. *The Mountain Geologist*, **14**, 75–99.

Karaman, O. (2012) Shoreline Architecture and Sequence Stratigraphy of Campanian Iles Clastic Wedge, Piceance Basin, CO: Influence of Laramide Movements in Western Interior Seaway. Masters Thesis, University of Texas at Austin, Texas, 137 pp.

Keighley, D., **Flint, S.**, **Howell, J.** and **Moscariello, A.** (2003) Sequence stratigraphy in lacustrine basins: a model for part of the Green River Formation (Eocene), southwest Uinta Basin, Utah, USA. *J. Sed. Res.*, **73**, 987–1006.

Kirschbaum, M.A. and **Hettinger, R.D.** (2004) Facies Analysis and Sequence Stratigraphic Framework of Upper Campanian Strata (Neslen and Mount Garfield Formations, Bluecastle Tongue of the Castlegate Sandstone and Mancos Shale), Eastern Book Cliffs, Colorado and Utah. *U.S. Geol. Surv. Digital Data Series.*

Kvale, E.P. (2011) Tidal Constituents of Modern and Ancient Tidal Rhythmites. In: *Principles of Tidal Sedimentology* (Eds A.R. Davis Jr and R.W. Dalrymple), Springer, Netherlands, 1–17.

Kvale, E.P. and **Archer, A.W.** (1990) Tidal deposits associated with low-sulfur coals, Brazil Fm.(Lower Pennsylvanian), Indiana. *J. Sed. Petrol.*, **60**, 563–574.

Labrecque, P.A., **Hubbard, S.M.**, **Jensen, J.L.** and **Nielsen, H.** (2011) Sedimentology and stratigraphic architecture of a point bar deposit, Lower Cretaceous McMurray Formation, Alberta, Canada. *Bull. Can. Soc. Petrol. Geol.*, **59**, 147–171.

Lamb, M.P., **Nittrouer, J.A.**, **Mohrig, D.** and **Shaw, J.** (2012) Backwater and river plume controls on scour upstream of river mouths: Implications for fluvio-deltaic morphodynamics. *J. Geophys. Res.*; Earth Surface, **117**, F01002.

Lawton, T. (1986) Fluvial systems of the Upper Cretaceous Mesaverde Group and Paleocene North Horn Formation, Central Utah: A record of transition from thin-skinned to thick-skinned deformation in the foreland region: Part III. Middle Rocky Mountains. In: *Paleotectonics and Sedimentation in the Rocky Mountain Region, United States* (Ed. J.A. Peterson). *AAPG Mem.*, **41**, 423–442.

Leeder, M. (1977) A quantitative stratigraphic model for alluvium, with special reference to channel deposit density and interconnectedness. In: *Fluvial Sedimentology* (Ed. A.D. Miall), *Can. Soc. Petrol. Geol.*, **5**, pp. 587–596.

Leeder, M. (1999) Sedimentology and Sedimentary Basins. From Turbulence to Tectonics. Blackwell Science Ltd., 594 pp.

Legarreta, L. and Uliana, M.A. (1998**)** Anatomy of hinterlanddepositional sequences: Upper Cretaceous fluvial strata, Neuquen basin, west-central Argentina. In: *Relative Role of Eustasy, Climate, Tectonism in*

Continental Rocks (Eds K.W.Shanley and P.J. McCabe), *SEPM Spec. Publ.*, **59**, 83–92. Society of Economic Paleontologists and Mineralogists,Tulsa, OK.

Legler, B., **Hampson, G.J.**, **Jackson, C.A.**, **Johnson, H.D.**, **Massart, B.Y.**, **Sarginson, M.** and **Ravnås, R.** (2014) Facies Relationships and Stratigraphic Architecture of Distal, Mixed Tide-and Wave-Influenced Deltaic Deposits: Lower Sego Sandstone, Western Colorado, *USA. J. Sed. Res.*, **84**, 605–625.

Leopold, L.B. and **Wolman, M.G.** (1960) River meanders. *Geol. Soc. Am. Bull.*, **71**, 769–793.

Lynds, R. and **Hajek, E.** (2006) Conceptual model for predicting mudstone dimensions in sandy braided-river reservoirs. *AAPG Bull.*, **90**, 1273–1288.

Mackey, S.D. and **Bridge, J.S.** (1995) Three-dimensional model of alluvial stratigraphy: theory and application. *J. Sed. Res.*, **65**, 7–31.

McGowen, J. and **Garner, L.** (1970) Physiographic features and stratification types of coarse-grained pointbars: Modern and ancient examples. *Sedimentology*, **14**, 77–111.

McLaurin, B.T. and **Steel, R.J.** (2000) Fourth-order nonmarine to marine sequences, middle Castlegate Formation, Book Cliffs, Utah. *Geology*, **28**, 359–362.

Miall, A. (2014) *Fluvial Depositional Systems*. Springer, 316 pp.

Miall, A.D. (1985) Architectural-element analysis: A new method of facies analysis applied to fluvial deposits. *Earth-Sci. Rev.*, **22**, 261–308.

Miall, A.D. (1988) Facies architecture in clastic sedimentary basins. In: *New perspectives in basin analysis* (Eds K.L. Kleinspehn and C. Paola). Springer, 67–81.

Miall, A.D. (1977) Lithofacies types and vertical profile models in braided river deposits: a summary. In: *Fluvial Sedimentology* (Ed. A.D. Miall), **5**, 597–604.

Miranda, M.C., De Fátima Rossetti, D. and **Carlos Ruiz Pessenda, L.** (2009) Quaternary paleoenvironments and relative sea-level changes in Marajó Island (Northern Brazil): Facies, δ13C, δ15N and C/N. *Palaeogeogr. Palaeoclimatol. Palaeoecol.*, **282**, 19–31.

Musial, G., **Reynaud, J.-Y.**, **Gingras, M.K.**, **Féniès, H.**, **Labourdette, R.** and **Parize, O.** (2012) Subsurface and outcrop characterization of large tidally influenced point bars of the Cretaceous McMurray Formation (Alberta, Canada). *Sed. Geol.*, **279**, 156–172.

Nami, M. and **Leeder, M.** (1977) Changing channel morphology and magnitude in the Scalby Formation (M. Jurassic) of Yorkshire, England. *Mem. Can. J. Petrol. Geol.*, **5**, 431–440.

Nanson, G.C. (1980) Point bar and floodplain formation of the meandering Beatton River, northeastern British Columbia, Canada. *Sedimentology*, **27**, 3–29.

Nanson, G.C. and **Page, K.** (2009) Lateral accretion of fine-grained concave benches on meandering rivers. Modern and Ancient Fluvial Systems. *Int. Assoc. Sedimentol. Spec. Publ.*, **6**, 133–143.

Nio, S.D. and **Yang, C.S.** (1991) Sea-level fluctuations and the geometric variability of tide-dominated sandbodies. *Sed. Geol.*, **70**, 161–193.

Nittrouer, J.A., **Shaw, J.**, **Lamb, M.P.** and **Mohrig, D.** (2012) Spatial and temporal trends for water-flow velocity and bed-material sediment transport in the lower Mississippi River. *Geol. Soc. Am. Bull.*, **124**, 400–414.

O'Brien, K.C. (2015) *Stratigraphic architecture of a shallow-water delta deposited in a coastal-plain setting: Neslen Formation, Floy Canyon, Utah, Colorado School of Mines*. Arthur Lakes Library, 77 pp.

Olariu, C., **Steel, R.J.**, **Olariu, M.I.** and **Choi, K.S.** (2015) Facies and architecture of unusual fluvial-tidal channels with inclined heterolothic strata: Campanian Neslen Formation, Utah, USA. In: *Fluvial-Tidal Sedimentology* (Eds P.J. Ashworth, J.L. Best and D.R. Parsons). Elsevier, 1 edn, 68, pp. 634.

Pemberton, S.G., **Flach, P.D.** and **Mossop, G.D.** (1982) Trace fossils from the Athabasca oil sands, Alberta, Canada. *Science*, **217**, 825–827.

Pitman, J.K., **Franczyk, K.J.** and **Anders, D.E.** (1986) Marine and Nonmarine gas-bearing rocks in Upper Cretaceous Neslen and Blackhawk foramtions, Eastern Uinta Basin, Utah-Sedimentology, Diagenesis and Source rock potential. *AAPG Bull.*, **70**, 1052–1052.

Plink-Björklund, P. (2015) Morphodynamics of rivers strongly affected by monsoon precipitation: Review of depositional style and forcing factors. *Sed. Geol.*, **323**, 110–147.

Posamentier, H. and **Vail, P.** (1988) Eustatic controls on clastic deposition II—sequence and systems tract models. In: Sea-Level Changes – An Integrated Approach (Eds C. Wilgus, B. Hastings, H. Posamentier, J. Van Wagoner, C. Ross and C. Kendall). *SEPM Spec. Publ.*, **42**, 47–70.

Pranter, M.J., **Ellison, A.I.**, **Cole, R.D.** and **Patterson, P.E.** (2007) Analysis and modeling of intermediate-scale reservoir heterogeneity based on a fluvial point-bar outcrop analog, Williams Fork Formation, Piceance Basin, Colorado. *AAPG Bull.*, **91**, 1025–1051.

Rampino, M.R. and **Sanders, J.E.** (1981) Episodic growth of Holocene tidal marshes in the northeastern United States: A possible indicator of eustatic sea-level fluctuations. *Geology*, **9**, 63–67.

Rasanen, M.E., **Linna, A.M.**, **Santos, J.C.R.** and **Negri, F.R.** (1995) Late Miocene Tidal Deposits in the Amazonian Foreland Basin. *Science*, **269**, 386–390.

Reineck, H.E. and **Wunderlich, F.** (1968) Classification and origin of flaser and lenticular bedding. *Sedimentology*, **11**, 99–104.

Russell, C.E., **Mountney, N.P.**, **Hodgson, D.M.** and **Colombera, L.** [this volume] Improving prediction of lithologic heterogeneity in fluvial point-bar deposits from analysis of meander morphology and scroll-bar pattern. *Int. Assoc. Sedimentol. Spec. Publ.*, **48**, 385–417.

Ryer, T.A. (1981) Deltaic coals of Ferron Sandstone Member of Mancos Shale: predictive model for Cretaceous coal-bearing strata of Western Interior. *AAPG Bull.*, **65**, 2323–2340.

Savrda, C.E. (1991) Teredolites, wood substrates and sea-level dynamics. *Geology*, **19**, 905–908.

Schumm, S.A. (1963) Sinuosity of alluvial rivers on the Great Plains. *Geol. Soc. Am. Bull.*, **74**, 1089–1100.

Schumm, S. and **Khan, H.** (1972) Experimental study of channel patterns. *Geol. Soc. Am. Bull.*, **83**, 1755–1770.

Shanley, K.W., **McCabe, P.J.** and **Hettinger, R.D.** (1992) Tidal influence in Cretaceous fluvial strata from Utah, USA: a key to sequence stratigraphic interpretation. *Sedimentology*, **39**, 905–930.

Shiers, M., **Mountney, N.**, **Hodgson, D.** and **Cobain, S.** (2014) Depositional Controls on Tidally Influenced Fluvial Successions, Neslen Formation, Utah, USA. *Sed. Geol.*, **311**, 1–16.

Shiers, M.N., **Hodgson, D.M.** and **Mountney, N.P.** (2017) Response of A Coal-Bearing Coastal-Plain Succession To Marine Transgression: Campanian Neslen Formation, Utah, USA. *J. Sed. Res.*, **87**, 168–187.

Simon, S.S. and **Gibling, M.R.** (2017b) Finegrained meandering systems of the Lower Permian Clear Fork Formation of north-central Texas, USA: Lateral and oblique accretion on an arid plain. *Sedimentology*, **64**, 714–746.

Simon, S.S. and **Gibling, M.R.** (2017b) Pedogenic Mud Aggregates Preserved In A Fine-Grained Meandering Channel In the Lower Permian Clear Fork Formation, North-Central Texas, USA. *J. Sed. Res.*, **87**, 230–252.

Simons, D.B. (1960) Sedimentary structures generated by flow in alluvial channels. Primary Sedimentary Structures, *SEPM Spec. Publ.*, **12**, 34–52.

Sisulak, C.F. and **Dashtgard, S.F.** (2012) Seasonal controls on the development and character of inclinced heterolithic stratification in a tide-influenced, fluvially dominated channel: Fraser River, Canada. *J. Sed. Res.*, **82**, 244–257.

Smith, D.G. (1987) Meandering river point bar lithofacies models: modern and ancient examples compared. In: *Recent developments in Fluvial Sedimentology* (Eds F.G. Ethridge, R.M. Flores and M.D. Harvey) *SEPM*, **39**, 83–91.

Smith, D.G., **Hubbard, S.M.**, **Leckie, D.A.** and **Fustic, M.** (2009) Counter point bar deposits: lithofacies and reservoir significance in the meandering modern Peace River and ancient McMurray Formation, Alberta, Canada. *Sedimentology*, **56**, 1655–1669.

Sønderholm, M. and **Tirsgaard, H.** (1998) Proterozoic fluvial styles: response to changes in accommodation space (Rivieradal sandstones, eastern North Greenland). *Sed. Geol.*, **120**, 257–274.

Speiker, E.M. (1949) The transition between the Colorado Plateaus and the Great Basin in central Utah. *Utah Geol. Soc. Guidebook*, **106**.

Stewart, D.J. (2009) Possible Suspended-Load Channel Deposits from the Wealden Group (Lower Cretaceous) of Southern England. In: *Modern and ancient fluvial systems* (Eds J.D. Collinson and J. Lewin). Blackwell Publishing, 369–384.

Tewari, R.C., **Hota, R.N.**, and **Maejima, W.** (2012) Fluvial architecture of Early Permian Barakar rocks of Korba Gondwana basin, eastern-central India. *J. Asian Earth Sci.*, **52**, 43–52.

Thomas, R.G., **Smith, D.G.**, **Wood, J.M.**, **Visser, J.**, **Calverleyrange, E.A.** and **Koster, E.H.** (1987) Inclined heterolithic stratification-terminology, description, interpretation and significance. *Sed. Geol.*, **53**, 123–179.

Tissot, B.P. and **Welte, D.H.** (1984) From kerogen to petroleum. In: *Petroleum Formation and Occurrence*. Springer, 160–198.

Turner, B. and **Eriksson, K.** (1999) Meander bend reconstruction from an Upper Mississippian muddy point bar at Possum Hollow, West Virginia, USA. *Fluvial Sedimentology*, **VI**, 363–379.

Tyler, N. and **Finley, R.J.** (1991) Architectural controls on the recovery of hydrocarbons from sandstone reservoirs. In: *The three-dimensional facies architecture of terrigenous clastic sediments and its implications for hydrocarbon discovery and recovery* (Eds N. Tyler and A. Miall). SEPM, *Concepts in Sedimentology and Paleontology*, **3**, 1–5.

van den Berg, J.H., **Boersma, J.R.** and **van Gelder, A.** (2007) Diagnostic sedimentary structures of the fluvial-tidal transition zone - Evidence from deposits of the Rhine and Meuse. *Geol. Mijnbouw*, **86**, 287–306.

Visher, G.S. (1965) Use of vertical profile in environmental reconstruction. *AAPG Bull.*, **49**, 41–61.

Walker, R.G. and **Cant, D.J.** (1984) Sandy fluvial systems. In: *Facies models*. Geoscience Canada Reprint Series, **1**, 71–89.

Wang, H., **Shao, L.**, **Hao, L.**, **Zhang, P.**, **Glasspool, I.J.**, **Wheeley, J.R.**, **Wignall, P.B.**, **Yi, T.**, **Zhang, M.** and **Hilton, J.** (2011) Sedimentology and sequence stratigraphy of the Lopingian (Late Permian) coal measures in southwestern China. *Int. J. Coal Geol.*, **85**, 168–183.

Weimer, R.J., **Howard, J.D.** and **Lindsay, D.R.** (1982) Tidal flats and associated tidal channels. Sandstone Depositional Environments: *AAPG Mem.*, **31**, 191–245.

Williams, G.P. (1986) River meanders and channel size. *J. Hydrol.*, **88**, 147–164.

Willis, A. (2000) Tectonic control of nested sequence architecture in the Sego Sandstone, Neslen Formation and upper Castlegate Sandstone (Upper Cretaceous), Sevier foreland basin, Utah, USA. *Sed. Geol.*, **136**, 277–317.

Willis, B.J. and **Tang, H.** (2010) Three-dimensional connectivity of point-bar deposits. *J. Sed. Res.*, **80**, 440–454.

Wright, P.V. and **Marriott, S.B.** (1993) The sequence stratigraphy of fluvial depositional systems: the role of floodplain sediment storage. *Sed. Geol.*, **86**, 203–210.

Yan, N., **Mountney, N.P.**, **Colombera, L.** and **Dorrell, R.M.** (2017) A 3D forward stratigraphic model of fluvial meander-bend evolution for prediction of point-bar lithofacies architecture. *Comput. Geosci.*, **105**, 65–80.

Young, R.G. (1957) Late Cretaceous cyclic deposits, Book Cliffs, Eastern Utah. *AAPG Bull.*, **41**, 1790–1774.

Young, R.G. (1955) Sedimentary facies and intertonguing in the Upper Cretaceous of the Book Cliffs, Utah, Colorado. *Geol. Soc. Am. Bull.*, **66**, 177–202.

Yoshida, S., **Willis, A.** and **Miall, A.D.** (1996) Tectonic control of nested sequence architecture in the Castlegate Sandstone (Upper Cretaceous), Book Cliffs, Utah. *J. Sed. Res.*, **66**, 737–748.

Int. Assoc. Sedimentol. Spec. Publ (2018) **48**, 47–80.

Toggling between expansion and translation: The generation of a muddy-normal point bar with an earthquake imprint

SHELBY JOHNSTON and JOHN HOLBROOK

Texas Christian University, Fort Worth, Texas, USA

ABSTRACT

Mud-dominated point bars are widely accepted as recording deposition by tidal influence, bar tails or counter point bars. Less understood are muddy point bars that lack these depositional origins and otherwise have the geometry of more traditional sandy point bars. This study seeks the cause of these 'muddy-normal' point bars by field examination of a point bar with features and architecture consistent with sandy deposits but containing mud-dominated internal lithofacies. This study examines a point bar in Late Cretaceous fluvial strata of the Dinosaur Park Formation in the Steveville badlands of Dinosaur Provincial Park, Alberta. Strikes and dips, palaeocurrents, photo panoramas and stratigraphic columns are used to determine accretion trajectories and lithologic trends throughout the bar with a focus on sand *vs*. mud accretion and its relation to accretion trajectory. The point bar alternates between sand-dominated and mud-dominated accretion sets, with mud comprising over 50% of the point bar by volume. Accretion sets are defined by consistency in accretion dips. Both mud and sand beds within accretion sets have current ripples and cross sets indicative of deposition by transport. This suggests that the mud layers were deposited by active accretion events and are not simple drapes. Muddy accretion sets consistently have orientations reflecting bar translation (parallel with palaeodip) and sandy accretion sets consistently have orientations consistent with bar expansion (normal to palaeodip). These data suggest that the muddy *vs*. sandy accretion sets record toggling between sand-favouring bar expansion and mud-favouring translational growth vectors. This bar toggle explains how to generate a mud-dominate point bar with general lobate geometry without imposing tidal drivers, bar abandonment, or asserting a fully counter-point-bar interpretation. This toggling between expansion and translation records periodic upstream to downstream shift in the point of attachment for flow momentum to the cutbank that is probably caused by unstable flood discharge trends over the life of the bar. Bar toggle should be considered a growth vector option for point bars along with more established translation and expansion. The point bar also has a strong palaeoseismic imprint in the form of liquefaction features and a large lateral spread near the tip that is contemporary with late bar growth. The source of this earthquake is uncertain but could record a currently unrecognised intraplate earthquake source or, intriguingly, could be associated with the nearby Bow City impact structure which occurred in the same time frame.

Keywords: Point Bar, Fluvial, Muddy, IHS, mud-dominated point bar, Expansion, Translation, Reservoir

INTRODUCTION

Point bars are typically considered sand-dominated deposits (Dixon, 1921; Allen, 1963; Allen, 1970; McGowen & Garner, 1970; Brice, 1974; Miall, 1978; Walker & Cant, 1984; Smith, 1987) but several authors (Thomas *et al.*, 1987; Smith, 1988; Smith *et al.*, 2009) cite examples of bars containing higher percentages of mud than sand. Mud-rich accretion sets usually have some sand and are collectively called inclined heterolithic strata (HIS; after Thomas *et al.*, 1987). IHS is a descriptive term and defines alternating layers of sandy, muddy strata arranged along subparallel *en*

Fluvial Meanders and Their Sedimentary Products in the Rock Record, First Edition.
Edited by Massimiliano Ghinassi, Luca Colombera, Nigel P. Mountney and Arnold Jan H. Reesink.

échelon accretion surfaces at low (~10 degrees) angles to horizontal bedding that are typically attributed to muddy point bar development.

IHS is common and usually interpreted to record tidal point bars, bar tails, or counter point bars (Smith, 1987, 1988; Rahmani, 1988; Gingras *et al.*, 1999; Choi *et al.*, 2004; Smith *et al.*, 2009; Choi, 2010; Dashtgard & Johnson, 2014). IHS formation is attributed to seasonal or random changes in flow rates, or in a tidal environment it may be caused by seasonal and biweekly migration of turbidity maxima (Smith, 1985; De Boer *et al.*, 1988; Smith, 1988; Fustic *et al.*, 2012; and Blum, 2015). Though IHS is commonly attributed to tidal conditions (Thomas *et al.*, 1987; Smith, 1988; Schoengut, 2011; Fenies *et al.*, 2012), Thomas *et al.* (1987) made no indication that tidal influence is a required condition for IHS deposition. Indeed, non-tidal occurrences are common (Thomas *et al.*, 1987; Dalrymple *et al.*, 1992). In non-tidal meandering rivers, IHS forms in two ways. Multiple meander cut off events with consecutive lateral migrations over previous cut offs result in the preservation of amalgamated fragments of heterolithic channel fill and periodic growth of a single point may make HIS if mud deposition is generally high (Reineck & Wunderlich, 1968; Thomas *et al.*, 1987; and De Boer *et al.*, 1988). The cut-off examples typically are confined to the outer growth bands of the bar but the IHS reflective of periodic growth may permeate the bar. Flow variance in counter point bars tends to generate IHS throughout, but these bars also tend also to have a down-stream-elongated geometry and convex accretion surfaces (Smith, *et al.*, 2009).

Mud-dominant IHS point bars deposited owing to either tidal influence (Thomas *et al.*, 1987; Smith, 1988; Schoengut, 2011; Fenies *et al.*, 2012), waning bar tails (Willis & Tang, 2010; Smith *et al.*, 2011; and Ielpi & Ghinassi, 2014), or counter point bars (Brice, 1974; Hooke, 1984; Smith *et al.*, 2009; Fustic *et al.*, 2010) are common place and are modestly well understood. Less understood are point bars that lack characteristics of these depositional origins, yet are mud dominant. These 'muddy-normal' point bars bear no obvious tidal influence, have the lobate geometry of normal expansion-dominate sandy point bars but are mud-rich point bars dominated by IHS throughout.

The goal of the current study is to evaluate the process(s) of these muddy-normal point bars. This proceeds by examining the internal architecture of a heterolithic point bar deposit within the Cretaceous Belly River Group of Dinosaur Provincial Park, Canada that has the geometry and sedimentary features of a muddy-normal point-bar. This point bar also has the overprint of slumping and liquefaction that we here interpret to record a large lateral spread and liquefaction associated with a large earthquake that occurred late in point-bar development.

Point-bar processes and types

Point bars form as side-attached bars on the inside bend of single thread meandering rivers; and form mostly by accumulation of sand and gravel as the bar laterally accretes and the opposing cutbank retreats (Wolman & Leopold, 1957; Allen, 1965; Mertes *et al.*, 1996; Constantine & Dunne, 2008; Jo & Ha, 2013; Nardin, 2012; and van de Legeweg *et al.*, 2014). Bank pull (from rapid cutbank erosion compared to bar accretion) and bar push (from rapid bar accretion compared to cutbank erosion) cause channel migration towards the outer bank and an increase in sinuosity of the channel with continued bar growth (Constantine & Dunne, 2008; Willis & Tang, 2010; and Eke, 2013). Migration normal to a channel bank is expansion, whereas migration obliquely downstream relative to a channel bank is translation (Daniel, 1971; Jackson, 1976; Nanson, 1980; and Bridge & Jarvis, 1982).

Traditional models show point bars to fine upward owing to an upward decrease in bed shear stress with decreasing water depth. Multiple stacked upward fining trends of accretion packages may comprise a larger fining trend resulting from bar erosion and reactivation following major floods or changes in growth vector with channel rotation (Smith, 1987; Thomas *et al.*, 1987; Bridge, 2003; Constantine & Dunne, 2008; Willis & Tang, 2010; and Durkin *et al.*, 2015a & b.). These mechanisms produce scours, lateral-accretion bed sets and current structures exhibiting migration along lateral accretion faces which can be observed in most point bar deposits (Smith, 1987; Thomas *et al.*, 1987; Bridge, 2003; Constantine & Dunne, 2008; Willis & Tang, 2010; and Hubbard, 2011). Common point bar models include the sandy-normal point bar, counter point bar and tidal point bar.

The sandy-normal point bar records the typical 'text book' meandering point bar model. This model is simplified (Fig. 1) with subparallel lateral accretion surfaces, usually spanning from the top of the bar to the bottom of the bar (Sundborg, 1956; Allen, 1963, 1970; McGowen & Garner,

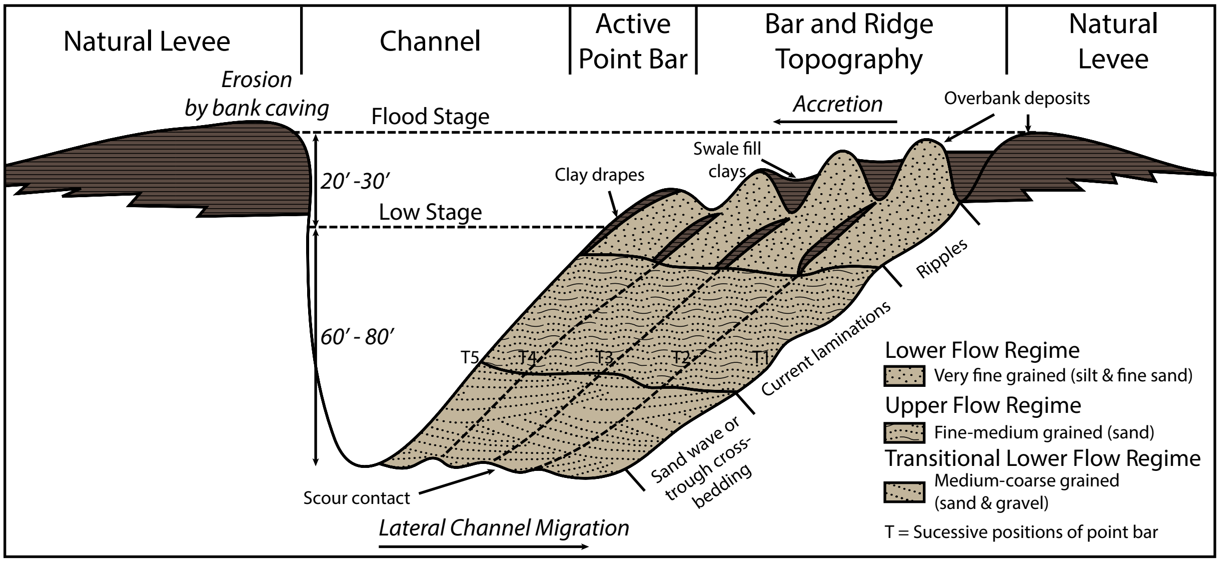

Fig. 1. (Above): From Saucier (1994), showing the internal sedimentary features of a sandy-normal point bar.

1970; Bluck, 1971; Bridge, 1975). These point bar deposits are typically sand-dominated with lower regime to some lower-upper regime sedimentary structures and minimal mud, most commonly in the form of relatively thin mud drapes between thicker sandy bed sets (Frazier & Osanik, 1961; Allen, 1970; and Walker & Cant, 1984). These bars are roughly the thickness of bank-full channel depth and form from a dominance of bar expansion compared to translation (Fig. 2) (Jackson, 1976; Nanson, 1980; and Bridge & Jarvis, 1982; Smith, 2006).

Counter point bars may be heterolithic with alternating accretion sets of sand and mud that form IHS deposits. Transition from normal point bar to counter point bar occurs across an inflection point separating the convex 'normal' point bar from the concave counter point bar during bar translation (Brice, 1974; Hooke, 1984; Smith *et al.*, 2009; and Fustic *et al.*, 2010). Translation pulls the channel from the concave bank downstream of the convex point bar and results in muddier bar-tail preservation (Smith *et al.*, 2009, 2011; Willis & Tang, 2010). Over time these bars accumulate elongate bodies with accretion sets that are concave to the channel in plane view (Fustic *et al.*, 2010; Brice, 1974; Hooke, 1984; and Smith *et al.*, 2009) (Fig. 3). Textural trends in counter point bars downriver from the crossover point include the thickening of silt-dominated facies, diminishing and fining of sand interbeds and general fining of grain-size within accretion sets (Fustic *et al.*, 2010; Brice, 1974; Hooke, 1984; and Smith *et al.*, 2009). Counter point bars thicken at the expense of normal point bars as they build away from the inflection point and eventually reach a maximum thickness equal to the full point bar (Fustic *et al.*, 2010; Brice, 1974; Hooke, 1984; and Smith *et al.*, 2009).

Tidal point bars are also characterised by IHS. Tidal environments have rhythmic fluctuations in water levels and current velocities due to tidal cycles; as such, IHS deposition is common (Smith, 1985; Thomas *et al.*, 1987; and De Boer *et al.*, 1988). Tidally induced IHS typically are heterolithic or clean sands inter-fingering with mud clast breccias. Typically, these mud clast breccias lay under heterolithic accretion-stratified sands, with clay layers more abundant in the uppermost portion (Smith, 1985; De Boer *et al.*, 1988; and Fenies *et al.*, 2012). Other indictors of tidally influenced point bars include cross-bedding within lenticular and wavy bedding and reactivation surfaces on top of the cross-beds (Reineck & Wunderlich, 1968; de Mowbray, 1983; Smith, 1985; and De Boer *et al.*, 1988) and marine trace fossils along accretion sets (Smith, 1985; Pattison *et al.*, 2005; Desjardins *et al.*, 2012). Tidal IHS point bars otherwise form by the same mechanisms of expansive or translating lateral accretion as other point bars.

A muddy-normal point bar has similar lobate geometries and convex accretion sets to a sandy normal point bar, but it has subequal to more